TP 8307 E

ALUMINUM-AIR (SALT WATER) BATTERY FOR VEHICLES

FINAL REPORT

Prepared for

Transportation
Development Centre

Transport Canada

by
Alcan International Ltd.

APRIL 1987

ALCAN

CA1
DTC 800
87
A42
c.2

mm

CA1
TC500
87
I42
c.2

ALUMINUM-AIR (SALT WATER) BATTERY FOR VEHICLES

Final Report

Prepared for
Transportation Development Centre
Transport Canada

by

Alcan International Limited

David S. Strong

TP 8307 E

Library and Information Centre / Centre de Documentation
RECEIVED / REÇU
APR 4 1989
Transport Canada / Transports Canada

April 1987

Alcan Report CSOR-87/E-005/10

41979

The contents of this report reflect the views of Alcan International Limited and not necessarily the official view or opinions of the Transportation Development Centre of Transport Canada.

Un sommaire en français de ce rapport est enclus avant la Table des matières.

Transport Canada / Transports Canada

Development / Développement

REPORT DOCUMENTATION FORM

1. Transport Canada Report No.	2. TDC Project No.	3. Recipient's Catalogue No.
TP 8307E	6282-6285	

4. Title and Subtitle	5. Report Date
Aluminium-Air (Salt Water) Battery for Vehicles	April 1987
	6. Performing Organization Report No.

7. Author(s)	8. Transport Canada File No.
David S. Strong	D1465-443

9. Performing Organization Name and Address	10. DSS File No.
Alcan International Limited 1188 Sherbrooke Street West Montreal, Quebec H3A 3G2	15SD.T8200-4-4530
	11. DSS or Transport Canada Contract No.

12. Sponsoring Agency Name and Address	13. Type of Report and Period Covered
Transportation Development Centre (TDC) 200 Dorchester Boulevard West Suite 601, West Tower Montreal, Quebec. H2Z 1X4	14. Sponsoring Agency Code

15. Supplementary Notes	16. TDC Project Officer
Partially funded by the DSS Unsolicited Proposals Fund and by the Energy R&D Panel of Energy, Mines and Resources.	John H. Morgan

17. Abstract

This report discusses the development of a 12-V, 250-W aluminum-air (salt water electrolyte) battery and its use to demonstrate the concept of range extension in electric vehicle using two types of battery.

Two 12-V 20-A multicell aluminum-air batteries were constructed and tested in a 24-V series configuration. They yielded 100 Wh/kg and 15 W/kg. The problems of heat removal, hydrogen dispersal and by-product management were resolved.

The batteries were then placed in parallel with lead-acid batteries in a 24-V golf cart. A device was developed for the aluminum-air battery to trickle-charge the lead acid battery. The hybrid system more than doubled vehicle range as compared to that obtained using lead-acid batteries only, with an equal mass and a similar capacity rating.

18. Key Words	19. Distribution Statement
Aluminum, air, salt water, electrolysis, fuel, cell, battery, electric vehicle.	A limited number of copies are available upon request from the Transportation Development Centre

20. Security Classification (of this report)	21. Security Classification (of this page)	22. No. of Pages	23. Price
None	None		

Canada

Transports Canada / Canada
Développement / Development

FORMULE DOCUMENTAIRE DU RAPPORT

1. N° du rapport Transports Canada	2. N° de l'étude — CDT	3. N° de catalogue du destinataire
TP 8307E	6282-6285	

4. Titre et sous-titre	5. Date du rapport
Aluminium-Air (Salt Water) Battery for Vehicles	Avril 1987
	6. N° du rapport de l'organisme exécutant

7. Auteur(s)	8. N° de dossier Transports Canada
David S. Strong	D1465-443

9. Nom et adresse de l'organisme exécutant	10. N° de dossier — ASC
Alcan International Limitée 1188 ouest, rue Sherbrooke Montréal (Québec) H3A 3G2	15SD.T8200-4-4530
	11. N° de contrat — ASC ou Transports Canada

12. Nom et adresse de l'organisme parrain	13. Genre de rapport et période visée
Centre de développement des transports (CDT) 200 ouest, boul. Dorchester Suite 601, tour ouest Montréal (Québec) H2Z 1X4	14. Code de l'organisme parrain

15. Remarques additionnelles	16. Agent de projet — CDT
Partiellement financé par le Programme des propositions spontanées du MAS et par le Programme énergétique d'Energie, Mines et Ressources.	John H. Morgan

17. Résumé

Ce rapport rend compte du développement de la batterie aluminium-air 12 volts, 250 watts, à électrolyte salin et du gain d'autonomie qu'elle a autorisé dans le cas d'un véhicule électrique mû par deux types différents de batteries.

Les deux batteries Al-air, 12 volts, 20 ampères réalisées ont été essayées dans une configuration 24 volts série, donnant 100 Wh/kg et 15 W/kg. Le problème de la chaleur, de l'hydrogène et des sous-produits dégagés a été résolu.

Ces batteries ont été par la suite branchées en parallèle aux batteries plomb-acide 24 volts d'une voiturette de golf. Un dispositif de régulation étudié exprès a permis aux batteries Al-air de recharger les batteries plomb-acide au fur et à mesure, ce qui a plus que doublé l'autonomie de la voiturette mue par les seules batteries plomb-acide, à masse égale et à capacité nominale comparable.

18. Mots-clés	19. Diffusion
Aluminium, air, eau saline, électrolyse, combustible, cellule, batterie, véhicule électrique.	Le Centre de développement des transports dispose d'un nombre limité d'exemplaires.

20. Classification de sécurité (de ce rapport)	21. Classification de sécurité (de cette page)	22. Nombre de pages	23. Prix
Non classifié	Non classifiée		

Canada

ACKNOWLEDGEMENTS

Alcan Wishes to thank the following people for their technical advice, endless enthusiasm, and constructive comments throughout the project.

Mr. J.H. Morgan (Project Officer)
Senior Development Officer
Transportation Development Centre
Montreal, Quebec

Dr. W. Adams
Coordinator, Electrochemical Science and Technology Centre
University of Ottawa
Ottawa, Ontario

Dr. M. Hammerli
Project Manager
Industry Policy Analysis
National Research Council
Ottawa, Ontario

The author also wishes to thank the members of the Alcan aluminum-air battery research and development teams in Kingston and Banburry, and the computer aided design specialists in Alcan Montreal for their contributions and assistance. Special thanks to those in the Kingston Labs machine shop, who always managed to turn out high quality workmanship within very tight deadlines.

This project was funded, in part, by the Unsolicited Proposals Fund of Supply and Services Canada and by the Energy Research and Development Panel, whose contributions are appreciated.

PREFACE

This report describes the development, design, and operation of a prototype multi-cell saline aluminum-air battery in an application as a range extender in a hybrid electric vehicle. The work was carried out at Alcan International's Research and Development Centres at Kingston, Ontario, Canada, and Banbury, England, over the past two years. Alcan provided 64% of the funds and the remaining 36% was provided under contract through the Transportation Development Centre (Transport Canada), the Unsolicited Proposals Fund (Supply and Services Canada), the National Research Council, and the Energy Research and Development Panel. Transport Canada's representative as project officer was Mr. J. Morgan.

This project was one of several steps towards the future development of an aluminum-air energy system capable of replacing the internal combustion engine in road vehicles. This project complements other longer-term work being carried out by Alcan and others in this field.

Government of Canada support for this program is in line with the recommendations of the 1981 Special Committee of the Canadian House of Commons on Alternate Energy and Oil Substitution. As pointed out in "Energy Alternatives", the Report of the Special Committee to the Parliament of Canada, the possible long-term benefits include pollution free road vehicles, reduced dependence on fossil fuels, greater exploitation of the Canadian hydro resource base and Canadian leadership in the development and exploitation of a new alternate energy technology. In the short term this program has provided a low-cost means for the practical evaluation of the technical and commercial feasibility of the aluminum-air powered vehicle and has helped to orient the long-term research and development program.

Alcan has made every effort to involve Canadian material suppliers and sub-contractors throughout the course of the project. For example, this includes two machine-shops in Kingston, an air-electrode supplier in Kingston, a prototype moldmaking shop in Cobourg, and a sub-contractor in Toronto. Although these were the main external contacts, there were countless other suppliers of materials and hardware as well, almost all of them Canadian based companies.

SUMMARY

1. BACKGROUND

Alternative technology power systems for road vehicles have been under active development since the energy crisis in 1973-74. Although electric vehicles have long been used in specialized applications, vans and passenger vehicles had only been produced on a small scale (bordering on novelty) before that time. The electric power systems had not been able to compare with the power and range of the internal combustion engine. Now, after more than a decade of effort, electric power storage and conversion devices such as batteries and fuel cells have taken major steps in performance and reliability.

When compared to typical batteries such as lead-acid or nickel-iron, metal-air cells have greater specific energy (Wh/kg) and energy density (Wh/L), as well as acceptable specific power (W/kg). Although there are many different types of metal-air cells, aluminum-air has very high specific energy (Wh/kg), second only to lithium-air, which is very difficult to work with, and has proven to be a reasonably practical system.

At the outset of this project, extensive research was ongoing, both inside and outside of Alcan, towards the long term development of an aluminum-air power system for road vehicles. Alcan made a very substantial commitment to this technology in 1981, with the ultimate goals being the use of pollution-free vehicles, reduced dependence on fossil fuels, beneficial use of Canadian hydro-electric power, and Canadian leadership in a new alternative energy technology.

As a part of this overall commitment, the Alcan aluminum-air battery project was proposed. This project was intended to demonstrate the state of saline aluminum-air battery technology, and to evaluate a hybrid vehicle concept, which is the coupling of a high energy, low power source with a low energy, high power source, to provide a combination of acceptable power and range. The work was carried out by Alcan International's Research and Development Centres in Kingston, Ontario, and in Banbury, England.

The actual detailed objectives, as outlined in the proposal, were as follows:

(i) To assess the current level of development of the aluminum-air battery for application as an auxiliary energy source for an electric vehicle

(ii) To analyse the performance of various battery systems when combined with the aluminum-air battery for road vehicle application

(iii) To package known technology and build a hybrid battery system for an industrial vehicle

(iv) To test and demonstrate the potential of the aluminum-air battery as a "range extender" and recharger for an industrial electric vehicle.

The scope of the study was defined to provide certain limitations on the development work, as the fields of aluminum-air batteries and electric vehicles are very broad. The electrolyte was to be saline only, rather than caustic, the latter of which allows for higher performance, but adds complexities due to safety and engineering considerations. In order to maintain a degree of practicality, the battery design was to remain as simple as possible to make it "user friendly". The aluminum-air battery was to allow for continuous use with only electrolyte and anode changes. The electric vehicle used in the tests was to be small, in the 24 to 36 volt range, and preferably an industrial or recreational vehicle. Finally, since the main intention of the study was to demonstrate the hybrid principle, the aluminum-air batteries were to be taken to the working prototype stage. Additional development towards commercialization of this type of battery was not within the scope of this project.

2. METHODOLOGY AND MAJOR DEVELOPMENTS

As described in the unsolicited proposal, it was intended to limit the project to the use of technology which already existed. However, it soon became apparent that existing technology at the time would limit the performance of the aluminum-air batteries. As a result, substantial effort went towards the development/improvement of technology, including both the process and the engineering.

Initial work concentrated on finding methods of extending the life of the electrolyte and reproducing results published by Alexander Despic of the University of Belgrade, which indicated that stirred electrolyte would extend the life of the cell and improve the voltage. It was found that electrolyte additives would not improve performance, and it was confirmed that stirring the electrolyte improved performance, although the method of stirring was demonstrated to be difficult in a practical sense.

As a result, the efforts in cell development increased rapidly. Two types of battery systems evolved as a result. One was a series of individual stirred cells, and the other was a multiple cell arrangement housed within a common stirred sump.

Many of the same problem areas were considered in both systems, but from a different approach. As it turned out, the final prototype consisted of the best developments from both locations, illustrating the benefits of this approach.

After many refinements in the technology, an optimized single cell was built using a practical air injection system which provided stirring, circulation, removed heat, settled much of the solid by-product, and diluted the produced hydrogen gas well below the lower explosion limit. The single cell reached the pre-determined goal of 100 Ah while remaining cleanable (actually reaching over 150 Ah) in a self-contained design requiring less than 10% parasitic power for operation.

The technology was integrated into a multi-cell battery with the cells sharing a common sump, initially in design form using a Computer Aided Design and Drafting system. This design was updated as the technology developed, and then the feasibility was put to the test in a three cell version of the common sump battery. With the exception of an air stagnation problem in the cathode cavity, the system worked successfully, producing the set goal of 300 Ah total discharge over 3 successive 100 Ah tests (on one set of anodes). At the end of each 100 Ah discharge, it was cleaned without disassembly by flushing with water.

The design was then altered to allow thermal convection to provide fresh air circulation to the cathodes, as well as to improve other parts of the system (for example, to allow anode change without major battery disassembly). This design was constructed in the full 14 cell size and first tested in a laboratory simulation, where it performed very well. Non-uniform stirring made the battery difficult to clean in the beginning, but this was mostly overcome by modifications to the air supply system. Seepage through the air cathodes in some cells created shorting from one cathode to another, resulting in rapid degradation and flooding of the affected cathodes, with subsequent loss in battery capacity. Despite this, the final prototype battery performed very well overall, and was able to demonstrate the main objective of hybrid vehicle power.

While battery development was progressing, other related issues were also being addressed. One of these was the acquisition of the test electric vehicle (a 24 volt, 500 watt single person golf vehicle), and its preparation for testing the hybrid battery power concept. This included mechanical changes and additions, as well as installation of instrumentation. The other major development was the design of an efficient charging control system to handle the combination of aluminum-air and lead-acid batteries. This was achieved as a final year project for an electrical engineering student at Southampton University, England, under contract from Banbury Labs.

The vehicle was first tested with lead-acid batteries only, and then with the aluminum-air/lead-acid combination to evaluate the benefits of the hybrid range extension concept. The driving time between recharges with the pair of 100 Ah lead-acid batteries supplied with the vehicle was about 3 hours with a 67% duty cycle. However, with the aluminum-air batteries

charging two 12 volt, 30 Ah lead-acid batteries in the hybrid arrangement, the corresponding time was over 6 hours, demonstrating a range extension of 100%. The range extension was limited due to leakage through several cathodes, causing cell failure and a voltage drop below the necessary level for charging. It is estimated that the aluminum-air batteries had only produced about 60 Ah, and would therefore have been able to run substantially longer, had the cathodes not failed. Another test was run on the following day with the vehicle operating for 4 hours before cell leakage again shut the system down. This illustrated further range extension, and also demonstrated that the battery could be re-started without disassembly.

3. CONCLUSIONS

As part of the major program of aluminum-air battery development for future vehicle or standby power, this project was intended to determine the performance capabilities of saline electrolyte aluminum-air batteries, and to ascertain whether an effective hybrid powered electric vehicle could be designed and demonstrated with the help of significant technical improvements achieved in the course of the project. It is now believed that the feasibility of the saline process technology has been established. However, engineering and materials development for this system is still required. Although the prototype battery was able to successfully reach the project specifications and demonstrate the range extender concept, more iterations of design and testing will be required before reliability and practicality are fully achieved.

Within the scope of this project, the objectives have been met, and the following conclusions have been reached:

(1) A multi-cell common sump, 12 volt, 20 ampere, saline aluminum-air battery has been developed that can produce 100 Wh/kg and 15 W/kg in its present form using injection molded parts. There is sufficient aluminum anode for three such runs. With minor refinements, the energy density can be increased substantially.

(2) Technology to remove heat, manage hydrogen, and manage the by-product in saline aluminum-air batteries has been developed and proven in both single cell and multi-cell batteries. The by-product management allows the battery to be cleaned at the end of a run by flushing the assembled battery with tap water.

(3) A multi-cell aluminum-air battery has been designed and built in such a fashion so as to be easily assembled and practical to operate. The battery can be cleaned and mechanically recharged (reloaded with aluminum anodes) with only minor disassembly. This same design can be easily adapted for any number of cells.

(4) A charging control system has been designed and demonstrated to efficiently control trickle charging from high energy aluminum-air batteries to high power lead-acid batteries operating in a hybrid electric vehicle system. This charging control system is also capable of acting as a controller for simple recharging of lead-acid batteries, separate from an electric vehicle.

(5) The range extension concept has been proven in an electric vehicle. The combination of aluminum-air batteries with small lead-acid batteries in a hybrid arrangement demonstrated twice the range of lead-acid batteries with similar charge ratings (100 Ah) without a noticeable reduction in power. At double the range, the aluminum-air batteries had produced about half of their available discharge capacity, but failed prematurely due to cathode leakage.

4. RECOMMENDATIONS

There are several items which are within reasonable scope of further study.

(1) The one item that presently limits the success of the saline aluminum-air battery is the air cathode, both in terms of operating performance and life expectancy. Although there are other methods of providing oxygen for the reaction, such as hydrogen peroxide or metallic oxides, atmospheric air is the simplest, and the supply is limitless. For that reason alone, air cathodes must be developed further to make them leak-proof, longer lasting, and less expensive. An alternative to longer life would be low cost "throw-away" cathodes. Alcan has already begun to independently study this area.

(2) Since the scope of this project was limited to the development of the required technology and demonstration of the range extender concept, there was no funding to study its impact on the performance and life of the lead-acid power batteries. In considering the operation of this system, it is recognized that the power (lead-acid) batteries would be exposed to a shallower discharge cycle. This is likely to have a highly beneficial effect on both the net charge obtainable from the power batteries, and their life, since they maintain close to a full charge throughout the operation of the hybrid system. This area is worthy of further study.

(3) This project has demonstrated the feasibility of a 100 Wh/kg saline battery capable of operating at 20 amperes at 14 volts over successive runs of several hours. Simultaneously, Alcan had built and operated (at its own expense) larger alkaline batteries capable of 300 Wh/kg. It is recommended that both systems be examined as potential range extenders.

SOMMAIRE

1. RAPPEL

La crise du pétrole de 1973-1974 a provoqué l'étude et le développement de nombreux systèmes de traction routière de substitution. Certes, il existait déjà des véhicules électriques destinés à des fins particulières, mais, avant cette date, les fourgonnettes et les voitures de tourisme mus à l'électricité ne se fabriquaient qu'en petites séries tant était forte l'emprise du moteur à combustion interne, supérieur en puissance et en autonomie. Aujourd'hui, une décennie plus tard, les générateurs électrochimiques - batteries et piles à combustible - ont fait d'énormes progrès, tant en performances qu'en fiabilité.

Par rapport aux accumulateurs classiques, au plomb-acide ou au nickel-fer, les batteries métal-air fournissent une énergie massique (Wh/kg) et une énergie volumique (Wh/L) bien supérieures, à une puissance massique (W/kg) restant quand même acceptable. Parmi les batteries métal-air, le couple aluminium-air vient au deuxième rang sur le plan de l'énergie massique, après le couple lithium-air qu'il surpasse cependant sur le plan de la facilité d'emploi.

Lorsque le présent programme a été lancé, le couple Al-air pour la traction routière faisait déjà l'objet de recherches intensives par Alcan et d'autres. En effet, dès 1981, Alcan avait décidé d'investir massivement dans cette filière, son but ultime étant la mise au point d'une source d'énergie de traction non polluante permettant à la fois de réduire notre dépendance des hydrocarbures, de valoriser nos ressources hydro-électriques et, enfin, de faire du Canada un chef de file dans le domaine des énergies de substitution.

Dans cette optique, Alcan a soumis une proposition visant à développer la technologie des batteries Al-air à électrolyte salin et à évaluer les performances d'un système hybride où une batterie haute énergie-faible puissance est couplée à une autre de type faible énergie-haute puissance, pour constituer un ensemble alliant puissance et autonomie suffisantes. C'est Alcan International Limitée qui a entrepris cette recherche, dans ses établissements à Kingston (Ontario) ainsi qu'à Banbury (Grande-Bretagne).

Les objectifs fixés à la recherche et indiqués dans la proposition étaient les suivants:

(i) Évaluer l'état d'avancement auquel est arrivée la batterie Al-air utilisable comme source d'énergie d'appoint en traction électrique routière.

(ii) Étudier les performances de divers types de batteries couplés à la batterie Al-air et utilisés pour la traction routière.

(iii) Appliquer les connaissances acquises à la réalisation d'une batterie hybride pour la traction des véhicules électriques de type industriel.

(iv) Faire l'essai et la démonstration de la batterie Al-air comme moyen d'accroître l'autonomie des véhicules électriques industriels, couplée à des batteries classiques dont elle assure la recharge.

La portée de la recherche a été nettement délimitée, les deux secteurs considérés, la batterie Al-air et la traction électrique routière, étant très vastes. Ainsi, 1) on s'en est tenu à l'électrolyte salin, malgré les performances supérieures de l'électrolyte alcalin, étant donné les complications que celui-ci apporte au niveau de la sécurité et de la fabrication; 2) on a voulu faire une batterie aussi simple que possible pour rendre son exploitation facile; 3) cette batterie devrait autoriser un fonctionnement continu avec le seul remplacement de l'électrolyte usagé et de l'anode; 4) le véhicule d'essai serait de petite taille, dans la gamme des 24 à 36 volts, de préférence de type industriel ou récréatif; et 5) la batterie serait amenée au stade de prototype fonctionnel, l'objectif de la recherche ayant pour objectif principal la validation du concept de la batterie hybride. Le développement en vue de la commercialisation de cette batterie n'entrait donc pas en ligne de compte.

2. MODE OPÉRATOIRE

Dans la proposition soumise, il avait été précisé que la recherche se fonderait sur les connaissances déjà acquises. Mais, très vite, il est devenu évident que, par cette restriction, on compromettrait les performances de la batterie Al-air. Il a donc fallu consentir un effort très important de développement et de perfectionnement, tant au niveau du procédé que des techniques utilisées.

La première tâche a été de rechercher le moyen de prolonger la durée de vie de l'électrolyse et d'arriver aux mêmes résultats que ceux décrits par Alexander Despic de l'université de Belgrade, lequel a trouvé que l'agitation de l'électrolyte permet d'obtenir non seulement une durée de vie plus longue des cellules, mais aussi une tension plus élevée aux bornes. Il a été déterminé qu'aucun additif ne permettait de réaliser ce résultat, mais que la filière agitation était valable, bien que, du côté pratique, elle se révélerait ardue à accomplir.

Dès lors, les efforts ont été concentrés sur le développement de la cellule électrochimique à deux types distincts de batterie; le premier étant constitué de cellules individuelles en série et agitées séparément, le

second, de plusieurs cellules, juxtaposées, logées dans un réservoir commun où se fait l'agitation.

Bon nombre des problèmes techniques communs aux deux types ont été abordés simultanément, mais envisagés selon une approche différente. Le prototype final qui en a résulté incorporait les meilleures idées de chaque filière, illustrant ainsi les avantages de la technique utilisée.

Après plusieurs perfectionnements, une monocellule optimisée a été réalisée, où un ingénieux système d'injection d'air provoquait l'agitation et la circulation de l'électrolyte, régulait la température, faisait se décanter la plupart des sous-produits solides et diluait l'hydrogène dégagé pour ramener sa concentration à un niveau bien au-dessous de la limite inférieure d'explosivité. Cette cellule a atteint l'objectif fixé de 100 Ah (réalisant en fait plus de 150 Ah), tout en demeurant accessible au rinçage, logée dans un boîtier et ne réclamant pas plus de 10 p. 100 de l'énergie fournie pour accomplir l'agitation.

Une batterie à plusieurs cellules partageant un même réservoir a été étudiée sur matériel DCAO (dessin et conception assistés par ordinateur), améliorée au fur et à mesure des progrès technologiques connexes et enfin éprouvée dans une version à trois cellules placées dans un réservoir commun. À part la stagnation de l'air dans la cavité cathodique, la batterie a bien fonctionné, délivrant au total les 300 Ah d'électricité prévus, à raison de trois décharges consécutives de 100 Ah chacune, sans remplacement des anodes. À la fin de chaque décharge 100 Ah, la batterie était rincée à l'eau sans avoir à être démontée.

Par la suite, le modèle a été modifié afin de permettre la libre circulation d'air neuf vers les cathodes par convection thermique et aussi pour améliorer certains autres aspects de la batterie, comme, par exemple, le remplacement de l'anode sans avoir à démonter la batterie. Ce modèle modifié a été réalisé dans une version pleine grandeur comportant 14 cellules et a été éprouvé en laboratoire où il a donné de bons résultats. Au début, le rinçage se faisait difficilement à cause de l'agitation inégale de l'électrolyte, mais on a vite pallié cet inconvénient par le perfectionnement de l'alimentation en air. Des fuites d'eau vers l'intérieur de certaines cathodes ont créé des courts-circuits, entraînant la dégradation rapide de celles-ci suivie de leur inondation, et provoquant des pertes de puissance. Néanmoins, le prototype final a donné de très bons résultats dans l'ensemble, ayant permis d'atteindre l'objectif principal qui était de valider le principe de la batterie hybride.

Entre-temps, les responsables ont fait avancer d'autres éléments du programme, comme l'acquisition du véhicule électrique devant servir aux essais, à savoir une voiturette de golf monoplace, 24 volts, 500 watts, et

sa préparation en vue des essais. Il s'agissait notamment de la modifier et de l'équiper d'instruments de mesure. Il y a eu aussi l'étude d'un système de régulation de la recharge, menée par un étudiant de dernière année en génie électrique de l'université de Southhampton (Grande-Bretagne), pour le compte des laboratoires de Banbury.

Les essais pratiques ont commencé avec la voiturette mue d'abord par les seules batteries plomb-acide, puis par la batterie hybride, le but étant de vérifier le gain d'autonomie réalisé. Le temps entre recharges des deux batteries plomb-acide 100 Ah fournies avec la voiturette a été d'à peu près trois heures, le facteur de marche étant de 67 p. 100. Mais, avec la batterie hybride, des batteries Al-air rechargeant deux batteries plomb-acide 12 volts 30 Ah, le temps correspondant a dépassé les six heures, soit un gain d'autonomie de 100 p. 100. Pourtant, les résultats ont souffert des fuites d'eau vers plusieurs des cathodes, provoquant la panne de celles-ci et une chute de tension à un niveau ne permettant plus la recharge. Il a été calculé que les batteries Al-air n'ont délivré que 60 Ah environ, mais qu'elles auraient pu fonctionner beaucoup plus longtemps, n'eût été la panne des cathodes. Le lendemain, la voiturette a fonctionné pendant quatre heures, l'apparition de fuites mettant un terme à l'essai. Néanmoins, un gain d'autonomie a été obtenu, et il a été démontré que la batterie pouvait être remise en marche sans avoir à être démontée.

3. CONCLUSIONS

Lancée dans le cadre du programme de développement de la batterie Al-air à électrolyte salin, soit pour la traction, soit comme source d'énergie d'appoint, la recherche visait à vérifier les performances de ce type de batterie et à prouver qu'un véhicule électrique efficace, mû par une source d'énergie hybride, pouvait être réalisé. Grâce aux perfectionnements apportés au fur et à mesure de l'avancement des travaux, on sait maintenant que ce type de batterie est du domaine du réalisable, bien qu'il nécessite encore une mise au point sur le plan du procédé et des matériaux. Cependant, même s'il a satisfait aux spécifications et permis de valider le concept de la batterie hybride, d'autres recherches et d'autres essais sont quand même nécessaires avant de pouvoir dire que l'objectif de fiabilité et de facilité d'emploi a été pleinement atteint.

Vu les limites imposées à la recherche, on peut dire que les objectifs ont été atteints et en tirer les conclusions suivantes:

(1) Une batterie aluminium-air, 12 volts 20 ampères à électrolyte salin, composée de plusieurs cellules groupées dans un réservoir commun a été réalisée, capable de fournir 100 Wh/kg et 15 W/kg dans sa forme actuelle, faite de pièces moulées par injection. L'anode d'aluminium suffit pour trois décharges. Par de légers

perfectionnements, l'énergie massique pourra être considérablement relevée.

(2) Le problème de la chaleur, de l'hydrogène et des sous-produits dégagés a été maîtrisé, dans les deux versions de la batterie: monocellulaire et multicellulaire. La technique d'élimination des sous-produits consiste à rincer la batterie avec de l'eau à la fin de chaque décharge.

(3) La batterie multicellulaire a été conçue de manière à en faciliter l'assemblage et l'emploi. Elle peut être nettoyée et rechargée mécaniquement (remplacement de l'anode d'aluminium) sans autre chose qu'un démontage très partiel. Un nombre quelconque de ces cellules peut être groupé pour former une batterie.

(4) Un dispositif de régulation de la recharge des batteries plomb-acide à haute puissance, à même les batteries Al-air à haute énergie, a été réalisé et éprouvé avec succès, dans une application de traction routière. Ce dispositif peut également servir à réguler la recharge ordinaire des batteries plomb-acide.

(5) Le gain d'autonomie d'un véhicule routier à bel et bien été vérifié, la mise en parallèle des batteries Al-air avec des batteries plomb-acide de petite taille ayant permis de doubler l'autonomie sur ces dernières, à capacité nominale égale (100 Ah) et sans réduction perceptible de la puissance, bien que les batteries Al-air n'aient délivré que la moitié de leur capacité avant la panne due aux fuites d'eau.

4. RECOMMANDATIONS

Les progrès suivants sont réalisables par une recherche plus poussée:

(1) La cathode d'air présente le seul obstacle au plein succès du couple Al-air à électrolyte salin, sur le plan tant des performances que de la durée de vie. Il existe, certes, d'autres moyens de produire l'oxygène nécessaire à la réaction, comme le peroxyde d'hydrogène ou les oxydes des métaux, mais l'oxygène dans l'air est plus simple à obtenir et la réserve est illimitée. Cette raison d'ailleurs milite en faveur des cathodes d'air, qu'il faudra mettre au point en les rendant étanches, durables et meilleur marché. Une autre solution serait d'avoir des cathodes bon marché, et jetables. C'est dans cette direction que Alcan a lancé sa recherche.

(2) Étant donné que la recherche était limitée à la mise au point de la technologie considérée et à la vérification du gain d'autonomie, on ne disposait pas de fonds permettant d'étudier son impact sur les

batteries plomb-acide sur le plan des performances et de la durée de vie. Mais du fait que, dans ce système, la décharge restera peu profonde, il est permis de croire que cet impact sera bénéfique en matière de capacité nette disponible et de durée de vie puisque, en fonctionnement hybride, ces batteries seront constamment maintenues à un état de charge proche du maximum. Ceci mérite d'être étudié plus à fond.

(3) Il a été bel et bien démontré qu'une batterie à électrolyte salin de 100 Wh/kg peut délivrer 20 ampères à 14 volts durant plusieurs heures, et sur plusieurs cycles successifs. Parallèlement, Alcan a réalisé et fait fonctionner (à ses frais) des batteries à électrolyte alcalin de plus grande taille, de l'ordre de 300 Wh/kg. Il est recommandé que ces deux types de batteries soient envisagées sous l'angle de leur utilisation comme moyen d'accroître l'autonomie des véhicules électriques routiers.

TABLE OF CONTENTS

1. INTRODUCTION 1
   1.1 Background 1
   1.2 Objectives and Scope of the Project 3

2. DISCUSSION 4
   2.1 Background Studies 4
      2.1.1 Electrolyte Additives 4
      2.1.2 Effect of pH and Stirring on Oxidation Products 5
      2.1.3 Effects of Electrolyte Temperature and Salt Concentration 6
      2.1.4 Effects of Stirring the Electrolyte 7
   2.2 Single Cell Development 9
      2.2.1 The First Engineered Single Cell 9
      2.2.2 The First Cell Stack Stirred by Reciprocated Electrolyte 9
      2.2.3 The 14 Cell Stack (Stirred by Reciprocated Electrolyte) 10
      2.2.4 Developments in the Single Cell 10
   2.3 Development Work for Optimised Single Cells..... 11
   2.4 Single Cell Development Towards the Common Sump Battery 11
      2.4.1 Full Development of Air (Gas) Injection Technology 12
   2.5 Development of the Multi-Cell Common Sump Battery 17
      2.5.1 The Common Sump Multi-Cell Battery Concept 17
      2.5.2 Shunt Current Tests on the Common Sump Design.... 18
      2.5.3 Shunt Current Tests on the Common Manifold/ Common Sump Design 19
   2.6 Setting Prototype Battery Parameters 19
   2.7 Development of the 12 Volt Prototype Battery with Computer Aided Design and Drafting 19
      2.7.1 CADD Design Three 21
   2.8 Feasibility Testing of the Multi-Cell Common Sump Battery: The Three Cell Version 22
      2.8.1 Design 22
      2.8.2 Construction 22
      2.8.3 Performance Testing 23
   2.9 The Final 12 Volt Prototype Battery 23
      2.9.1 Design 23
      2.9.2 Bench Test of the Prototype Battery 27
   2.10 Selection of the Electric Test Vehicle 29
   2.11 Charging Control System 30
   2.12 Electric Vehicle Performance Tests 31

3. CONCLUSIONS 32

4. RECOMMENDATIONS 32

LIST OF TABLES

Table 1	Comaprison of Metal-Air Batteries.....	1
Table 2	Effect of NaCl Concentration and KCl in a Stirred Cell at 30 mA/cm^2.....	7
Table 3	Reaction Product Results from Static and Reciprocated Cells	7
Table 4	Behaviour of 3 Cell Stack.....	9
Table 5	Single Cell Performance Test Results.....	13
Table 6	Single Cell Performance Test Results.....	14
Table 7	Single Cell Performance Test Results.....	15
Table 8	Single Cell Performance Test Results.....	16
Table 9	Shunt Current Tests.....	20
Table 10	Three-Cell Common Sump Battery Performance Results.....	24
Table 11	Electric Vehicle Weight Breakdown.....	28

LIST OF FIGURES

Figure 1	Schematic operation of an aluminum-air battery.....	2
Figure 2	Voltage and current efficiencies.....	34
Figure 3	Flow cell power performance in 7% NaCl.....	35
Figure 4	Conductivity versus cell capacity.....	36
Figure 5	Waste from stagnant cell.....	37
Figure 6	Waste from reciprocated cell.....	37
Figure 7	The 25 cm^3 test cell.....	38
Figure 8	Hydrogen evolution tests on 5* alloy.....	39
Figure 9	Galvanostatic polarization in 12% NaCl with 5* alloy..	40
Figure 10	Hydrogen evolution rate versus temperature.....	41
Figure 11	The first single cell design.....	42
Figure 12	The first single cell assembly.....	43
Figure 13	Performance of a single reciprocated cell.....	44
Figure 14	Temperature and weight loss of a 3 single cell stack..	45
Figure 15	14 Single cell stack test assembly.....	46
Figure 16	Cell voltages for 14 single cell stack test.....	47
Figure 17	Current efficiencies of a 14 single cell stack test...	48
Figure 18	Slant bottom single cell.....	49
Figure 19	Schematic of test connections.....	50
Figure 20	Performance of various cathode connections.....	51
Figure 21	Schematic of circulated cell.....	52
Figure 22	Schematic of gas injection cell (front view).....	53
Figure 23	Schematic of gas injection cell (side view).....	54
Figure 24	Conceptual air cathode cassette.....	55
Figure 25	Conceptual battery cover.....	56
Figure 26	Conceptual battery case.....	57
Figure 27	Conceptual anode support rack.....	58
Figure 28	Shunt current test box.....	59
Figure 29	Shunt current test with common manifold.....	60
Figure 30	CADD design 3 (1).....	61
Figure 31	CADD design 3 (2).....	61
Figure 32	CADD design 3 (3).....	62
Figure 33	CADD design 3 (4).....	62
Figure 34	CADD design 3 (5).....	63
Figure 35	CADD design 3 (6).....	63
Figure 36	CADD design 3 (7).....	64
Figure 37	CADD design 3 (8).....	64
Figure 38	Three cell battery - air cathode cassette.....	65
Figure 39	Three cell battery - front view.....	66
Figure 40	Three cell battery - side view.....	67
Figure 41	Three cell battery - top view.....	68
Figure 42	Three cell battery test apparatus.....	69
Figure 43	Three cell battery performance.....	70
Figure 44	Final prototype design - air cathode cassette..... (front view).....	71
Figure 45	Final prototype design - battery end view.....	72
Figure 46	Final prototype design - cathode support frame.....	73
Figure 47	Final prototype design - cathode cassette assembly....	74
Figure 48	Final prototype design - partial side view.....	75
Figure 49	Final prototype design - partial side (section) view..	76
Figure 50	Final prototype design - top view.....	77

LIST OF FIGURES (cont'd)

Figure 51 Final CADD design (1)..... 78
Figure 52 Final CADD design (2)..... 78
Figure 53 Final CADD design (3)..... 79
Figure 54 Final CADD design (4)..... 79
Figure 55 Final CADD design (5)..... 80
Figure 56 Final CADD design (6)..... 80
Figure 57 Final CADD design (7)..... 81
Figure 58 Final CADD design (8)..... 81
Figure 59 Final CADD design (9)..... 82
Figure 60 Final CADD design (10)..... 82
Figure 61 Final CADD design (11)..... 83
Figure 62 Constructed battery (1)..... 83
Figure 63 Constructed battery (2)..... 84
Figure 64 Final prototype battery bench test..... 84
Figure 65 Final prototype battery performance test results..... 85
Figure 66 Final prototype battery cell voltages..... 86
Figure 67 Final prototype battery temperatures..... 87
Figure 68 Final prototype battery - three day results..... 88

1. INTRODUCTION

1.1 Background

Several types of batteries have been developed which make use of the oxygen in the air as the cathodic reactant. The most obvious advantage of the oxygen cathode is its low weight and very high capacity. The resulting cell has, at the cathode, the identical membrane that is found in a hydrogen fuel cell, and the technology of metal air batteries had benefited in recent years from the attention given to research on the cathode membranes. Four metals, namely aluminum, zinc, magnesium, and lithium have been extensively studied for use in metal air systems. The properties of these metals are compared in Table 1. Hitherto only zinc has been used on any scale in metal air batteries where it requires a caustic electrolyte to perform well. It can be seen in the table that aluminum's properties should yield a very desirable performance.

Table 1 Comparison of Metal-Air Batteries

Metal	Electrochemical equivalent Ah/g	Theoretical cell voltage* V	Theoretical specific energy Wh/g	Operating voltage V
Li	3.86	3.4	13	2.4
Al	2.98	2.7	8.1	1.6
Mg	2.20	3.1	6.8	1.4
Ca	1.34	3.4	4.6	2.0
Zn	0.82	1.6	1.3	1.2

* Cell voltage with oxygen cathode

Aluminum can operate in electrolytes with pH ranging from acidic to basic and has been studied for mechanically rechargeable metal air batteries with a neutral to caustic electrolyte. Figure 1 schematically illustrates the aluminum-air battery. The capacity (i.e. Wh/litre and Wh/kg) of the battery is generally limited by the electrolyte rather than the anode. This is because the dissolution of aluminum into the electrolyte results initially in the formation of soluble complexes with either chloride or hydroxyl ions which eventually precipitate out as aluminum hydroxide in various structural forms. Unless this precipitation process is managed (i.e. delayed or controlled), the result is premature battery failure and the electrolyte can effectively solidify, making emptying or cleaning for re-use difficult, if not impossible.

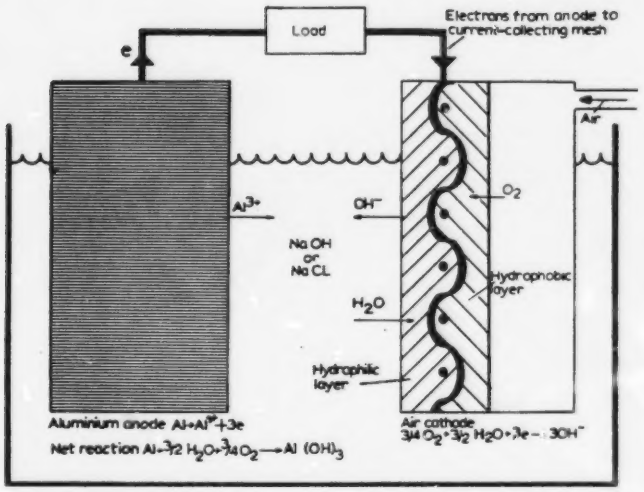

Figure 1 Schematic Operation of an Aluminum-Air Battery

In Alcan's proposal (The Electric Vehicle Project, CSO: E-005-84, 11 March 1984), it was suggested that the capacity limit that could be reached in a stagnant saline aluminum-air cell was around 200 Wh/litre. At that point, the cell by-product had solidified. Alexander Despic at the University of Belgrade had suggested that a stirred cell could have double the capacity and still be cleanable. He had also shown that such a cell could sustain one volt at a current density of 50 ma/cm^2.

Dr. Despic was retained as a consultant to this project and this report begins by describing the early attempts that were made to duplicate his work. The report then goes on to describe the development of a feasible battery in which heat, hydrogen, and the precipitate are managed. That battery has been tested and it produces a stack voltage of 14 volts and current of 20 amperes. The battery is easily capable of exceeding 100 Wh/kg and 15 W/kg between electrolyte changes, and carries sufficient aluminum for three such runs.

It should be borne in mind that this project constituted only a fraction of the effort that Alcan has committed to aluminum batteries. During the same time period, Alcan has worked on caustic batteries and taken their practical electrolyte capacity up to 1000 Wh/litre. The battery described in this report will have one set of applications; other aluminum batteries

will be able to meet other needs. The battery described here will be particularly suitable for applications where there is concern over the use of a caustic electrolyte, and will have earlier consumer appeal than caustic systems.

1.2 Objectives and Scope of the Project

The purpose of this study was to design and build a hybrid battery system into an electric vehicle using aluminum-air batteries to extend the limited range of conventional electric vehicle batteries.

The objectives of the project were four-fold:

(i) To assess the current level of development of the aluminum-air battery for application as an auxiliary energy source for an electric vehicle

(ii) To analyse the performance of various battery systems when combined with the aluminum-air battery for road vehicle applications

(iii) To package known technology and build a hybrid battery system for an industrial vehicle

(iv) To test and demonstrate the potential of the aluminum-air battery as a "range extender" and recharger for an industrial electric vehicle.

The scope of the study was defined so as to provide certain limitations on the development work, as the fields of aluminum-air batteries and electric vehicles are very broad. The electrolyte was to be saline only rather than caustic, the latter of which allows for much higher power densities, but adds many complexities due to safety and engineering considerations. In order to maintain a degree of practicality, the battery design was to remain as simple as possible to make it "user friendly". The aluminum-air battery was to be re-usable to allow for continuous use with only electrolyte and anode changes. The electric vehicle used in the tests was to be small, in the 24 to 36 volt range, and preferably an industrial or recreational vehicle. Finally, since the main intention of the study was to demonstrate the hybrid principle, the aluminum-air batteries were to be taken to the working prototype stage.

As described in the initial unsolicited proposal, it was intended to limit the project to the use of fundamental technology which was already published. However, it soon became apparent that this would limit the performance of the aluminum-air batteries. As a result, substantial effort went towards the development of process technology as well as engineering.

Process problems were identified as cell life, cleaning and re-usability. These were overcome with a few novel, but very simple techniques. Solutions to the engineering problems presented themselves after component testing. The only significant problem that remained by the end of the

project was the life and cost of the air cathodes. If air cathodes were a small fraction of the cost of the battery, they could affordably have a limited lifetime. However, they are still very expensive from the existing suppliers, and the best available cathode can only be used in saline batteries of this type for about 100 hours, roughly equivalent to 5 sets of aluminum anodes of the size used in this battery. Cathode cost is only now beginning to drop with mass production and market competition. Since cathode development was not within the scope of this project, no attempt was made to improve on their performance. Alcan now has an independent cathode development project underway, and preliminary results are promising.

The main body of the report has been broken down to describe several areas of development. In each section, the work is described more or less chronologically, However, in many cases, there was more than one subject area under development at the same time, and hence the subject order in the report is not necessarily chronological.

Every attempt was made in the preparation of this report to cover all of the significant work that occurred throughout the project. However, should more detail be required, the reader can refer to the original unsolicited project proposal, "The Alcan Electric Vehicle Project", CSO: E-005-84, or any of the nine progress reports written throughout the project, CSOR-84/E-005/1 to 4, CSOR-85/E-005/5 to 8, and CSOR-86/E-005/9. These are all under DSS file 15SD.T8200-4-4530. Some or all of these reports may have restricted access pending coverage of proprietary information. These reports also provide a more chronological description of the progress, and several subjects are covered repeatedly over several reports as continuing developments occurred.

2. DISCUSSION

2.1 Background Studies

The first few months of the project were spent as planned on the cell science rather than cell design and engineering. Topics included electrolyte additives, cell chemistry and operating characteristics (using small laboratory aluminum-air cells), and cell thermal and electrolyte management. These last two items continued throughout the project and will be mentioned in later sections of the report as well. The main results and conclusions of the preliminary work are described in the following discussion.

2.1.1 Electrolyte Additives

Formation of alumina gel in aluminum-air cells with NaCl electrolyte limits operating performance and cell life. The obtainable energy density depends

on the NaCl concentration and current density, but under typical "optimum" conditions, it can reach about 0.25 Ah/ml of electrolyte. Gel formation and properties may be changed by chemical additives or mechanical stirring.

An effort was made to control the gel formation using chemical additives of two main types; flocculants, mostly based on polyacrylamide, both anionic and cationic, and secondly, organic anions, which were all complex aluminum ions and were known to stabilize solutions of polybasic aluminum chloride used for water treatment.

The flocculants were intended to prevent the gel from stabilizing by causing the formation of solid aluminum hydroxide particles which would fall out of suspension. Some of the flocculants tested include Percol 728, 727, 512, E10, 455, and 351 (all produced by Allied Colloids). None were successful in significantly increasing the performance or life of the cell. Some did appear to coagulate alumina, but the effect was only noticeable at the beginning of the operation. It appeared that the flocculant material was being used up or adsorbed by the reaction products. Continuous feed of the flocculant may solve this, but at the price of increased complexity and cost.

Organic anions tested included tartrates, oxalates, and formic acid. None of these improved the performance by more than 10%, which is about the level of reproducibility of the tests. Some are detrimental to the performance, creating additional parasitic corrosion or polarization effects.

Other additives tested include dispersants (polyethylene oxide, Dispex N40, Antiprex A, and Antiprex 461), fine alumina (7 micron and 1 micron), inorganic anions (SO4-2, F-), and stannate.

In later tests, aliquots of saturated mercuric chloride were added to the electrolyte in an attempt to created the same effect as having mercury alloyed in the anode. This seemed to generate a small beneficial effect on potential, but the cell life suffered. Mercury was also considered to be environmentally unacceptable, and was not tested further.

One other additive, 0.8 M sodium sulphate, was suggested by Professor A. Despic, an acting consultant to the project. This was tested in both KCl and NaCl electrolytes, and in both cases, performed worse than the electrolytes with no additives whatsoever.

2.1.2 Effect of pH and Stirring on Oxidation Products

In early work, indications were that quiescent cells produced either gibbsite or bayerite as a product of oxidation, whereas "stirred" cells generated pseudo-boehmite. The first two products tend to create cell failure prematurely by choking off the reaction with the gelatinous by-product. On the other hand, pseudo-boehmite forms into small particles which tend to settle out of the active cell area, if allowed to. It was

thought that the stirring action prevented the formation of varying pH layers in the electrolyte, and as a result, produced the desirable pseudo-boehmite by-product. An attempt was made to artificially control pH in order to produce pseudo-boehmite without stirring.

In one case, the pH was adjusted to 1.8, 2.9, 7.1, 10.9, and 12.0 using HCl or NaOH. Pseudo-boehmite was not formed in any case, and the maximum energy density was obtained in the neutral solution.

In another series of tests, the electrolyte was buffered by a 0.5 M solution of CH_3COOH + CH_3COONa or NH_4OH + NH_4Cl. The pH values were 4.0, 5.5, 6.8, 9.0, and 10.0. Again, pseudo-boehmite did not form, and local pH values were quite different than those of the buffers. Apparently, buffers could not prevent the pH changes from occurring at the electrodes. Indications were that pseudo-boehmite would only form if sufficient stirring was applied.

2.1.3 Effects of Electrolyte Temperature and Salt Concentration

Accurately monitored voltage measurements were made at various cell temperatures over a range from 3 to 50 degrees Celcius, with current densities ranging from 10 to 46 mA/cm^2, in salt concentrations from 3 to 20% by weight. These results were generated in a small flowing cell. In general, the voltages fall off as the temperature is reduced below ambient. This fall-off is greatest for 7% NaCl at high current densities. The effect is almost entirely due to a reduction of the anode potential with temperature.

Figure 2 summarises voltage efficiency vs. current efficiency at several temperatures and current densities. It appears that the best overall efficiency is demonstrated in 7% NaCl, although results are somewhat scattered. This is supported further by a plot of power efficiencies at varying temperatures shown in Figure 3. The power efficiency generally falls as the battery temperature is raised and the highest efficiency is found at temperatures below 30 degrees C.

In later tests with stirred electrolyte (to be described in more detail further in the report), the effects of varying salt concentration became even more clear. Table 2, below, illustrates the results of these tests.

There is an obvious increase in electrolyte capacity with increasing salt concentration. Figure 4 demonstrates a relationship between electrolyte conductivity and cell capacity. This suggests that the life of a cell is controlled by the conductivity of the electrolyte and that the cell eventually dies when its conductivity falls below a certain level.

In choosing a salt concentration for optimum performance, all of these factors (potential, electrolyte capacity, efficiency) were considered, and the logical choice was the 12% NaCl, which had only marginally less power efficiency, but substantially more capacity.

Table 2 Effect of NaCl Concentration and KCl in a Stirred Cell at 30 mA/cm^2

	7%NaCl	12%NaCl	20%NaCl	20%KCl
Time to current fall off (hours)	28	33	42	52
Total capacity	0.27	0.34	0.37	0.42

2.1.4 Effects of Stirring the Electrolyte

As has been briefly noted earlier in the report, electrolyte stirring has an effect on the performance and characteristics of the cell. This effect was first pointed out by Professor Despic, who had demonstrated this effect by simply reciprocating the electrolyte up and down with an amplitude of about 10% of cell height and a period ranging from a second or so to several seconds. The chief result of the stirring is the change in reaction product from a gelatinous compound which tends to plug the cell to a granular solid, which seems to maintain fluidity in the cell and improve cleanability.

Small scale cell tests were then carried out with electrolyte reciprocation (reversing electrolyte flow in the cell) and the results are tabulated below in Table 3.

Table 3 Reaction Product Results from Static and Reciprocated Cells

	Static Cell	Reciprocated Cell
Energy Density	0.2 Wh/ml	0.2 Wh/ml
Reaction	Bayerite, gibbsite (Figure 5)	Mainly pseudo-boehmite with minor amounts of bayerite and gibbsite (Figure 6)
Form of Products	Gelatinous, plus hard solids	Early settling precipitate plus liquid
Cell Characteristics	Anode difficult to remove, cell difficult to clean	Anode easier to remove, cell easier to clean
Spent Electrolyte	High alumina content (several percent)	Low alumina content (several ppm)

Although there was no apparent increase in energy density (in terms of electrolyte capacity), there were definite advantages to the stirred cell, chiefly in terms of by-product management and ease of cleaning. Despic's results indicated that reciprocation should push energy density up over 0.3 Ah/ml, but this was not demonstrated in this test. Possible reasons for the discrepancy are Despic's use of a smaller anode/cathode gap and lover quality anodes. Other variations include the possibility of different calculation techniques, such as energy output being calculated from metal consumed, rather than watts produced.

Another test with a smaller anode/cathode gap (about 5mm, as opposed to 7 mm used in the previous tests) produced about 0.25 Ah/ml, slightly more than the first tests, but still substantially less than reported by Despic.

Further experimentation was performed in a flowing cell as shown in Figure 7. With this cell, various frequencies of flow reversal and magnitude of flow rate could be accurately generated. In discharges using a peristaltic pump running at 60_2 ml/minute, with an anode/cathode gap of 3 current density of 30 mA/cm^2, flow in one direction for 1 minute followed by flow reversal for 30 seconds, an energy density of 0.36 Wh/ml was achieved.

Substantial additional work was done with the flowing cell and in some cases, electrolyte capacity reached 0.4 Ah/ml. These results, however, were generated under closely controlled conditions, and are not necessarily reproducible in full scale cells. Some of the most recent work was a comparison of hydrogen generation obtained by running a reciprocated aluminum-air battery at various current densities and various temperatures with hydrogen evolution obtained from operating galvanostatically in an electrochemical corrosion cell. The results from the reciprocated battery are shown in Figure 8, and some from the galvanostatic cell in Figures 9. The hydrogen evolution rate increases with current density and temperature in most cases, and is almost linear. Taking this one step further, by comparing the slopes of all of these lines and other results as shown in Figure 10, it becomes apparent that the hydrogen evolution rate is much higher in the reciprocated battery, particularly at higher temperatures, where it is about three times as great as the galvanostatic cell. The effect of stirring on both disturbing the near-surface electrolyte and enhancing the mechanical break-up of the anode is probably the cause. The alloy type can significantly alter the results, however, since some alloys tend to dissolve along grain boundaries, undercutting small pieces of anode until they fall off (resulting in low efficiency), while other alloys dissolve much more uniformly and do not break up, even in a reciprocated environment. The latter alloy types are the aim of the anode development program. Even with higher hydrogen evolution (lower efficiency), the stirred batteries have better operating performance and longer life than stagnant batteries.

2.2 Single Cell Development

The background work on cell chemistry, additives, and electrolyte management used a variety of aluminum-air cells. Theses include: the "cube" cell, which contained two separate cells, each with an active electrode area of about 20 cm^2; the flow cell, which is really a micro-scale cell with only a few square centimeters of electrode area; and a number of other larger cells with anode/cathode gaps ranging from 3 to 7 mm. This report will describe in detail the development from the first "engineered" cell and its many variations through to the multi-cell common sump prototype battery.

2.2.1 The First Engineered Single Cell

The first cell, which was designed around parameters generated in early tests, was the so-called 60 Ah cell, shown in detailed drawings in Figure 11, and assembled (minus the air cathode for clarity) in Figure 12. This cell was the basis for almost all developments which were generated in this project, with the exception of the concept of the common sump (an assembly of cells operating within one common electrolyte box) multi-cell battery, and one idea that spawned from a later 3 cell common sump battery test.

The performance of the original cell, using electrolyte stirred by reciprocation, is shown in Figure 13 at 25 ma/cm^2. Cell output was about 100 Ah (0.25 Ah/ml not including make-up water) and performance was quite acceptable for a first test.

2.2.2 The First Cell Stack Stirred by Reciprocated Electrolyte

In order to learn more about the operation of the cells, a 3 cell stack of individual cells was set up and discharged at constant current density. Results listed in Table 4 indicate that operating temperature rises dramatically with current density, and that the centre cell, which was operating at a higher temperature than the other two cells, had the highest voltage. However, the higher temperatures also result in a higher water loss. Figure 14 illustrates the data in graphical form. This information led to the decision to go one step further.

Table 4 Behaviour of 3 Cell Stack

C.D. mA/cm^2	End Deg C	Centre Deg C	Wt. Loss gm/hr/cell	Volts End Cell	Volts Centre Cell
5.525	23.0	25	2.7	1.248	1.281
11.050	36.5	42	5.0	1.167	1.220
16.550	46.5	53	10.0	1.105	1.171
22.100	52.5	61	12.0	1.071	1.140
27.600	65.0	75	21.0	0.969	1.104

2.2.3 The 14 Cell Stack (Stirred by Reciprocated Electrolyte)

After evaluating the results of the 3 cell stack, a 14 cell version was built and evaluated. The individual cells were assembled in a row with gaps of about 1 cm between each cell. Reciprocation was generated by a pressure/vacuum pump operating at a frequency of about 15 cycles per minute. This pump alternately pushed/pulled liquid in and out of a separated "leg" at the side of each cell, resulting in the electrolyte level in the cell rising and falling about 1 cm from the mean, and hence creating a reciprocating effect. A large fan was set up off to the side of the cell stack to provide cooling, and the load drawing the power was an electric trolling motor operating in a barrel of water. The battery and test apparatus are shown in Figure 15.

The stack was run for 4.5 hours at the full speed setting before the test ended. Although most of the cells were still operational, 2 had fallen below 0.5 volts due to inadequate stirring. This was the first indication of the difficulty in both providing the electrolyte stirring and maintaining uniformity across all of the cells. With the fan on, temperature of the stack was fairly uniform around 50 degrees C, but with the fan shut off for 10 minutes, the temperature rose to 60 degrees C. Figure 16 illustrates the variation between individual cell voltages, and the two low cells are clearly seen as early as two hours into the test. Figure 17 shows the current efficiencies for each cell, and it should be noted that there is no obvious correlation between efficiency and voltage from these results.

Also generated in this test were the voltage losses in the electrical connections. Although only simple (though logical) connections were used, the voltage loss totalled only 0.4 volts across the whole battery. This represents a 3% voltage loss and was not considered to be significant. The total charge drawn from the stack was only 60 Ah, but sufficient information was produced from this test to carry on development work for many months.

2.2.4 Developments in the Single Cell

The development of the single cell took two somewhat different paths. In Banbury, the effort was concentrated on obtaining the best possible performance from the single cell, with the intention of creating larger batteries from a series stack of individual cells. This effort took aim at optimising areas such as electrical connections and fluid flow/solids settling problems. On the other hand, the Kingston effort was focussed on developing technology to optimise the single cell which could be applied to an integrated multi-cell battery, that is, one that does not consist of a number of single cells, but is a unit within itself. Many of the same problem areas were considered, but from a different viewpoint. As it turned out, the final prototype consisted of the best developments from both locations, illustrating the benefits of this approach.

2.3 Development Work for Optimised Single Cells

Preliminary work on the original version of the single cell identified the areas that could benefit from refinements. In particular, these were the electrical connections and the methods of reciprocating/stirring for longer life and ease of cleaning. Improvements in both areas, along with some additional changes in cell design were achieved in several steps.

Cells were operated with an external reservoir, pump, and low flow air injection for stirring. After some experimentation, 6.0 mm^2 cable was selected and a modified cell design as shown in Figures 18 and 19 was evaluated. Comparative discharge curves are illustrated in Figure 20, and the benefits of the improved connections are evident, especially when current density exceeds 50 mA/cm^2.

All of these cells were tested in 12% NaCl with electrolyte pumped at 250 ml/min with flow reversal of 60 seconds forward and 30 seconds reverse. To improve turbulence, air was bubbled in through a small tube in the bottom of the cell.

Due to pumping and cleaning problems in the earlier versions, the third cell was given a slanted bottom for better electrolyte flow, a sealed lid, and a different electrolyte suction port. The schematic arrangement for this cell is shown in Figure 21. A total discharge was achieved for this cell over a period of 16 hours at a current density of 20 mA/cm^2, and over 190 Ah were obtained before the anode was totally consumed. (It should be noted that with an outboard reservoir system, excess electrolyte is provided, and as a result, the anode can dissolve completely before the electrolyte capacity is exceeded. By not pushing the electrolyte capacity to the limit, cell cleaning is easier due to the lower concentration of solids).

The cell was completely cleanable after the run, and the by-product was found to be mainly pseudo-boehmite.

2.4 Single Cell Development Towards the Common Sump Battery

With the experience of the 14 cell stack test, it was realized that one of the main weaknesses in the technology was the method of "stirring" in order to prevent the formation of gelatinous by-products which would result in premature cell failure. The electro-mechanical device used in the 14 cell stack test was cumbersome, inefficient, and non-uniform across the cell stack. There were other problems to be resolved as well, such as cell cooling, hydrogen handling, cell cleaning, and solids management. These problems were considered while keeping in mind the goal of the integrated battery, that is, a multi-cell battery contained in one simple assembly. This created additional difficulty, since the objective necessitated the optimising of almost all parameters, especially the discharge capacity

available from the electrolyte (Ah/ml), in order to keep the unit self-contained and within a minimal volume. One other objective was to keep the parasitic power requirements as low as possible, as the battery was intended to be self-supporting. This steered the development as much as possible away from pumps, fans, and other ancillary equipment.

The milestones set for the development were discharges of 100 Ah at a peak current density of 50 mA/cm^2 between electrolyte changes, and 300 Ah total from each anode without disassembly for cleaning or replacement.

2.4.1 Full Development of Air (Gas) Injection Technology

Air bubbling at low flow rates had been demonstrated as a good method of achieving cell stirring, but it was realized that, at higher flow rates and in appropriately designed cells, this could be taken several steps further in order to provide cooling, dilute the produced hydrogen, and even generate circulation currents (like pumping) within the cell. These developments occurred over many single cell tests, and a condensed description of the technology and its development follows.
The results of 54 single cell tests are presented in Table's 5, 6, 7, and 8. The tests from 1 to 43 represent the majority of the development on the air injection technique and the related cell design, while tests 44 to 54 are related to anode and cathode evaluation and are not relevant here. (A total of 82 tests were run during the project, the last 40 or so related mostly to anode and cathode evaluation.)

It is important, when reviewing this data, to note that the "cell life" referred to in the Tables or in the text does not necessarily indicate that the cell "died" after this amount of discharge. In some cases, the cells were shut down at a discharge of about 100 Ah to determine their cleanability at this point. In other cases, a minimum voltage of 0.85 V (the minimum average cell voltage for 14 cells to produce 12 volts) was used as the criteria for "failure". Generally, when the cells were stopped, either due to reaching desired discharge or minimum voltage, they could have continued producing useful energy for some time.

The optimised design of the single cell, upon which was based the first construction of the common sump battery, is summarised as follows:

(a) The gas injection system consisted of a T-shaped tube (Figures 22 and 23) extending up from the bottom of the cell. The cross tube was suspended just below the active area of the cell in order to improve circulation and reduce the chance of plugging the bubble holes. The bubble holes were located 45 degrees either side of vertical in the lower half of the tube. The holes were 0.63 mm (0.025") diameter and were drilled in opposing pairs in 5 equally spaced positions along the tube. Air injection rate for this size of cell was found to be best around 1 liter/minute. This rate provided adequate turbulence,

Table 5 Single Cell Performance Test Results

Exp #	Cell Type	Air Cath	Al Anode	Load (Ohm)	Air Inj. (4Min)	Performance									Comments
						Act. Time (Min)	Max Volt. (Volts)	Time To Max (Min)	End Volt. (Volts)	Ave. Volt. Volts	Test Dur'n (H)	Cell Life (A-H)	Cell Eff. (%)	Max Temp (°C)	Clean (0-10)	
1	S	Hur	Buk	0.1	0.5	5	1.01	15	0.96	0.97	6	58	65	41	9	
2	S	Hur	Buk	0.05	0.75	1	0.93	1	0.49	0.79	4.5	70	52	50	5	
3	S	Hur	Buk	0.1	0.5	3	1.03	22	0.68	0.98	7.0	69	62	39	2	
4	S1	Hur	Buk	0.1	0.75	3	1.03	5	0.95	0.96	7.0	68	67	36	7	
5	S1	Hur	Buk	0.05	0.6	No	0.80	50	0.68	0.77	4.8	77	60	49	10	
6	S1	Hur	Buk	0.1	0.75	4	1.00	40	0.83	0.95	9.2	88	67	36	10	
7	S1	Hur	Buk	0.1	0.75	7	0.97	90	0.88	0.95	10.5	99	69	37	10	
8	S2	Em	Buk	0.1	1.0	2	1.14	60	0.76	1.01	8.1	81	55	41	0	
9	S1	Em	Buk	0.1	1.0	1	1.13	40	0.68	1.07	14.2	155	63	35	1	
10	S1	Hur	Buk	0.1	1.0	2	1.09	70	0.90	1.03	10.5	108	60	35	10	
11	S1	Em	Buk	0.1	1.0	1	1.19	60	1.08	1.12	9.0	101	58	38	8	
12	S1	Hur	Buk	0.1	1.0	1	1.12	60	1.02	1.07	9.3	100	66	36	0	
13	S1	Hur	Buk	0.1	None	2	1.10	38	0.85	1.00	5.5	55	55	47	10	
14	S1S	Hur	Buk	0.1	1.0	3	1.12	58	0.86	1.01	12.6	128	63	40	9	
15	S1S	Hur	Buk	0.1	1.0	1	1.11	56	0.85	1.02	12.5	128	59	40	2	
16	SS	Hur	Buk	0.1	1.0	1	1.06	56	0.88	1.01	11.0	111	63	38	9	
17	S2	Hur	Buk	0.1	1.0	1	1.11	23	0.99	1.04	10.7	111	62	39	8	
18	S2	Hur	Buk	0.1	1.0	2	1.06	35	0.93	1.01	10.0	100	63	37	10	18,19,20 are triple
19	S2	Hur	Buk	0.1	1.0	1	0.94	15	0.85	0.90	8.8	79	63	34	2	Test, Hence one efficiency

Table 6 Single Cell Performance Test Results

Exp #	Cell Type	Air Cath	Al Anode	Load (Ohm)	Air Inj. (4Min)	Performance										Comments
						Act. Time (Min)	Max Volt. (Volts)	Time To Max (Min)	End Volt. (Volts)	Ave. Volt. Volts	Test Dur'n (H)	Cell Life (A-H)	Cell Eff. (%)	Max Temp (°C)	Clean (0-10)	
20	S2	Hur	Buk	0.1	1.0	5	1.01	55	0.86	0.96	9.8	94	63	35	9	
21	S2	Hur	Bdw	0.1	1.0	53	0.88	93	0.85	0.82	6.8	55	70	40	6	Test of Caustic Alloy in Salt Elect.
22	S2	Hur	Xab 05	0.1	1.0	2	1.05	20	0.96	1.02	10.1	103	67	40	10	Production Alloy
23	S2	Hur	Xab 05	0.1	1.0	4	1.07	26	0.66	0.95	15.4	146	67	44	7	Production Alloy
24	S2	Hur	Bun	0.05	1.0	41	0.87	240	0.85	0.82	11.6	95	75	46	9	
25	S2	Hur	Buk	0.05	1.0	3	0.95	82	0.86	0.90	14.3	129	61	55	9	
26	S2	Dc	Clg	0.05	1.0	4	0.93	75	0.86	0.87	7.8	135	85	51	10	
27	S2	Dc	Buk	0.05	1.0	1	0.95	140	0.82	0.90	7.2	128	63	59	10	
28	S2	Hur	Clg	0.05	1.0	1	0.93	30	0.84	0.90	6.92	123	79	50	8	
29	S2	Hur	Clg	0.1	1.0	1	1.05	25	0.99	1.02	10.1	103	78	39	9	
30	S2	Hur	Clg	0.05	1.0	None	N/A	N/A	N/A	N/A	N/A	N/A	N/A	N/A	N/A	Did not activate
31	S2	Hur	Clg	0.05	1.0	1	0.91	12	0.89	0.89	2.9	51	74	52	9	31 and 32 are consecutive
32	S2	Hur	Clg	0.05	1.0	19	0.87	60	0.83	0.84	6.75	114	74	50	9	Hence same Eff. for both
33	S2	Hur	Clg	0.05	1.0	7	0.88	22	0.84	0.86	5.4	92	78	47	10	Continuation of 31 and 32
34	S2	Em	Clg	0.05	1.0	2	1.01	5	0.89	0.96	7.2	138	70	50	10	34,35, and 36 are consecutive. Hence same efficiency
35	S2	Em	Clg	0.05	1.0	1	0.96	9	0.89	0.92	4.4	81	70	45	10	

Table 7 Single Cell Performance Results

Exp #	Cell Type	Air Cath	Al Anode	Load (Ohm)	Air Inj. (4Min)	Performance										Comments
						Act. Time (Min)	Max Volt. (Volts)	Time To Max (Min)	End Volt. (Volts)	Ave. Volt. Volts	Test Dur'n (H)	Cell Life (A-H)	Cell Eff. (%)	Max Temp (°C)	Clean (0-10)	
36	S2	Em	Clg	0.05	1.0	1	0.94	14	0.86	0.90	5.2	94	70	45	10	
37	S2	Em	Clg	0.05	1.0	1	1.01	19	0.91	0.96	5.0	96	68	48	10	
38	S2	Hur	Clg	0.05	1.0	1	0.97	14	0.87	0.92	5.6	103	73	48	10	New Huron Cath. from here on
39	S2	Hur	Clg 05	0.05	1.0	1	0.91	44	0.88	0.89	6.1	107	79	46	10	39 & 40 are consecutive tests
40	S2	Hur	Clg	0.05	1.0	18	0.89	800	0.86	0.85	5.2	88	79	46	9	
41	S2	Em	Clg	0.05	1.0	1	0.98	15	0.88	0.92	6.53	119	72	47	10	41 & 42 are consecutive tests.
42	S2	Em	Clg	0.05	1.0	1	0.93	35	0.86	0.89	2.2	39	72	45	10	
43	S2	Em	Clg	0.05	1.0	1	0.99	210	0.85	0.93	4.6	86	70	46	10	
44	S	Hur	Buk	0.1	None	1	1.15	18	0.84	1.07	4.7	51	54	54	1	Anode/cathode tests
45	S	Hur	Clg	0.1	None	1	1.10	15	0.80	0.97	4.5	44	74	47	1	Andoe/cathode tests
46	S2	Em	Buk	0.05	1.0	1	1.04	15	0.83	0.97	6.8	131.4	57.6	54	7	Anode/cathode tests
47	S2	Em	Clg	0.10	1.0	1	1.14	1	1.04	1.09	10.0	109	75.5	39	10	Anode/cathode tests
48	S	Hur	Xab 05-A	0.10	None	1	1.04	22	0.87	0.96	4.7	45	65	32	2	Anode tests re heat-treatment
49	S	Hur	Xab 05-B	0.10	None	1	1.01	16	0.79	0.91	4.7	43	64	31	2	Anode tests re: heat-treatment
50	S	Hur	Xab 05-C	0.10	None	1	1.06	16	0.85	1.01	4.7	47	65	26	2	Anode tests re: heat-treamtent
51	S	Hur	IOI -F	0.10	None	1	1.03	28	0.84	0.97	6.2	60	64	30	2	TB[2] abide tests efficiency

Table 8 Single Cell Performance Results

Exp #	Cell Type	Air Cath	Al Anode	Load (Ohm)	Air Inj. (4Min)	Performance									Comments
						Act. Time (Min)	Max Volt. (Volts)	Time To Max (Min)	End Volt. (Volts)	Ave. Volt. Volts	Test Dur'n (H)	Cell Life (A-H)	Cell Eff. (%)	Max Temp (°C)	Clean (0-10)	
52	S	Hur	IOI -B	0.10	None	1	1.02	18	0.71	0.95	6.2	59	79	34	2	TB^2 anode tests
53	S	Hur	IOI -M	0.10	None	3	1.01	20	0.80	0.94	4.2	39	75	35	2	TB^2 anode tests
54	S2	Hur	Xab 05-C	0.05	1.0	2	0.94	5	0.83	0.88	6.2	110	67	51	9	

circulation, and heat removal for most operating conditions. Air injection provided more than double the life and higher voltage than a stagnant cell while also making cleaning possible with water flushing.

(b) The cell had two recirculation paths, one on each side of the electrode area. A baffle between the active area and the return path extended from below the air tube (to catch any stray bubbles and direct them up the active side) to slightly above the top of the active area. this recirculation technique apparently added an additional 25 - 50% usable life beyond having air injection alone, while also providing additional improvement in the ease of cleaning.

Some of the individual single cell tests such as 23, 26, 27, 34, 41, and 46 were taken well beyond the 100 Ah goal. These durations, in the range of 130 - 150 Ah, represent the maximum life expectancy while maintaining good cleanability with this system. Hence, electrolyte discharge capacities of 0.3+ Ah/ml are achievable in an easily cleanable cell design.

2.5 Development of the Multi-Cell Common Sump Battery

Two of the main objectives in this project were: to package technology and build a hybrid battery system for a vehicle, and; to test and demonstrate the potential of the aluminum-air battery as a "range extender" and a recharger for an electric vehicle. In order to achieve these objectives, it was necessary to design and build a battery that could operate in these conditions. The battery had to be practical in order to allow for sensible evaluation, and also to demonstrate that aluminum-air technology could be packaged so that anyone could operate it with only modest instruction. These objectives helped focus the idea of the integrated multi-cell battery, preferably contained in a simple battery case and assembled with logical, effective components.

2.5.1 The Common Sump Multi-Cell Battery Concept

The original design concept for the multi-cell common sump battery, where all the anodes and cathodes share a common sump, is covered in U.S. Patent number 4,626,482. At this early stage, very little was known about the operating parameters required, or for that matter, whether a common sump battery was feasible, considering it had only been tested in a 2 volt battery. It was assumed that some form of stirring would be required, that heat needed to be removed, that hydrogen would have to be safely vented, sealed electrical connections would be required, and electrolyte would have to be drained.

The concept was based on the need for simple assembly and replaceable components. The basic unit was the "air cathode cassette" shown in Figure 24. This consisted of a narrow rectangular box with fins on the bottom and both sides to separate individual cells (fins only shown on bottom in sketch). Each side of the cassette had a separate air cathode sealed into

place. A series of 15 of these cassettes would slide into the lid, Figure 25, using a dovetail assembly. The lid and cathode cassettes, together as one unit, would then be inserted into the main battery box, Figure 26, with each air cathode cassette falling between two aluminum anodes. The aluminum anodes would be held in proper position in a rack (Figure 27), which would be lifted out of the box as one unit for ease of cleaning and assembly.

This concept was an "inside-out" version of the original single cell. Rather than containing the anode and electrolyte inside the narrow cell, which can create some difficulty in mechanical recharging and cleaning, the electrolyte was contained within the main battery box, surrounding the anodes but remaining outside the air pockets formed by the air cathode cassettes. The only apparent disadvantages of this design were the necessity to seal the electrical connections where they penetrated the box, and the possible need to feed air into the air cathode pockets due to their top open only design.

2.5.2 Shunt Current Tests on the Common Sump Design

The feasibility of the common sump design depended on minimizing shunt currents between the cells. Because each cell operates at about a 1 volt higher or lower voltage than its neighbour (due to the series connection), there is a natural potential for current to flow from cell to cell through electrolyte paths, generating heat and wasting useful energy. In the common sump design, there was a small clearance between the edge of the fins and the common sump box through which the current could pass. It was hoped that the cross-sectional area of this clearance was small enough, and the lengthened electrolyte path between the active area of each cell (due to the fins) was long enough, to render the shunt current between cells insignificant. It should be noted at this point that a tightly sealed cell design was considered, but it was concluded that this would very quickly become difficult, if not impossible to re-assemble due to the build up of the ever present by-product.

A test apparatus was built to evaluate the shunt current situation. It consisted of a simple model of the common sump box, with 15 sliding plastic dividers as shown in Figure 28. A 14 volt potential was applied with 12% NaCl electrolyte in the box, and the current flow was measured at 65 mA, an insignificant amount. In order to simulate improper battery assembly, each divider was lifted 3 mm off the bottom of the sump, and the current was then measured at 600 mA. Although this value was greater, it would only exist in a severely misassembled battery, and would not significantly affect the battery performance. Similar tests were performed on adjacent cells using a potential of 1.2 V, and similar results were found. Based on these results, the design was considered to be quite safe from deleterious shunt current effects around the cell dividers.

2.5.3 Shunt Current Tests on the Common Manifold/Common Sump Design

The next feature introduced to the common sump multi-cell battery was the common manifold. This manifold is simply a reservoir spanning the length of the battery with tubes for electrolyte connection to each cell (between dividers inside the battery box). This manifold was designed for several purposes. First, it would provide one point for supplying make-up water to all cells (to replace water lost due to evaporation through the cathodes and saturated in the exhaust gas). Secondly, it would maintain an equal electrolyte level in each cell by pressure equalisation. Thirdly, it would provide one common connection through which the battery could be filled with electrolyte to begin operation, or to be flushed with water for cleaning after operation.

However, it was realised that such a manifold would create another electrolyte path between cells, possibly resulting in shunt current losses. Therefore, another apparatus was set up to evaluate this concept, as shown in Figure 29. Various tube lengths were used to determine the minimum acceptable length, and 12 cm was found to be optimum in terms of shunt currents and practicality. Table 9 presents the results both with and without the common side manifold. The shunt current increased from 65 mA in the common sump box only, to 150 mA with the common manifold attached. These results were very promising, not only confirming that a common side manifold was feasible, but also suggesting that the addition of another common manifold on the exit ports could be added, generating a total shunt current of only about 250 mA, a very acceptable figure.

2.6 Setting Prototype Battery Parameters

Having considered the project scope and objectives, the following specifications were set as realistic goals:

- 12 Volts minimum potential
- 20 Amperes peak current
- 100 Ampere-hours minimum between electrolyte changes
- 300 Ampere-hours between anode replenishment
- flush cleanable without disassembly
- no "on-board" processing of by-product (self-contained)
- gas injection for agitation, cooling, and hydrogen dilution
- easy assembly/disassembly for anode change

It should be noted that these design specifications were set before they had actually been accomplished, and as a result, they helped continue the push towards better performance.

2.7 Development of the 12 Volt Prototype Battery With Computer Aided Design and Drafting

Due to the changing nature of the prototype design, it was decided that the use of Computer Aided Design and Drafting (CADD) would be extremely beneficial in this project. Alcan's Engineering Division in Montreal was

Table 9 Shunt Current Tests

Condition	No. of Cells	Potential (volts)	Shunt Current (milliamps)
Dividers Down	14	14	65
One Divider up 3 mm	1	1	150
All Dividers up 3 mm	14	14	600

Common Sump Battery With Side Manifold

(12 cm Connections)

Condition	No. of Cells	Potential (volts)	Shunt Current (milliamps)
Dividers Down	14	14	150
One Divider up 3 mm	1	1	200
All Dividers up 3 mm	14	14	700

equipped with a full mainframe CADD system, and their facilities were used extensively in this area. Over the course of the project, four generations of CADD prototype designs were produced. The first three versions were generated as development of the single cell battery progressed. As new ideas were proven, they were incorporated into the CADD design. Since these ideas were developed in the single cell, the CADD provided an opportunity to evaluate, in 3 dimensions, their inclusion into the multi-cell design, often resulting in substantial modifications, since the multi-cell unit was an "inside-out" version of the single cell. The final CADD was produced after construction and testing of a 3 cell common sump unit, both of which will be described in later sections of the report.

2.7.1 CADD Design Three

After producing the first two developmental versions of the CADD design, the third generation CADD is shown in Figures 30 to 37. This version contained a much higher degree of engineering as opposed to conceptual design, and the result was a tightening up of dimensions which produced a battery with clean, simple lines and effective inclusion of the required technology.

Figure 30 shows the basic common sump battery box. There are no grooves or hanger protrusions on the inside to create area of by-product agglomeration. The box is back to the flat bottom design, which had proven to be more effective than slant bottom for the self-contained by-product, and made more effective use of space. One additional advantage of the flat bottom is that the air cathode cassettes could be designed as identical halves, resulting in only one mold for manufacturing, rather than the slant bottom which required left and right halves. The inlet and exit manifolds, Figure 31, were designed to be integral assemblies which could be molded as one piece.

The anodes, shown in Figure 32, are designed to be inserted from the side into spaces between the air cathode cassettes, before the cassette assembly is dropped into the battery box. This would allow assembly as a unit, without having to drop the anodes in one by one. This also eliminated the problem with having to deal with two sets of holes in the inner lid, one set to the cathode cassettes and the other set to the cells where the anodes were dropped through. The only disadvantages were that the cassettes had to be removed for anode change, and the anodes themselves were an odd shape with a "dog leg" tab, which would result in some extra wasted metal in manufacturing.

Figures 33 to 37 illustrate the rest of the battery assembly. The air cathode cassettes incorporated vertical bars on each side of the cathode area, with elevated tabs on the top and bottom of the bars. When assembled, the tabs on the bars on adjoining cassettes were pressed against each other, leaving a gap exactly the same size as the anode cross-section. With the anode inserted, the gaps were filled, forming baffles which contained the injected air bubbles and rising electrolyte. In this

version, the air injection tubes entered the cells from the side (the "T" tubes extending from the bottom had not yet been developed), and the holes in the tube were all located in the area within the electrode width, so that they did not bubble up the return legs in the side. The baffles had not yet been designed to enclose the tube.

2.8 Feasibility Testing of the Multi-Cell Common Sump Battery: The Three Cell Version

2.8.1 Design

The single cell had been the basis for development throughout the project, with the exception of the shunt current tests. All of the developments had been designed into the common sump multi-cell battery on paper, but it had not been demonstrated that this concept would actually work. In order to design an optimised 14 cell (12 volt) battery, it was decided that the concept would be proven and de-bugged on a 3 cell version of the same design.

The design is shown in machine drawings in Figures 38 to 41, and is basically the same as the third CADD design with the exception of the "T" type air injection tube, the extension of the side baffles to enclose the injected air within the electrode area, and the addition of another manifold to collect and vent the injected air/hydrogen.

As expected, the cathode cassette , Figure 38, was made from two identical halves, with the cathode mounted on the inside of the cassette to keep the electrical connections away from the electrolyte. The end view, Figure 40, illustrates the layout of the rest of the battery. All three of the "T" type air injection tubes were fed from a common manifold located directly under the centre of the battery floor. The side and exit manifold remain the same as in the CADD version. On top of the inner lid is another manifold which collects the exhaust gas (the injected air plus hydrogen) and vents it all through one port. This manifold also serves a second purpose by acting as a water flush manifold during cleaning (without disassembly). The holes through the inner lid into the manifold are cut so as to act as linear nozzles, providing a wide spray to clean as much of the electrode area as possible. One other point that becomes obvious at this point is that the multi-cell design has "dead" ends, that is, the air cathode cassettes at each end of the battery have one side that is not active. This was considered in the design stages and it was decided that it was best to be left this way since making different cassettes for the end cells would add complexity and cost. The solution was to simply insert a plastic blank in place of the air cathode on the outer side of the end cassettes to avoid the waste of the expensive air cathode material.

2.8.2 Construction

The battery was fabricated by the Kingston Laboratories' machine shop in order to ensure high quality and observe the progress regularly in case

design modifications were necessary. The plastic composition used was clear acrylic, definitely not a production material, but very machinable, easy to see through, and proven many times over in single cell tests. The ability to visually inspect the battery before and during operation was considered to be vital to performance evaluation.

2.8.3 Performance Testing

The arrangement for the 3-cell common sump battery test is shown in Figure 42. In the first two runs, problems were encountered with electrolyte leakage and lack of fresh air in the cathode cassettes. The leakage was due to an assembly oversight, but the air supply problem in the cathode cassettes was related to the "pocket" design. Although air circulation had been considered as a potential problem with this design, it was not expected to be so evident at the relatively low current densities.

Having identified this problem, tests 3, 4, and 5 were run with air continuously supplied to the cathode cassettes at about 1 litre per minute. Run number 5 is typical of these three tests and the discharge results are shown graphically in Figure 43. The results from all three tests are illustrated in tabular form in Table 10. In all three cases, the performance was excellent, and a total charge of 310 Ah was produced over the three tests (without disassembly - only water flush cleaning), exceeding the project goal of 300 Ah with the same set of anodes. Even at the end of the third test, the battery was still delivering an average of 0.91 V per cell, well above the minimum of 0.85 V.

The time and expense of interposing the 3 cell version on the way to the multi-cell design as a proof of concept phase was considered to be worthwhile. The identification of the one "bug" avoided a very simple, but very serious flaw in the final prototype battery.

2.9 The Final 12 Volt Prototype Battery

2.9.1 Design

Having identified what appeared to be the only serious flaw in the 3 cell battery test, the final design incorporated a modification to the air cathode cassettes and battery cover which would provide air flow to the cathodes with natural convection or, if necessary, with a very low power fan. However, the design modifications did not stop there. When the side loading anodes had been considered in previous designs, it was thought that dropping the complete cassette assembly into the box with the anodes in place would be the most effective method of assembly. It was unexpectedly found to be difficult to keep the cassettes from fanning out with the anodes in place, making insertion into the box difficult. It was also recognized that partial disassembly should not necessarily be required just to replace the anodes. Therefore, the final design also incorporated features to allow for top loading anodes.

Table 10 Three-Cell Common Sump Battery Performance Results

Exp #	Cell Type	Air Cath	Al Anode	Load (Ohm)	Air Inj. (4Min)	Performance										Comments
						Act. Time (Min)	Max Volt. (Volts)	Time To Max (Min)	End Volt. (Volts)	Ave. Volt. Volts	Test Dur'n (H)	Cell Life (A-H)	Cell Eff. (%)	Max Temp (°C)	Clean (0-10)	
M-3	Mc-3 29/4	Em	Clg	.171	3.0	1	1.04	14	0.94	0.97	4.5	78	N/A	59	10	Front Cell
						1	1.04	20	0.94	0.97	4.5	78	N/A	62	10	Middle Cell
						1	1.04	18	0.98	1.01	4.5	78	N/A	61	10	Back Cell
						1	3.12	16	2.85	2.98	4.5	78	N/A	N/A	N/A	Total Battery
M-4	Mc-3 30/4	Em	Clg	.171	3.0	1	1.03	20	1.01	1.013	6.5	111	N/A	61	8	Front Cell
						1	1.00	20	0.87	0.95	6.5	111	N/A	64	8	Middle Cell
						1	1.01	10	0.93	0.96	6.5	111	N/A	61	6	Back Cell
						1	3.04	20	2.82	2.921	6.5	111	N/A	N/A	N/A	Total Battery
M-5	Mc-3 1/5	Em	Clg	.171	3.0		1.04	22	0.99	1.00	7.4	121	59	62	9	Front Cell
						3	0.94	22	0.81	0.88	7.4	121	59	63	9	Middle Cell
						3	0.99	17	0.93	.911	7.4	121	63	57	7	Back Cell
						3	2.96	22	2.74	2.79	7.4	121	59.9	N/A	N/A	Total Battery

The basic change to allow air circulation in the cathode cassettes was the inclusion of air intake channels formed in the frame on either side of the cathode. This can be clearly seen in Figure 44, both in the front and top view. In order to create a convective circulation effect, the air intake channels had to be separated from the main cassette air pocket. As illustrated in Figure 45, this was achieved with baffles in the battery cover on each side of the battery, forming air intake manifolds within the cover. The main air pocket in the cassette was vented directly through the top of the cover to the environment. When the battery is operating, heat transfer takes place through the air cathodes, warming the air in the cassettes. As the air is heated, it rises out of the battery through the cover. As this occurs, fresh, cooler air will be drawn through the intake vents in the sides of the battery cover and down through the air channels into the cassettes. The baffled chambers on each side of the battery cover have holes which mate exactly with the air channel holes in the top of the cathode cassettes, thus preventing the fresh air from mixing with the gasses (injected air and hydrogen) within the battery itself.

The top loaded anode no longer has the "dog leg" tab, but rather the tab comes straight up from one edge of the anode. Substantial modifications to the inner lid were made to allow for the top loading anode. The inner lid has two sets of slots, one set for the cathode cassette air to rise out through, and a second, wider set for the anodes to drop through. Since the anodes have to be sealed within the battery to minimize water loss and prevent battery gasses from escaping freely, a second plastic cover slides over the inner lid. This cover seals over the holes where the anodes penetrated, but allows clear passage from the air cathode cassette pockets. Small holes, shaped like linear nozzles, are cut through this cover over the anodes, but are themselves covered by the exhaust manifold. This allows battery gasses to exhaust in a controlled fashion through the exhaust manifold. Vertical baffles on the cathode cassettes which divide the active and return electrolyte areas have the inside corners cut out to hold the anode in place as shown in Figure 50.

One other modification was made to the air cathode support frames which are glued, along with the cathode, to the inside of the air cathode cassette halves. These frames are simply a series of plastic bars with elevated sections at intermittent points as shown in Figure 46. Although these frames are thin and made of plastic, when the cassette halves are assembled, the elevations on opposing frames touch as illustrated in Figure 47, thereby supporting each other against the liquid pressure exerted by the electrolyte. Not only does this drastically reduce the chance of leaks due to adhesive failure, but it also almost eliminates "boving" of the cathode under electrolyte pressure, which can result in increased anode/-cathode gap and hence lower performance.

Partial side views of this design are shown in Figures 48 and 49, and a cutaway top view is shown in Figure 50. Handles have been added onto the inner lid, both to allow easier assembly/disassembly and to add structural support over the length of the inner lid.

The final 12 volt prototype aluminum-air battery design is thoroughly illustrated in the CADD photographs shown in Figures 51 to 63. These computer drawings are identical to the fabricated battery.

Figure 51 shows one half of a cathode cassette. The air channels on both sides of the cathode area are quite evident. The cutouts on the bottom fin are only included in the end cells, and are there to allow easier draining of the electrolyte from the "dead" ends of the battery. Shunt current is obviously not of concern on the ends.

Figure 52 shows an anode in place against one air cathode cassette. Note how half the thickness of the anode (at the edges) is contained within the side baffles. The anode would become fully contained with the neighbouring cassette beside it. The anode rests on tabs below the air cathode.

Figure 53 shows a cutaway view of the basic battery box. The side and exit manifolds which attach to the box are shown in Figure 54, and the air manifold, "T" tubes, and exit manifold (directly under the air manifold) are seen in Figure 55. The complete battery box with manifolds and tubes is shown in Figure 56.

The whole inner lid assembly is shown in Figure 57. Note here that the exhaust manifold now covers the small centre slots and the handles/-structural braces are in place. The cover plate holding the exhaust manifold slides from the end and is held in place by tabs extending from the handles.

Figure 58 shows a cutaway view of the battery top cover. The top plate has been removed to illustrate the operation of the air cathode venting system. The sidewall on the near side is removed to show the baffle and the holes in the bottom of the manifold which mate with the air channels in the cassettes. On the far side, the side plate is seen with ventilation holes through which fresh air is drawn to feed the cathode cassettes.

Figure 59 shows a cutaway of the assembled battery. The cassettes, inner lid, sliding lid cover, and handles are clearly seen. Since the anodes and connections cannot be seen in this view, an exploded cutaway view is shown in Figure 60. The anode tabs and cathode wires are seen extending out from the top of the battery. In this case, the cathode connections are brought up through the air cathode pockets, but in future batteries, the cathode connection would likely be molded into the plastic cassette frames. This exploded view also provides a good view of the other features previously described.

The complete battery is shown assembled in Figure 61. All ventilation holes to the environment are now evident, the ones on the sides being cathode intake air, and on the top spent cathode air exhaust. The small round hole in the centre of the cover is the vent for the injection air and hydrogen mixture. The hydrogen is diluted by the injection air to a level

below 1%, well below the lower explosion limit of 4% (based on calculations and confirmed by measurement). This vent could be brought out through one end of the battery, if desired. Being a prototype, the cover is simply held in place with elastic rings stretched from the battery handles to the tabs in the cover.

Figures 62 and 63 are photographs of the the actual constructed battery, assembled and ready for operation. The weight breakdown of the final prototype battery and its auxilliary components is outlined in Table 11.

2.9.2 Bench Test of the Prototype Battery

Before testing of the prototype battery on board the electric vehicle, it was decided to perform a fully instrumented bench test over a three successive day, 300 Ah total discharge. The test apparatus, shown in Figure 64, illustrates the overall layout, including data logging computer system and the 12 volt power supply which was driving the air pump. The air pump could have been driven by the battery itself, with a parasitic current draw of about 2 A (10% of the peak current capacity of the battery), but for accuracy in measuring performance, it was powered separately in this case.

The bench test results pointed out two new problems. The first was that the air manifold did not distribute air uniformly over all 14 cells. This was improved somewhat by pulsing the flow into the manifold, creating pressure waves, but was only demonstrated manually and could not be done constantly throughout the test. As a result, those cell which were receiving low or no air injection dropped in voltage faster and were much more difficult to clean. This problem was drastically improved in the third run by introducing the air injection from both ends of the air manifold. Since the air pump was a reciprocating type, pressure pulses were created within the manifold itself from the meeting of the two pressure fronts at the middle of the manifold. As a result, air distribution was much more uniform and performance and cleanability were both vastly improved.

The second problem was more significant, yet not a function of the battery design or technology. During the first day of testing, it was noticed that some of the air cathodes were weeping, allowing liquid to seep through the membrane into the air pocket. This resulted in two problems. First, the liquid contact with the metal grid within the cathode began to corrode the grid, as noted by the green colour of the corrosion product. This would eventually lead to cathode failure, assuming the cathode had not exceeded its useful life first. However, more significantly, when the seepage through the cathodes allowed the liquid to fill the air pocket to the cathode level, a short circuit was created across the air pocket from one cathode to the other (since cathodes in the same air cathode cassette are operating different cells). This short circuit not only created performance losses, but also corroded the metal grid in one cathode at the expense of the other. This caused rapid deterioration of the "sacrificial"

Table 11 Electric Vehicle Weight Breakdown

Vehicle Wt. - No. Batteries	87 kg
One 100 AH Lead-Acid Battery	41 kg
Vehicle Plus two 100 AH Batteries	169 kg
One 30 AH Lead-Acid Battery	10 kg
One 100 AH Al-Air Battery (Acrylic)	17.6 kg
Air Pump and Make-up Water (per battery)	2.5 kg
Modified Vehicle Wt.	
Instrumentation, Pumps, Battery Tray, etc.)	142 kg
With 2-30 AH Lead-Acid Batteries	142 kg
With 2-100 AH Al-Air Batteries	180 kg

cathode, and in a short time a hole was generated through it, since without the grid there was no structural support against the head of electrolyte. This resulted in the need to disassemble the battery after the second test to replace a number of the cathodes. However, in the third test, two more cells failed by the same mechanism. The cathode manufacturers are aware of the problem, and claim that it can be overcome. By project completion, no replacement cathodes had yet been received or tested. However, Alcan had begun an air cathode development and analysis program, and preliminary results are promising.

Considering these cathode failures, the battery performed very well, generating discharges of 97, 97, and 88 Ah on each day for a total of 282 Ah (just slightly short of the 300 Ah goal) and 3570 Watt-hours. The assembly worked very well in practice, and only required the addition of gasketing in certain areas in order to operate on a moving vehicle. With the exception of the cells that did not receive sufficient air injection in the first two runs, the battery was cleanable with water flushing. The voltage was well above the 12 volt minimum for the first two tests, and operated above 10 volts throughout the third test with two cells completely flooded.

The detailed performance results are presented in Figures 65 to 68. Figure 65 illustrates the battery performance on one of the three days of testing. The discharge curves are fairly smooth, and are typical of all three tests. The individual cell voltages for the same test are shown in Figure 66.

Figure 67 shows the individual cell temperature curves for the same day. In all three tests, the end cells were significantly cooler than the others, which were quite uniform. The average operating temperature at this current density (around 40 mA/cm^2) was about 60 degrees Celsius. On the third day the temperature fell off somewhat as several of the air pockets filled with electrolyte and shut down.

Figure 68 shows the voltage and current performance over the three days of testing. There is a marginal drop in performance from day 1 to day 2, and a more significant drop in day 3. The larger drop is a direct result of the flooded air pockets, and is not representative of the potential battery performance with proper air cathodes. In a side test, the battery was found to be able to peak at well over 30 amperes at about 12 volts. It is also projected that the battery could produce up to 150 Ah in a single discharge and still be cleanable, providing suitable air cathodes were used.

2.10 Selection of the Electric Test Vehicle

While the battery development was ongoing, so was the search for a vehicle to effectively demonstrate the hybrid range extender concept using a combination of aluminum-air and lead-acid batteries. After considering several electric vehicles, one that was considered to be ideal in size and

nature was a 24 volt one person golf cart, known as a "Batricaddy" and produced by a British company called Batricar. The basic specifications are as follows:

Wheelbase	95.3 cm
Track	73.7 cm
Length	165.1 cm
Width	91.4 cm
Height	111.8 cm
Average range	19 km on undulating terrain
Maximum speed	13 - 16 km/hr
Maximum gradient	1:5 with complete safety
Motor type	24 volt, 500 watt, permanent magnet traction motor
Controller	fully solid state with integral proportional electric braking
Batteries	two 100 Ah traction monoblocks (supplied)

This vehicle is very well suited for this project. The 500 watt motor is equivalent to the peak output of the two aluminum-air batteries, and it is unlikely that the motor would draw the full 500 watt capacity even in continuous use. Therefore, the aluminum-air batteries should be able to maintain a high charge level on the lead-acid power batteries. It was found later that the acceleration currents drawn from the motor were over 100 amperes, with brief power surges of around 2 kilowatts.

The vehicle was modified in order to accept the aluminum-air batteries, instrumentation, air pumps, make-up water reservoirs, etc. The original battery holders were changed so that alternate lead acid batteries (30 Ah) could be used. The weight breakdown of the modified vehicle and its components is shown in Table 10.

2.11 Charging Control System

In order to operate a hybrid system consisting of high power, low energy batteries and low power, high energy batteries, a suitable interface is required between the two battery types to control the charging rate. In this case, it was necessary to hold the charging current to a peak of 20 amperes (the maximum output of the aluminum-air batteries) and allow it to drop as necessary to avoid over-charging the lead-acid batteries. The charging control system was also required to be as efficient as possible to avoid energy losses in the form of heat. Rather than discuss the technical aspects in the main body of the report, the details are explained in appendix B.

All indications from the vehicle performance tests indicated that the circuit performed very well, allowing smooth current fluctuations as required up to a peak of 20 amperes. According to the appended report, the charging efficiency ranged from 60% at 5 A to over 90% at 17 A. This efficiency is considered to be excellent for this application.

2.12 Electric Vehicle Performance Tests

The vehicle was tested with the originally supplied 100 Ah lead-acid batteries first to provide a baseline performance to which the hybrid system could be compared. With a 67% duty cycle (ie. continuous operation for 4 minutes, idle for 2 minutes, repeated) around a test track, the vehicle ran for about 3 hours, at which time the lead-acid batteries were completely dead.

The vehicle was then tested with the 30 Ah deep-discharge lead-acid batteries which would be used in the hybrid arrangement as the power batteries. With these only, the vehicle was able to run the course for a little over one hour, but the duty cycle was decreased to less than 50% in the later part of the test in order to keep the vehicle running. The effective operating lifetime was actually slightly less than one hour.

The aluminum-air batteries were then installed with the charging system and the 30 Ah lead-acid batteries (recharged). With a continuous 67% duty cycle over the same course, the vehicle ran for over 6 hours on the first day before the test was stopped due to electrolyte leakage into several air pockets. This test demonstrated a range extension of about 100% before the problem occurred. At this point, the aluminum-air batteries had produced only about 60 Ah, and the cells which were not "flooded" were still producing operational voltage. A second run was attempted and the vehicle ran for 4 hours before leakage again shut the system down. In both cases, the electrolyte leakage appeared to begin as "seepage" through the cathodes, which then partially filled the air pocket to the cathode level. This resulted in electrical shorting from opposing cathodes and sacrificial dissolution of one of the metal grids, allowing the creation of larger leaks and eventually complete flooding.

Portable data logging equipment was used on the vehicle while it was running the tests, but for various reasons, the data was inconclusive and could possibly be misleading. During operation of the vehicle, it is estimated that the average current was 13-15 amperes, and the vehicle motor voltage varied from 20 to 28 volts, depending on operating conditions.

Although the data recorded could not be used effectively to fully analyse the operation the system, the general results clearly demonstrate the range extension using the aluminum-air/lead-acid hybrid system. From the results, extrapolation to the expected life of the aluminum-air batteries indicates a potential range extension of 3 to 4 times that of similarly sized lead-acid batteries.

3. CONCLUSIONS

The following conclusions can be drawn from the results of the project:

(1) The multi-cell common sump, 12 volt, 20 ampere, saline aluminum-air battery which has been developed can produce 100 Wh/kg, 15 W/kg, and 300 Wh/litre (of electrolyte) between electrolyte changes in its present form. There is sufficient aluminum anode for three such runs. With minor refinements, the energy density can be increased substantially.

(2) The technology to remove heat, manage hydrogen, and manage the by-product in saline aluminum-air batteries has been developed and proven in both single cell and multi-cell batteries. The by-product management allows the battery to be cleaned at the end of a run by flushing with water, and no disassembly is required.

(3) A multi-cell aluminum-air battery has been designed and built in a fashion so as to be easily assembled and practical to operate. The battery can be cleaned and mechanically recharged (reloaded with aluminum anodes) with only minor disassembly. This same design can be easily adapted for various numbers of cells.

(4) A charging control system has been designed and demonstrated to efficiently control trickle charging from high energy aluminum-air batteries to high power lead-acid batteries operating in a hybrid electric vehicle system. This charging control system is also capable of acting as a controller for simple recharging of lead-acid batteries, separate from an electric vehicle.

(5) The range extension concept has been proven in an electric vehicle. The hybrid aluminum-air/lead-acid battery system doubled the range of lead-acid batteries with the same charge rating and mass. At this range, the aluminum-air batteries had produced only about half of their potential discharge, but stopped prematurely due to a material quality problem.

4. RECOMMENDATIONS

There are several items which are within reasonable scope of further study:

(1) The one item that presently severely limits the success of the saline aluminum-air battery is the air cathode, both in terms of operating performance and life expectancy. Although there are other methods of providing oxygen for the reaction, such as hydrogen peroxide or metallic oxides, atmospheric air is the simplest, and the supply is limitless. For that reason alone, air cathodes must be developed further

to make them leak-proof, longer lasting, and less expensive. An alternative to longer life would be low cost "throw-away" cathodes. Alcan has already begun to independently study this technology.

(2) Since the scope of this project was limited to the development of the required technology and demonstration of the range extender concept, there was no funding to study the impact on the performance and life of the lead-acid power batteries. In considering the operation of this system, it is recognized that the power (lead-acid) batteries are not exposed to a standard deep discharge cycle. This effect could possibly have beneficial effects on both the net charge obtained from the power batteries, and their life, since they maintain close to a full charge throughout the operation of the hybrid system. This area is worthy of further study.

(3) This project has demonstrated the feasibility of a 100 Wh/kg saline battery capable of operating at 20 amperes at 14 volts over successive runs of several hours. Simultaneously, Alcan had built and operated (at its own expense) larger alkaline batteries capable of 300 Wh/kg. It is recommended that both systems should be examined as potential range extenders for Road Vehicles. A brief analysis of power systems for road vehicles is provided in Appendix B.

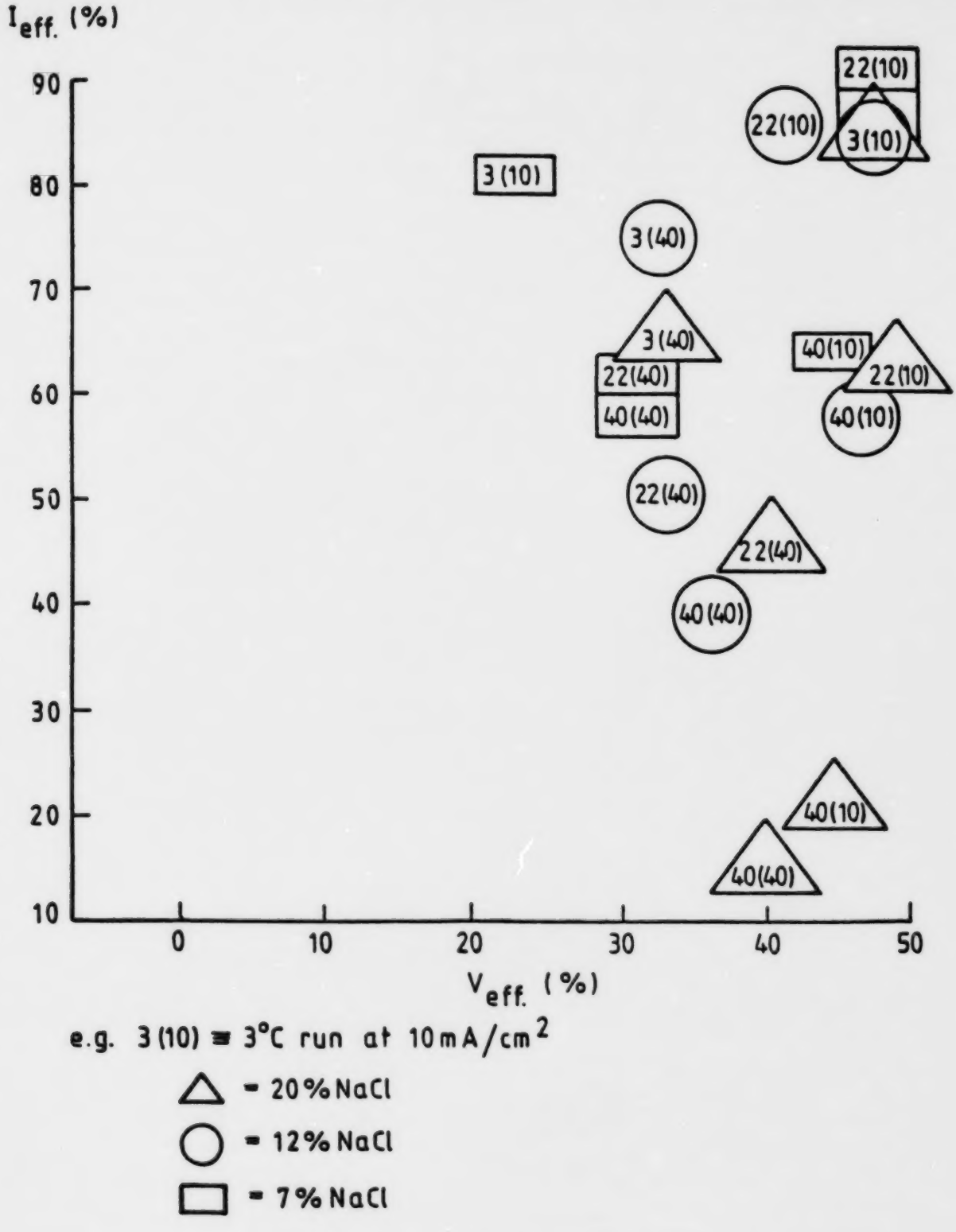

Figure 2 Voltage and current efficiencies

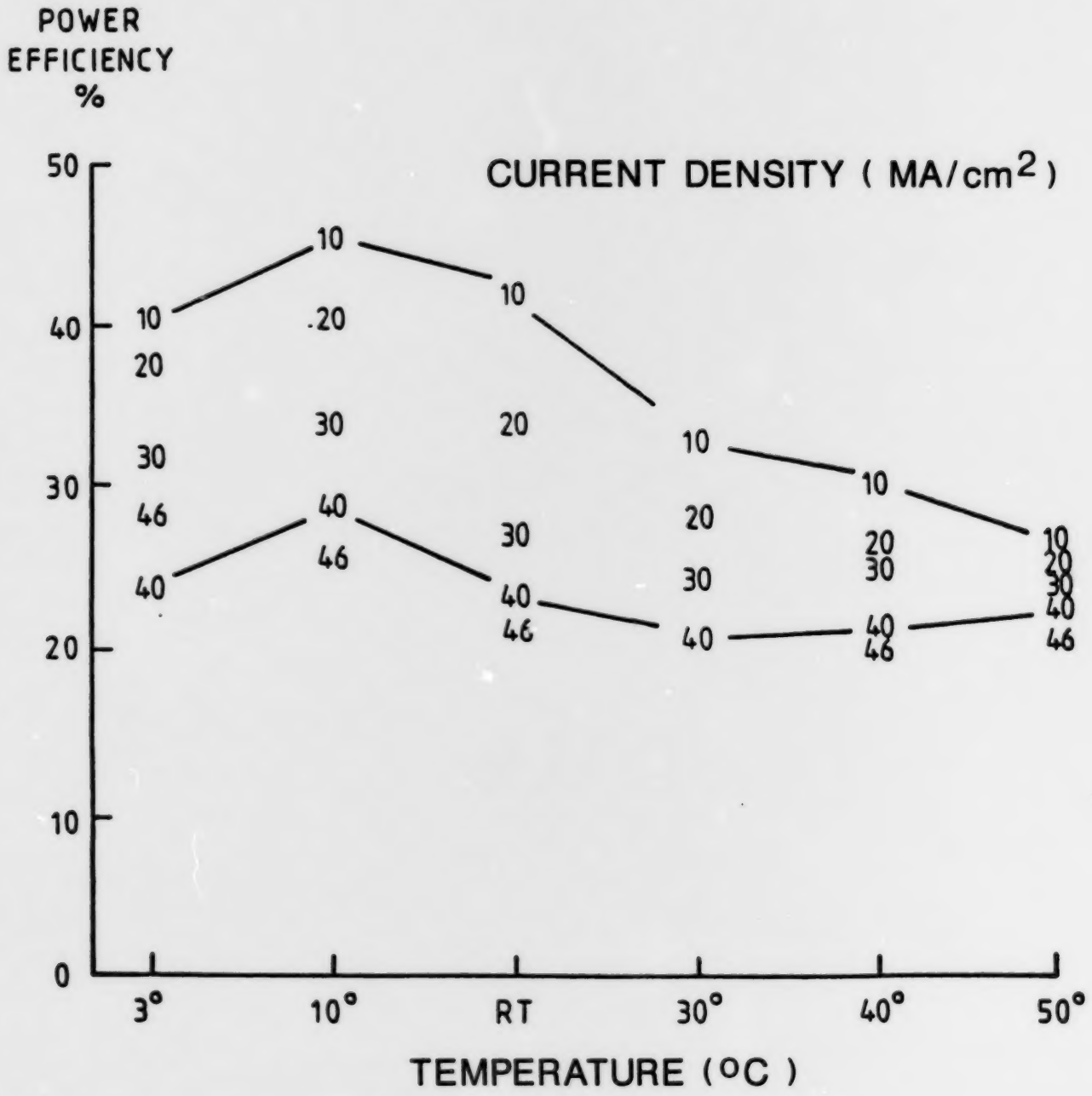

Figure 3 Flow cell power performance in 7% NaCl

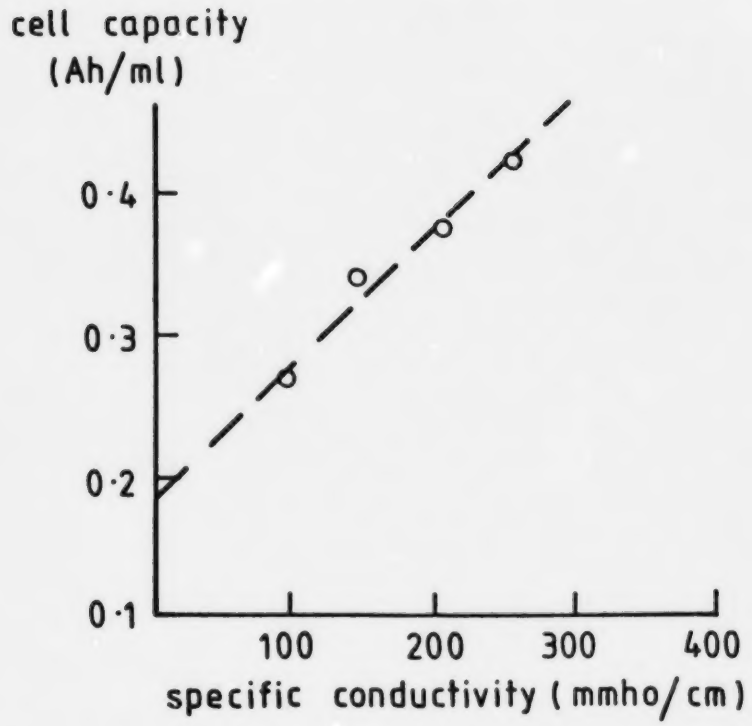

Figure 4 Conductivity versus cell capacity

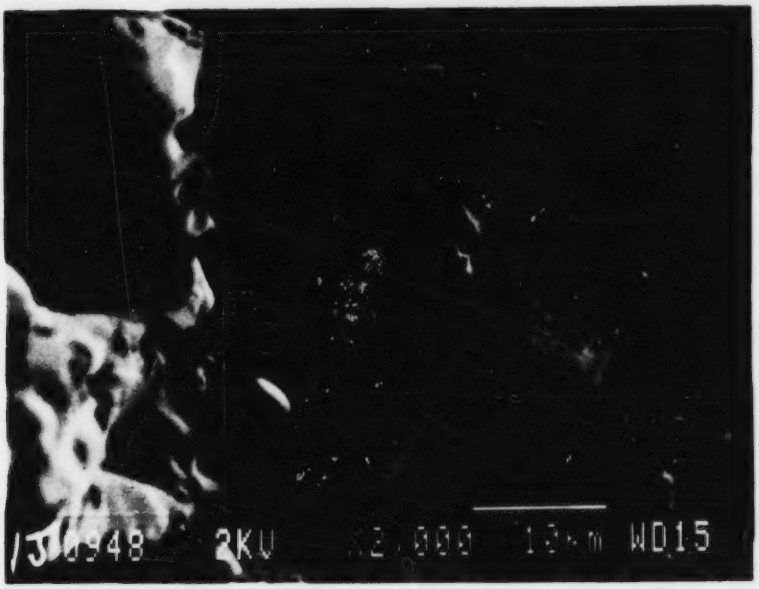

Figure 5 Waste from stagnant cell

Figure 6 Waste from reciprocated cell

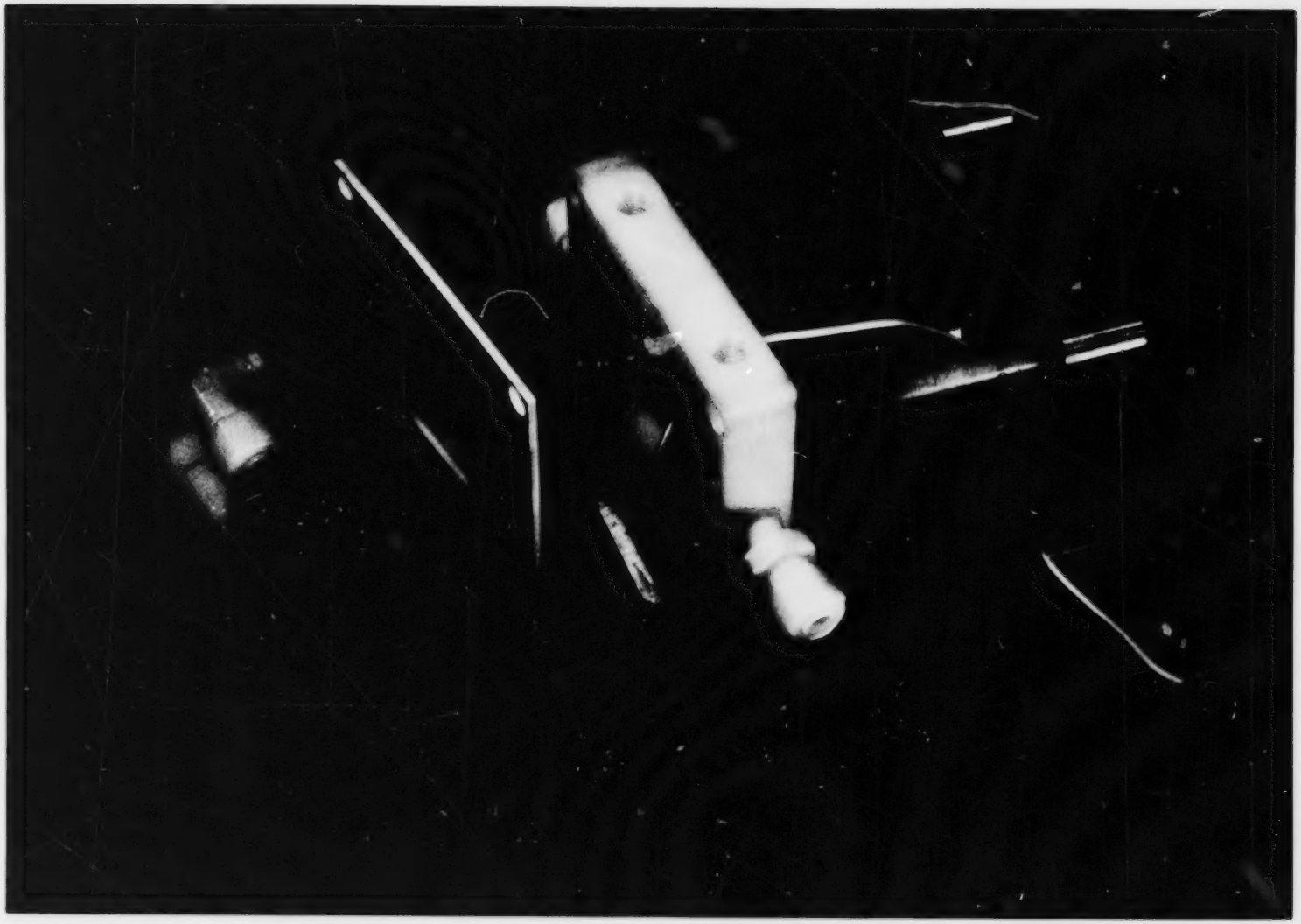

Figure 7 The 25 cm^3 test cell

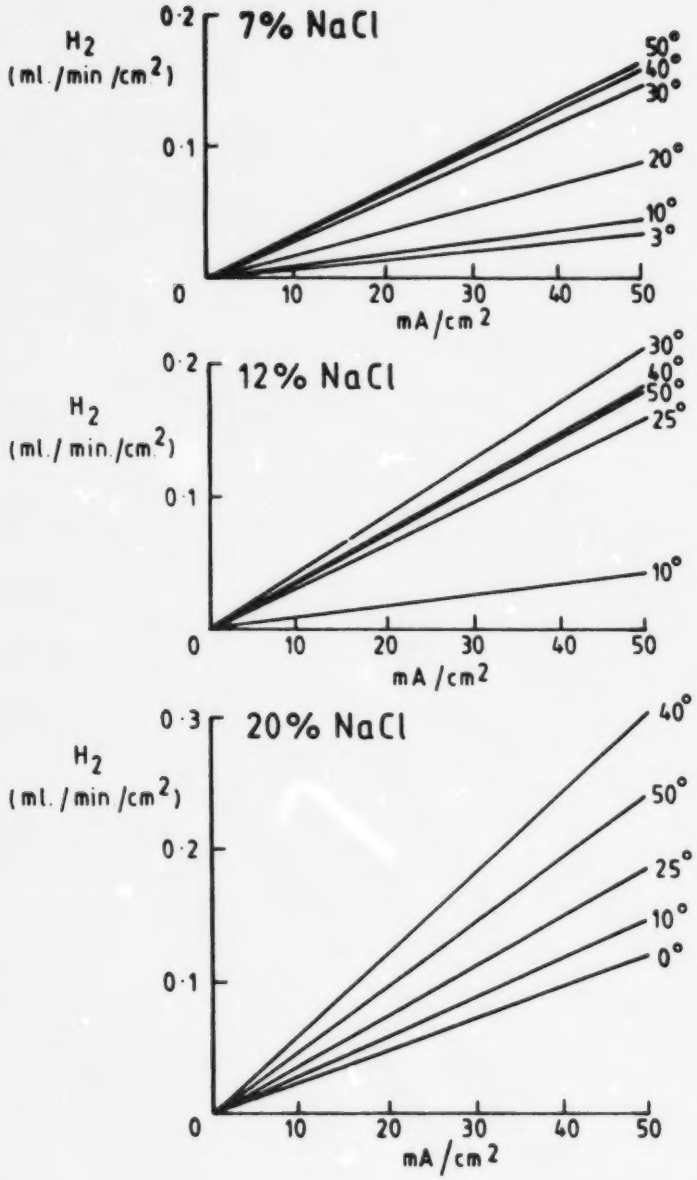

Figure 8 Hydrogen evolution tests on 5* alloy

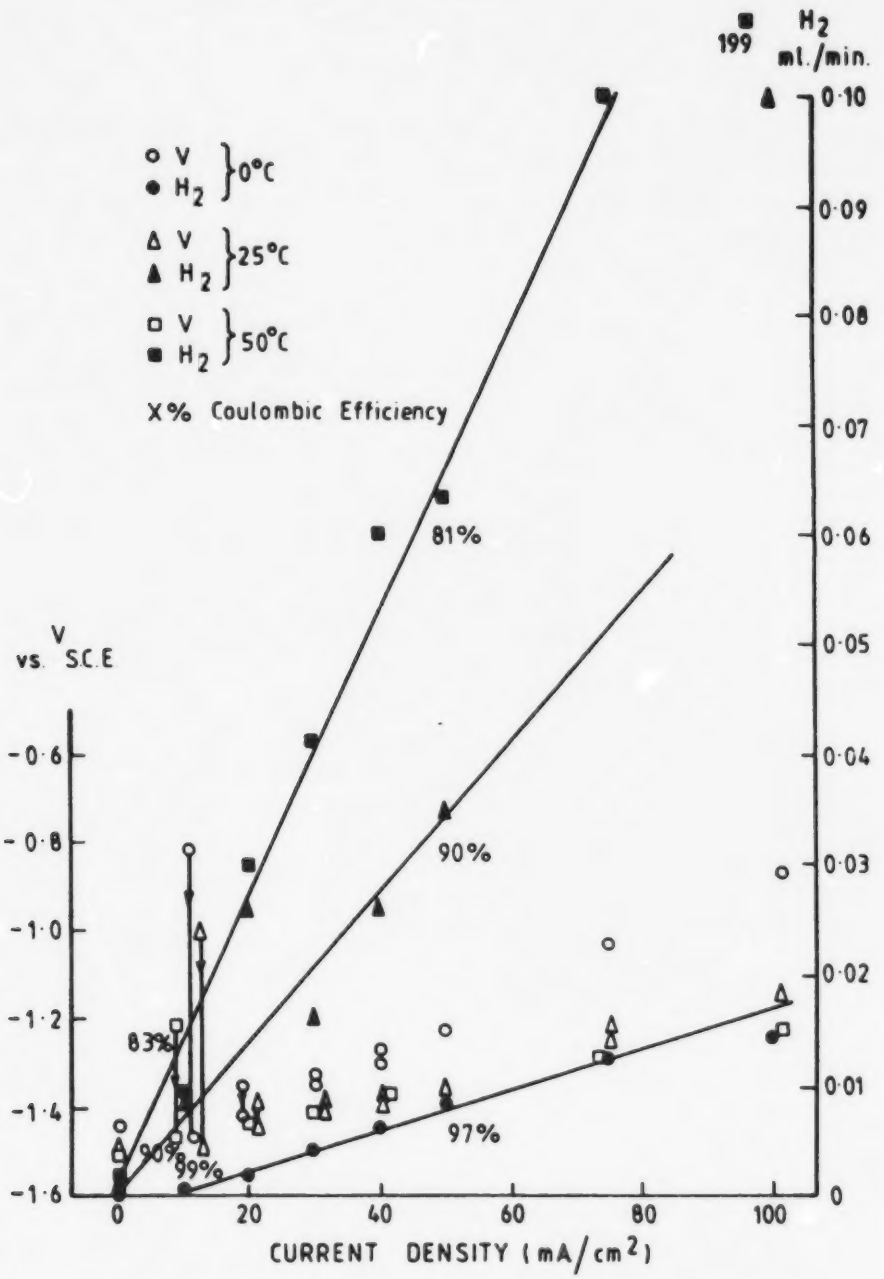

Figure 9 Galvanostatic polarization in 12% NaCl with 5* alloy

BATTERY TESTING

5* ALLOY / EMC CATHODE

Hydrogen evolution rate vs. temperature
for different NaCl concentrations

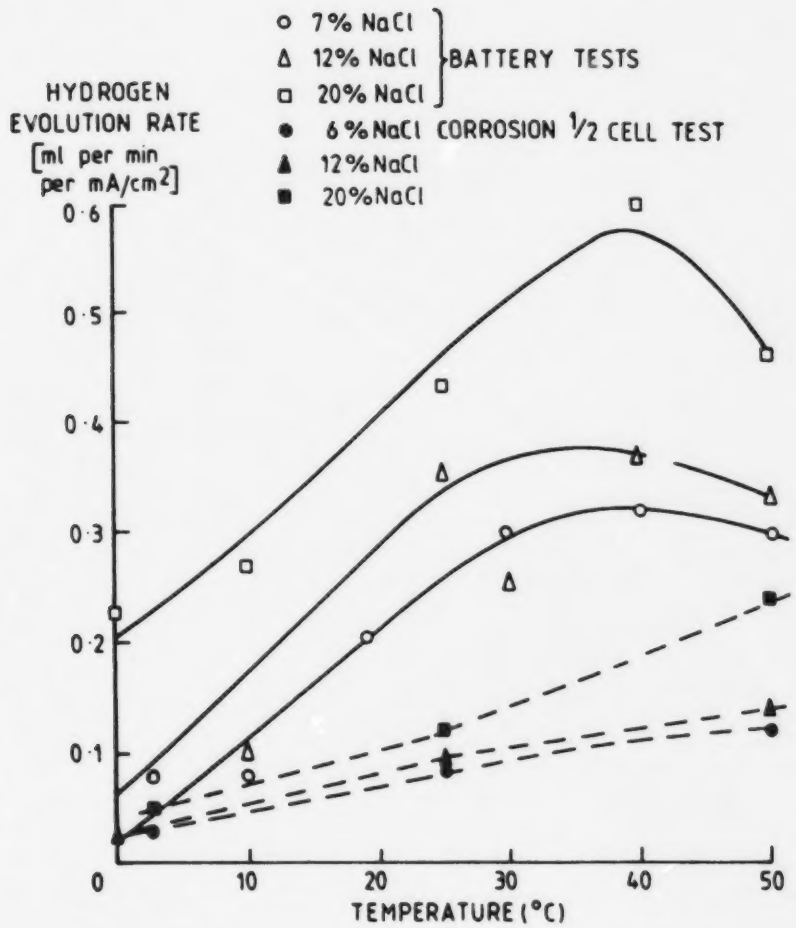

Figure 10 Hydrogen evolution rate versus temperature

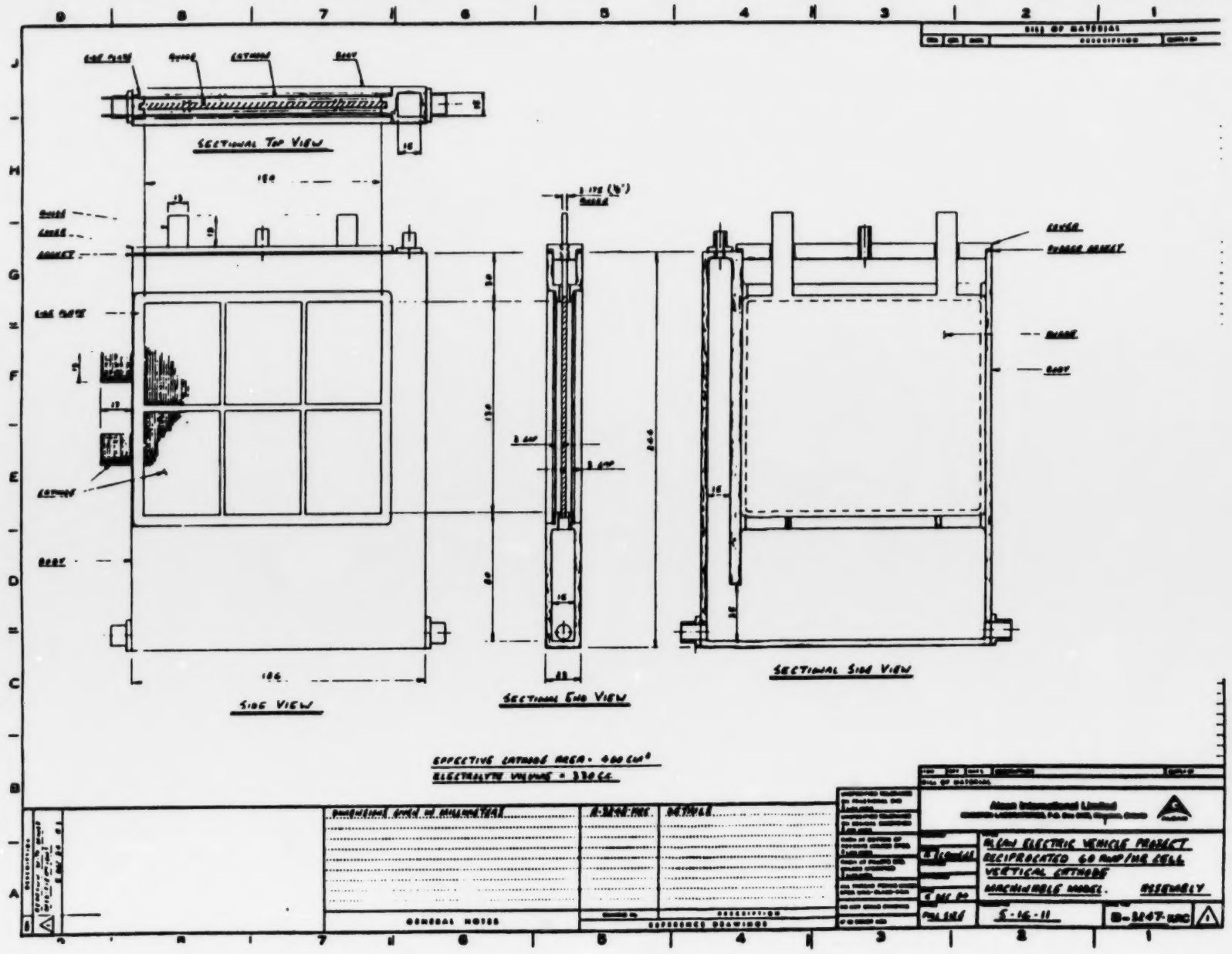

Figure 11 The first single cell design

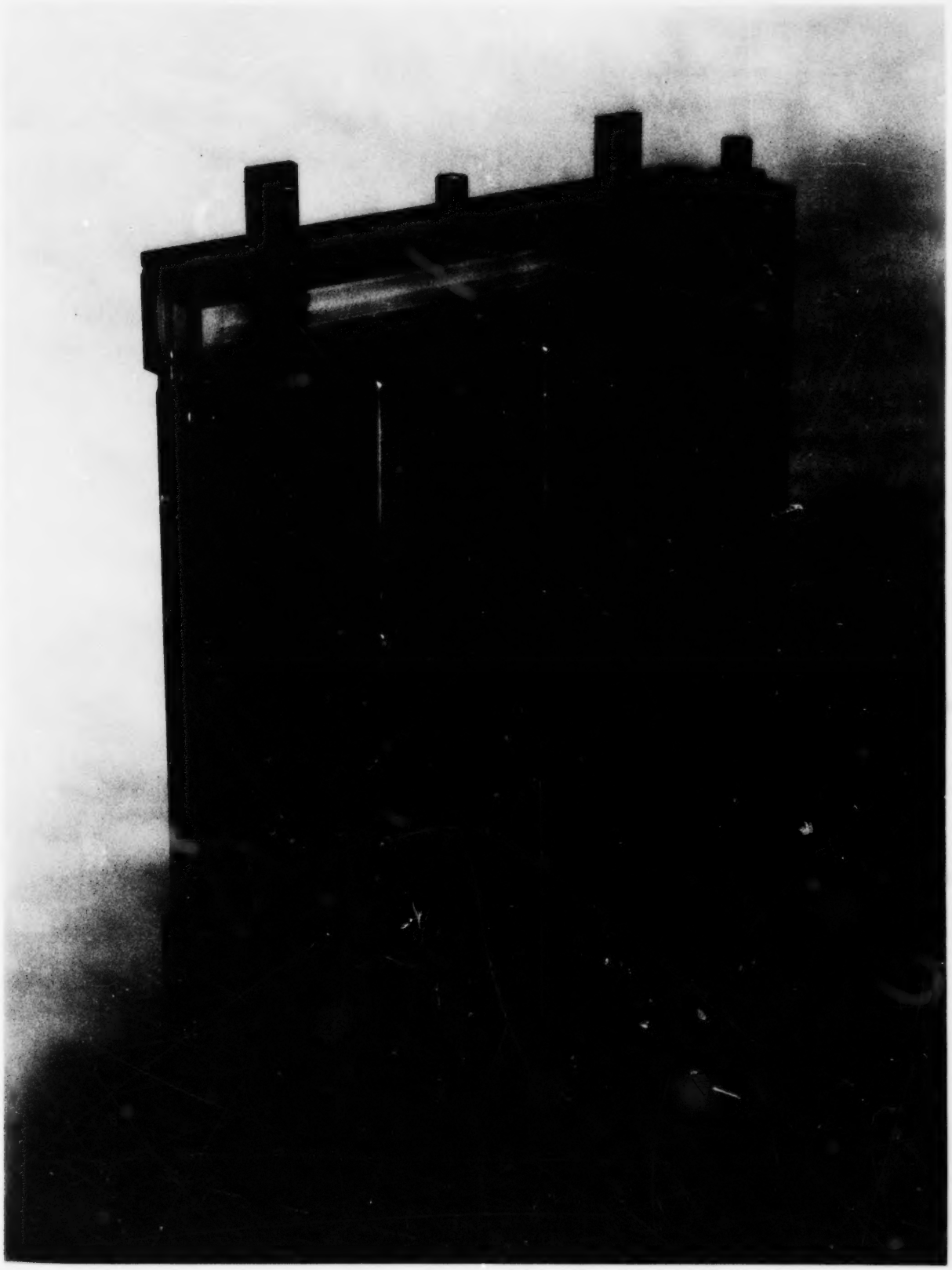

Figure 12 The first single cell assembly

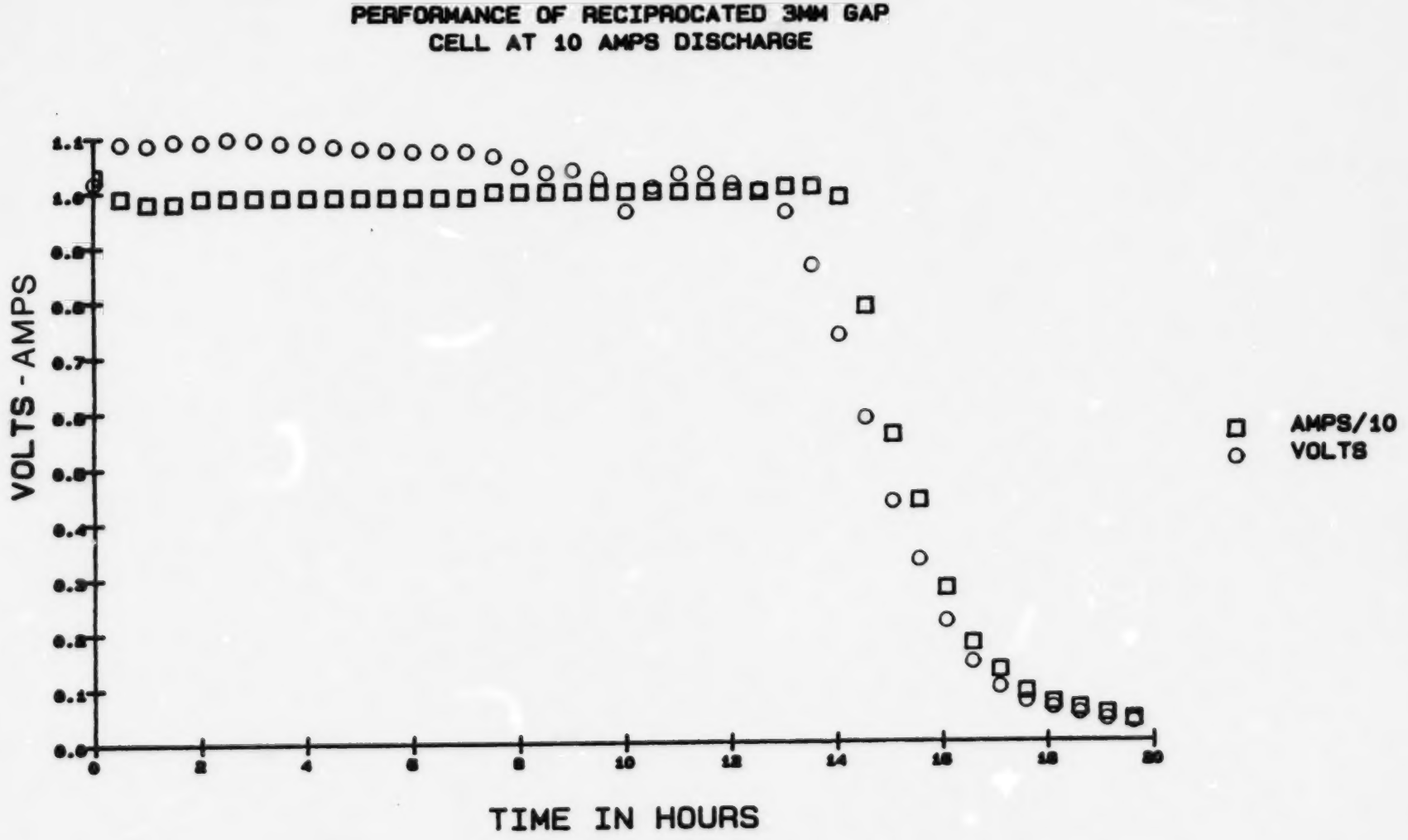
PERFORMANCE OF RECIPROCATED 3MM GAP
CELL AT 10 AMPS DISCHARGE
VOLTS - AMPS
TIME IN HOURS
AMPS/10
VOLTS
HURON CATHODE; 12% NACL; ELECTROLYTE REPLENISHMENT UP TO 12 HOURS;
EXPT #P000220; EFFICIENCY 58%; ANODE BSI

Figure 13 Performance of a single reciprocated cell

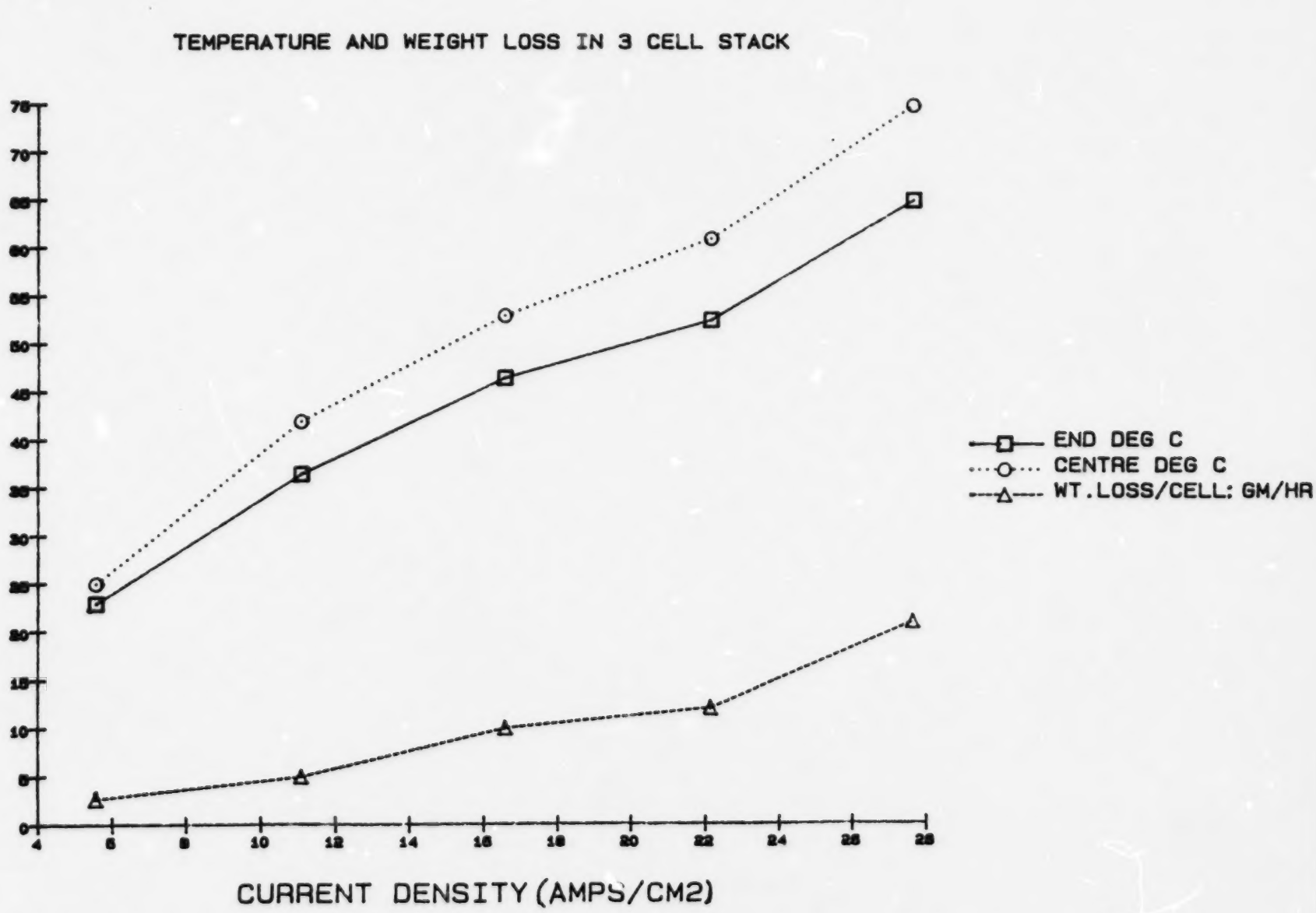

Figure 14 Temperature and weight loss of a 3 single cell stack

Figure 15 14 Single cell stack test assembly

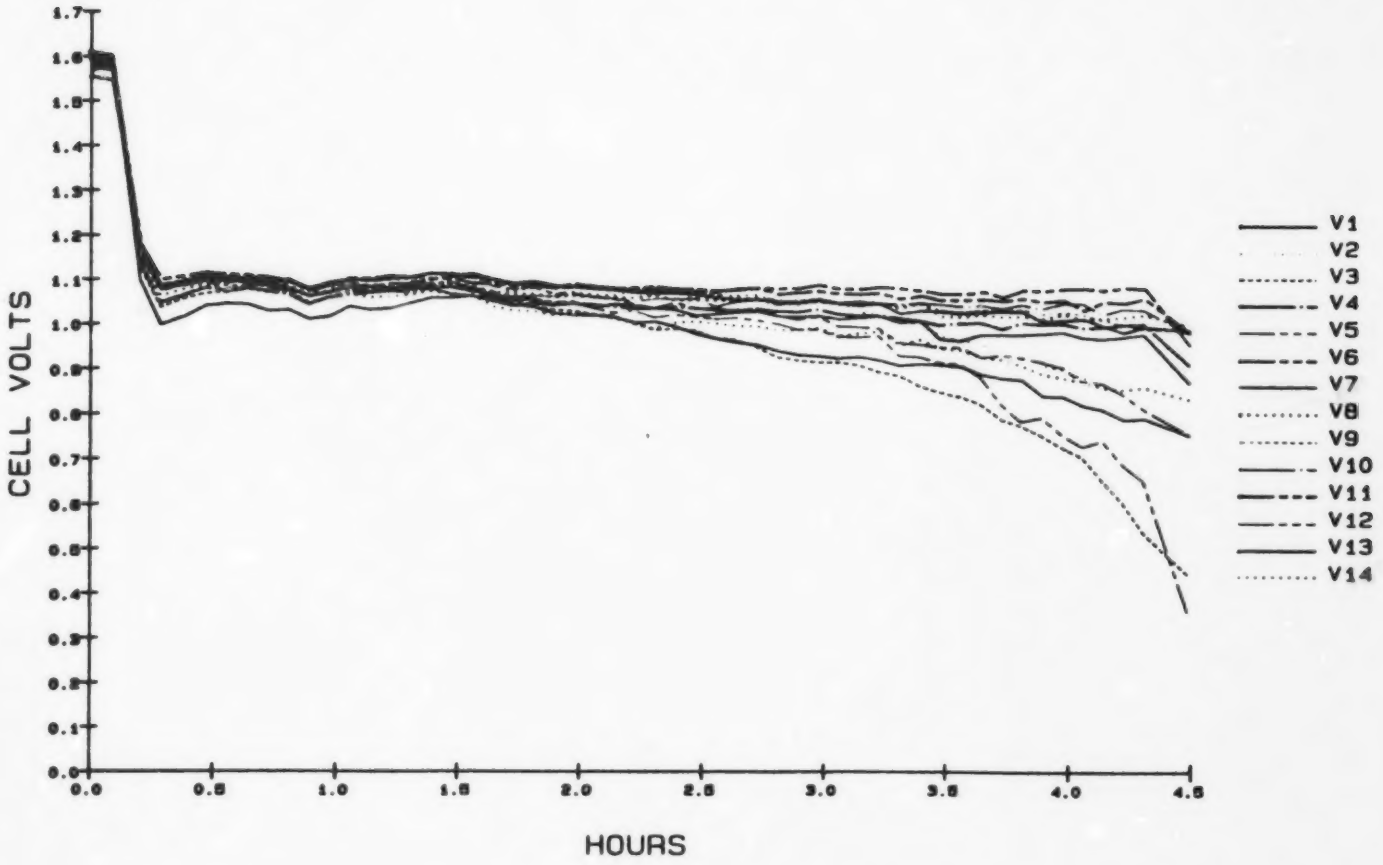

Figure 16 Cell voltages for 14 single cell stack test

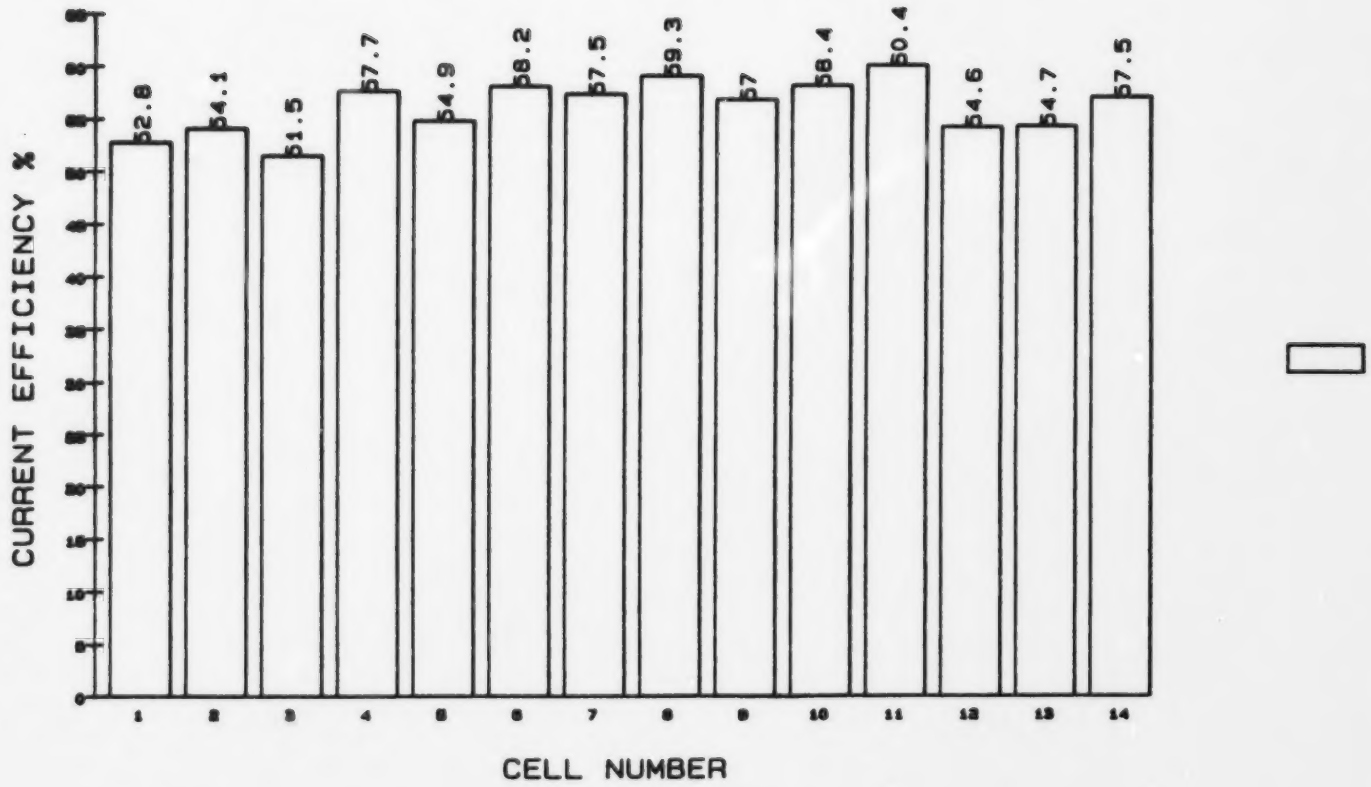

Figure 17 Current efficiencies of a 14 single cell stack test

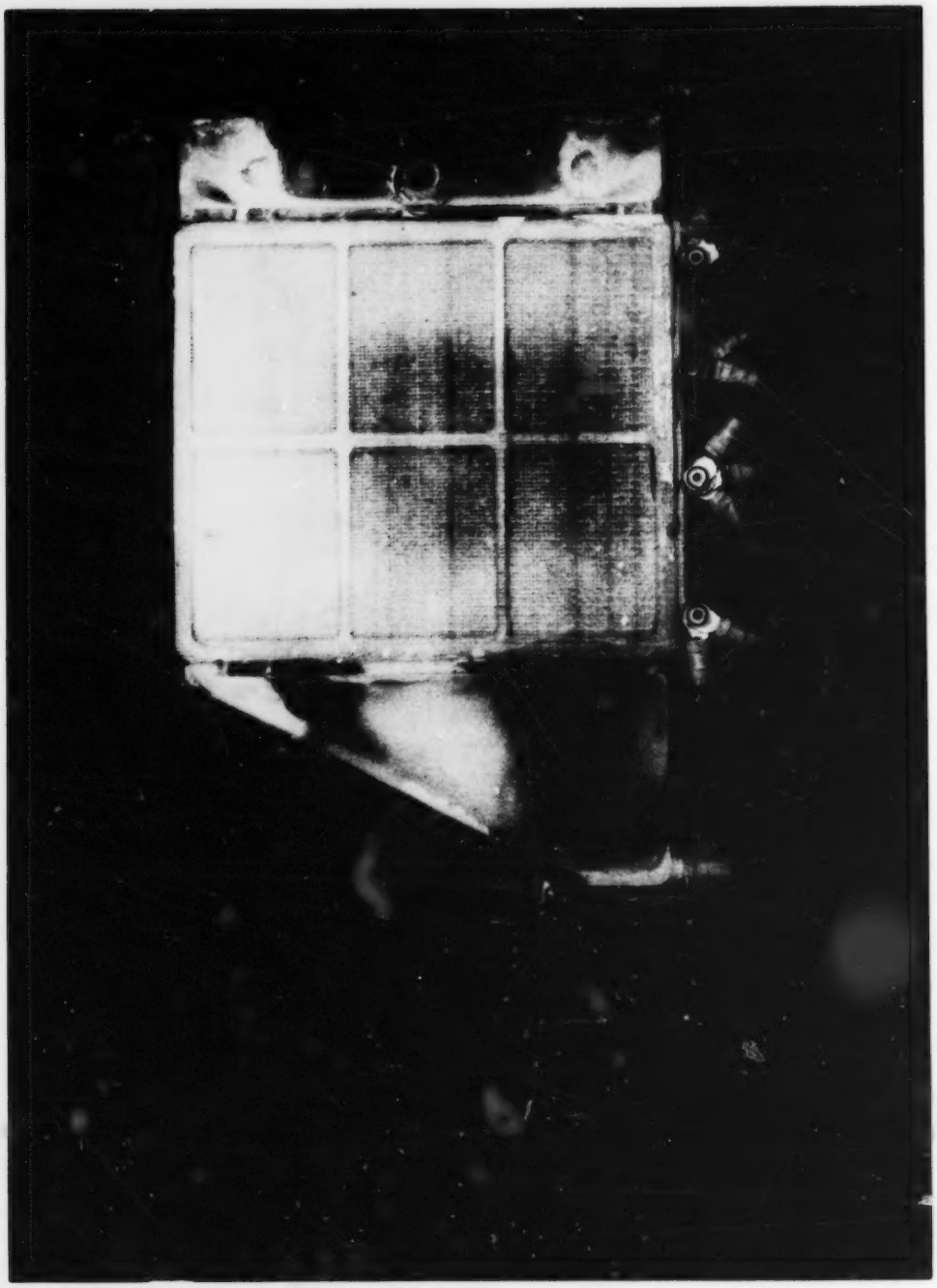

Figure 18 Slant bottom single cell

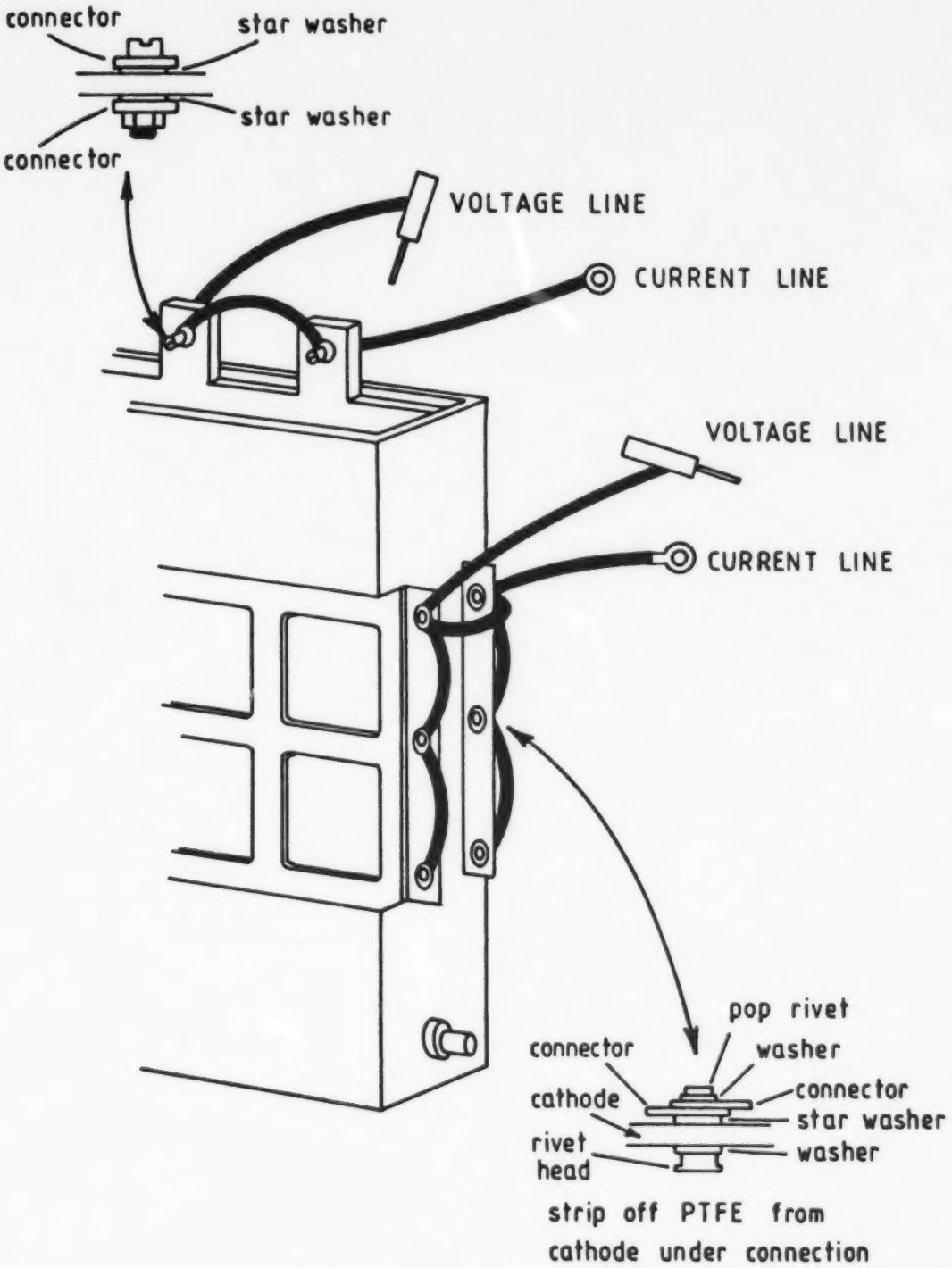

Figure 19 Schematic of test connections

IMPROVED V-i PERFORMANCE WITH BETTER TERMINATIONS

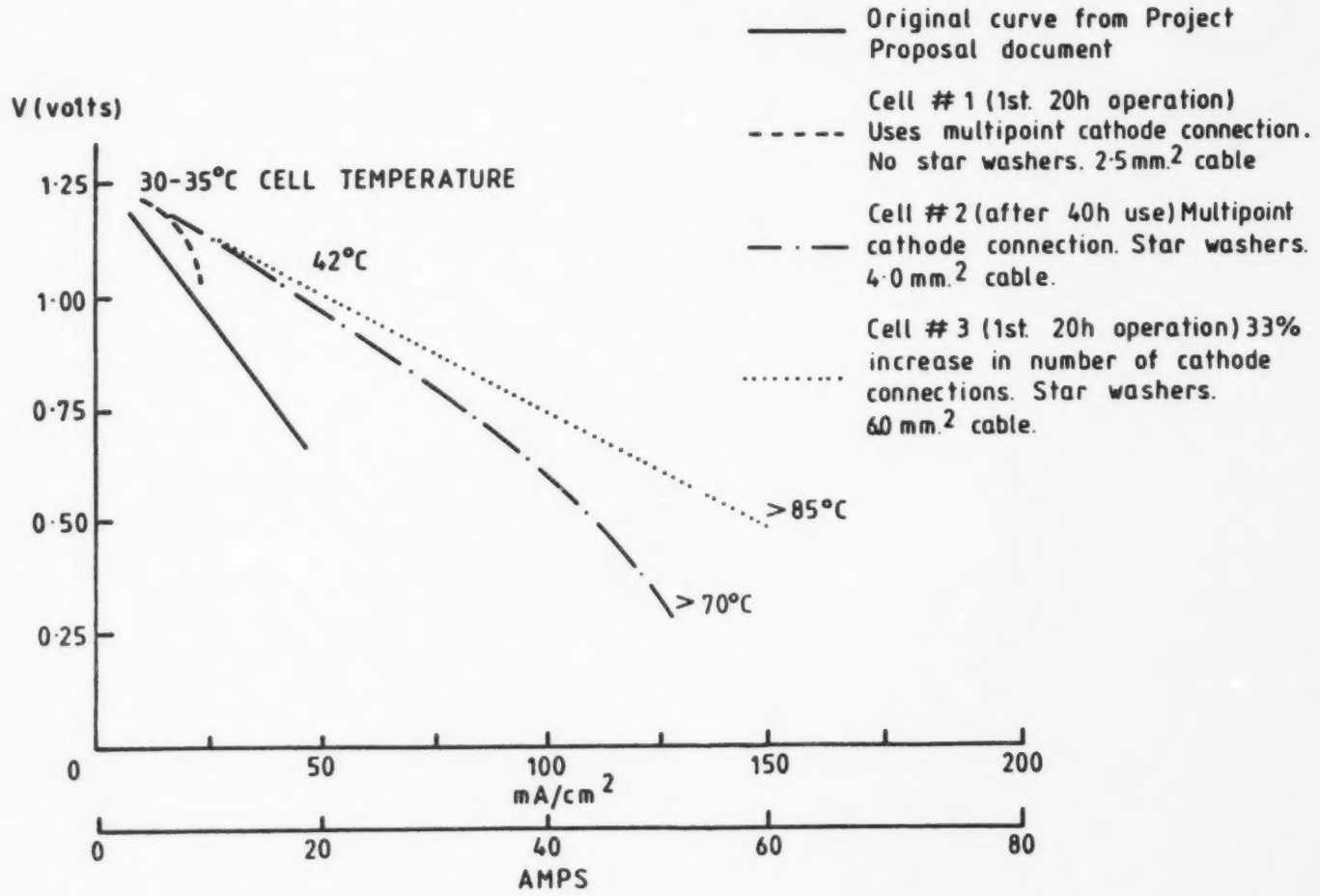

Figure 20 Performance of various cathode connections

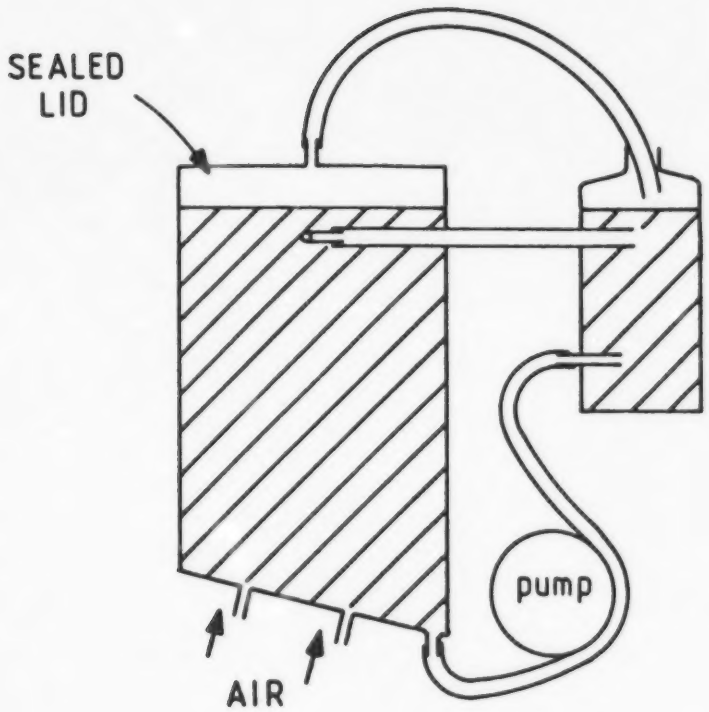

Figure 21 Schematic of circulated cell

Gas Injection Aluminum/Air Battery (Double Return)

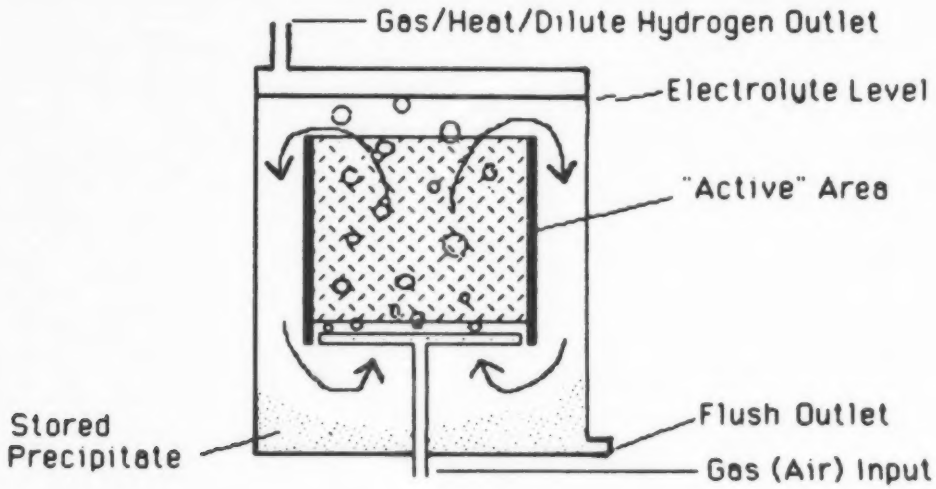

Figure 22 Schematic of gas injection cell (front view)

Gas Injection Aluminum/Air Battery

Side View (Cross-section)

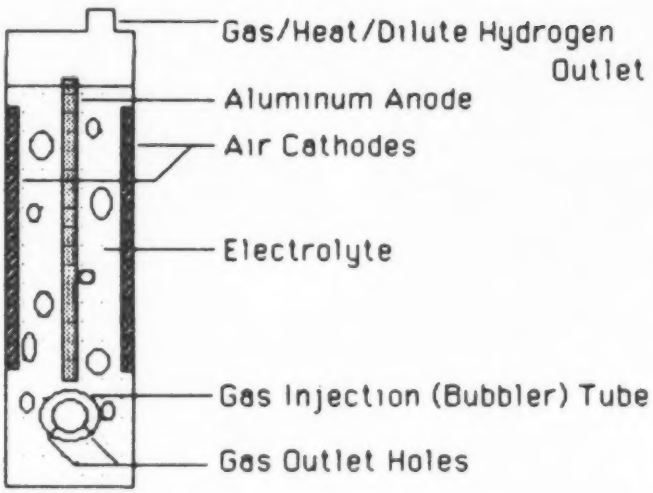

Figure 23 Schematic of gas injection cell (side view)

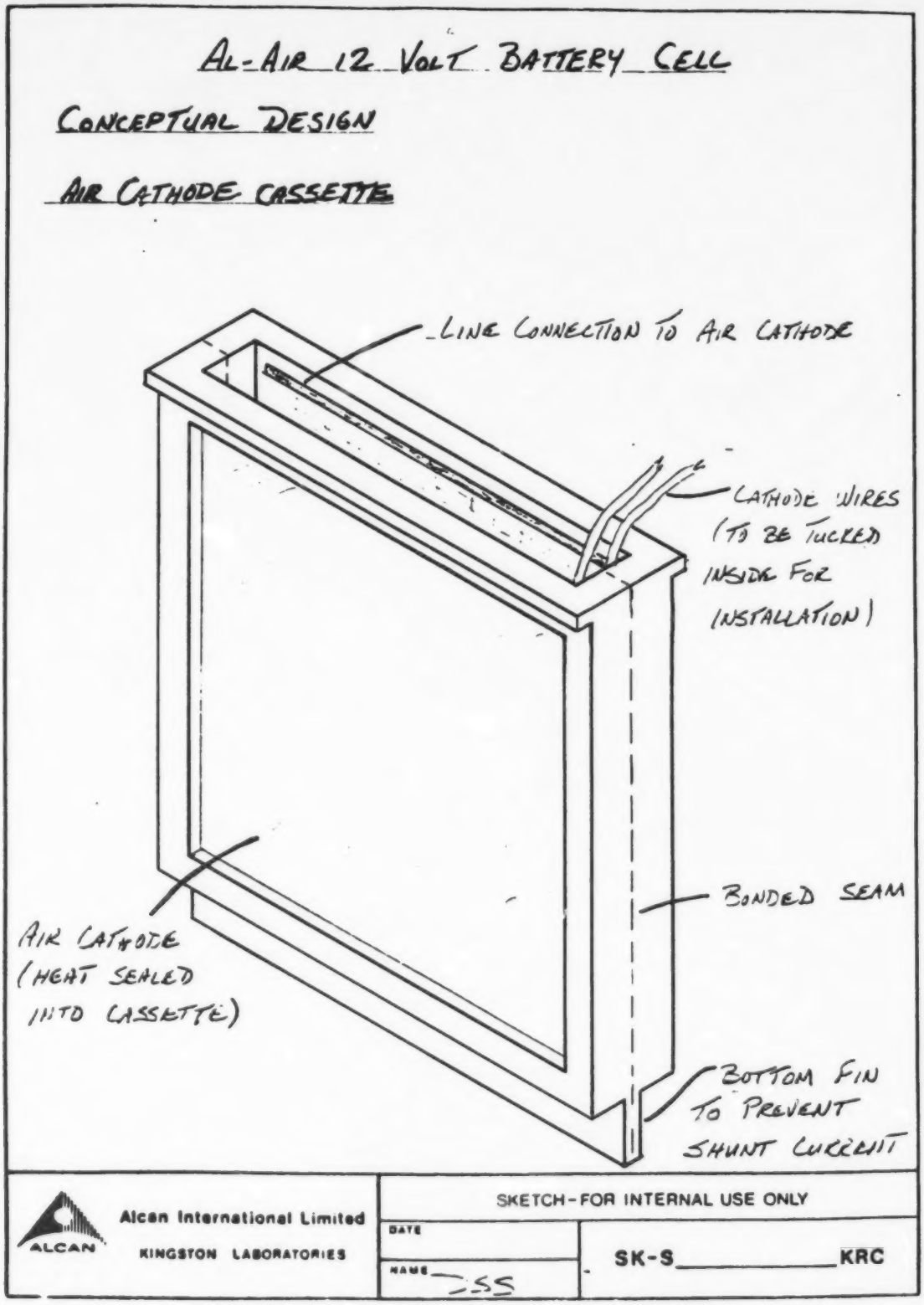

Figure 24 Conceptual air cathode cassette

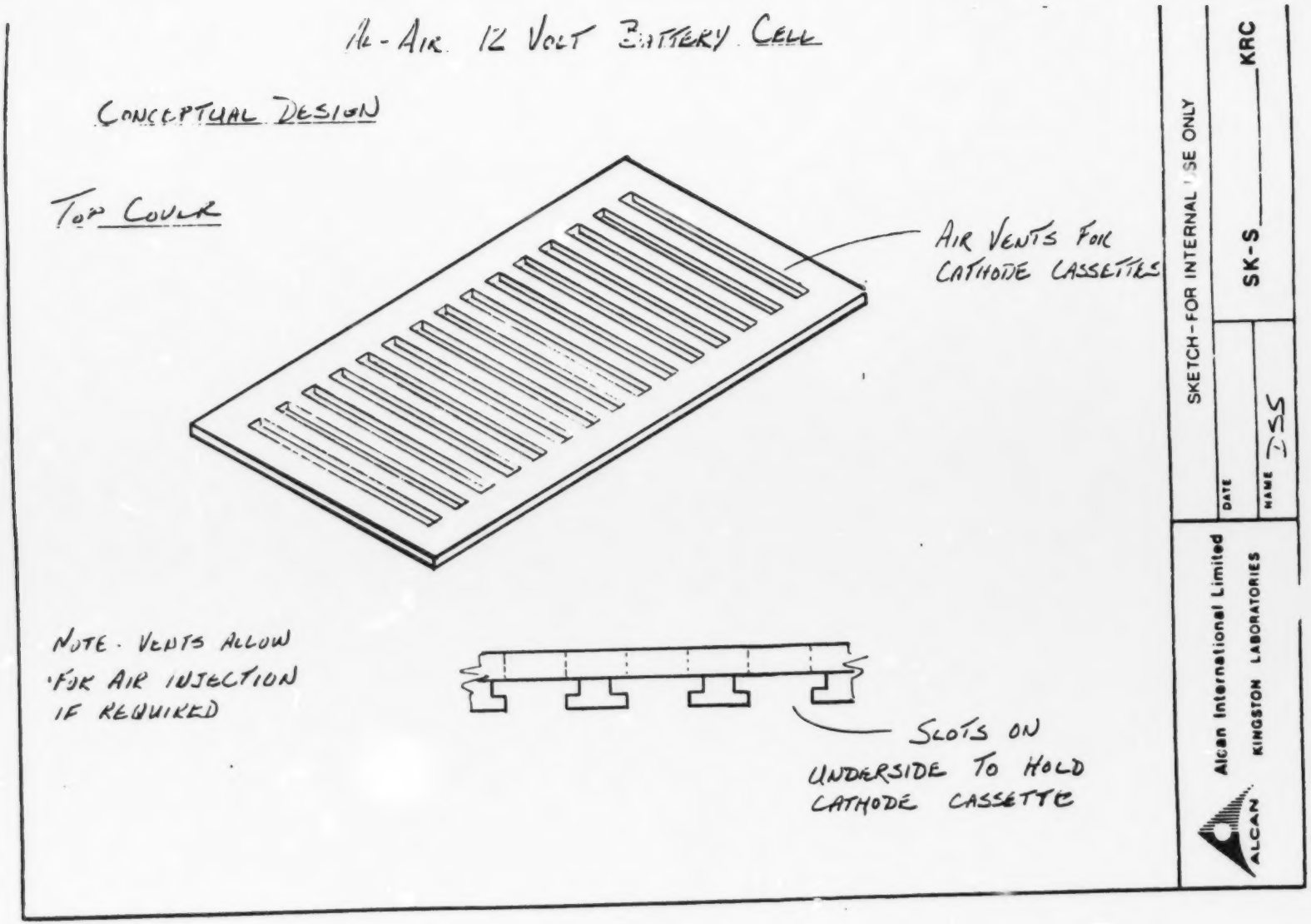

Figure 25 Conceptual battery cover

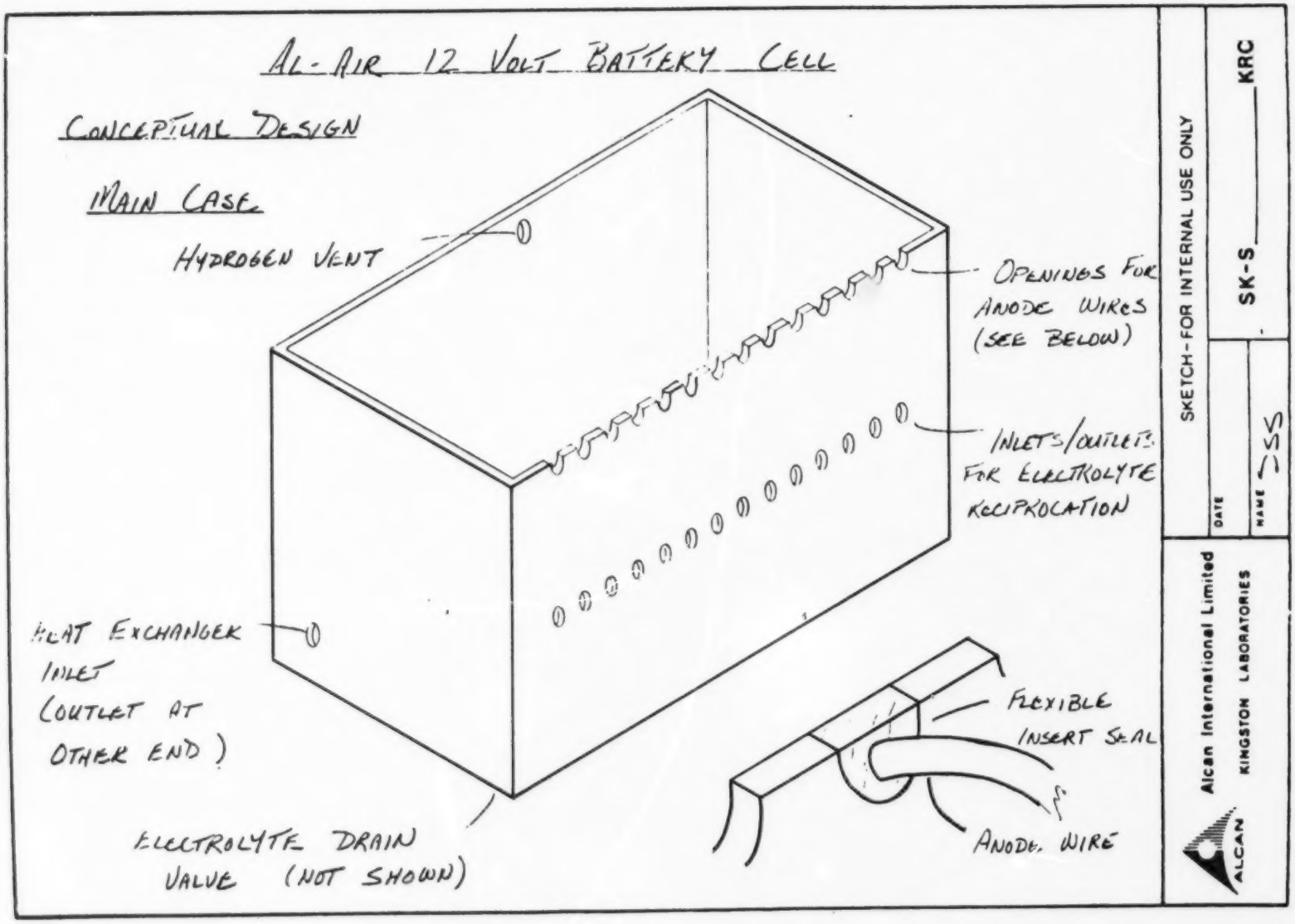

Figure 26 Conceptual battery case

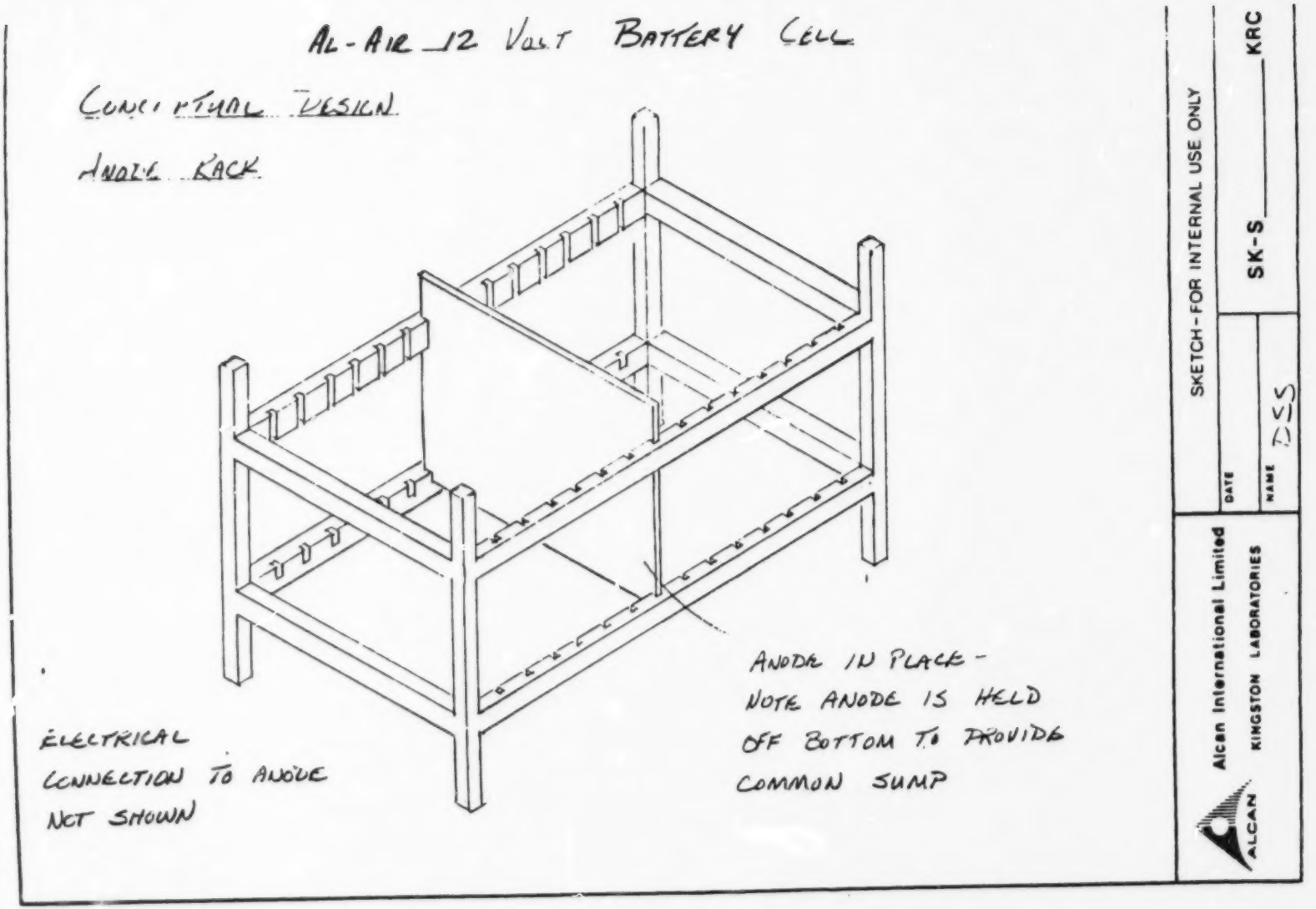

Figure 27 Conceptual anode support rack

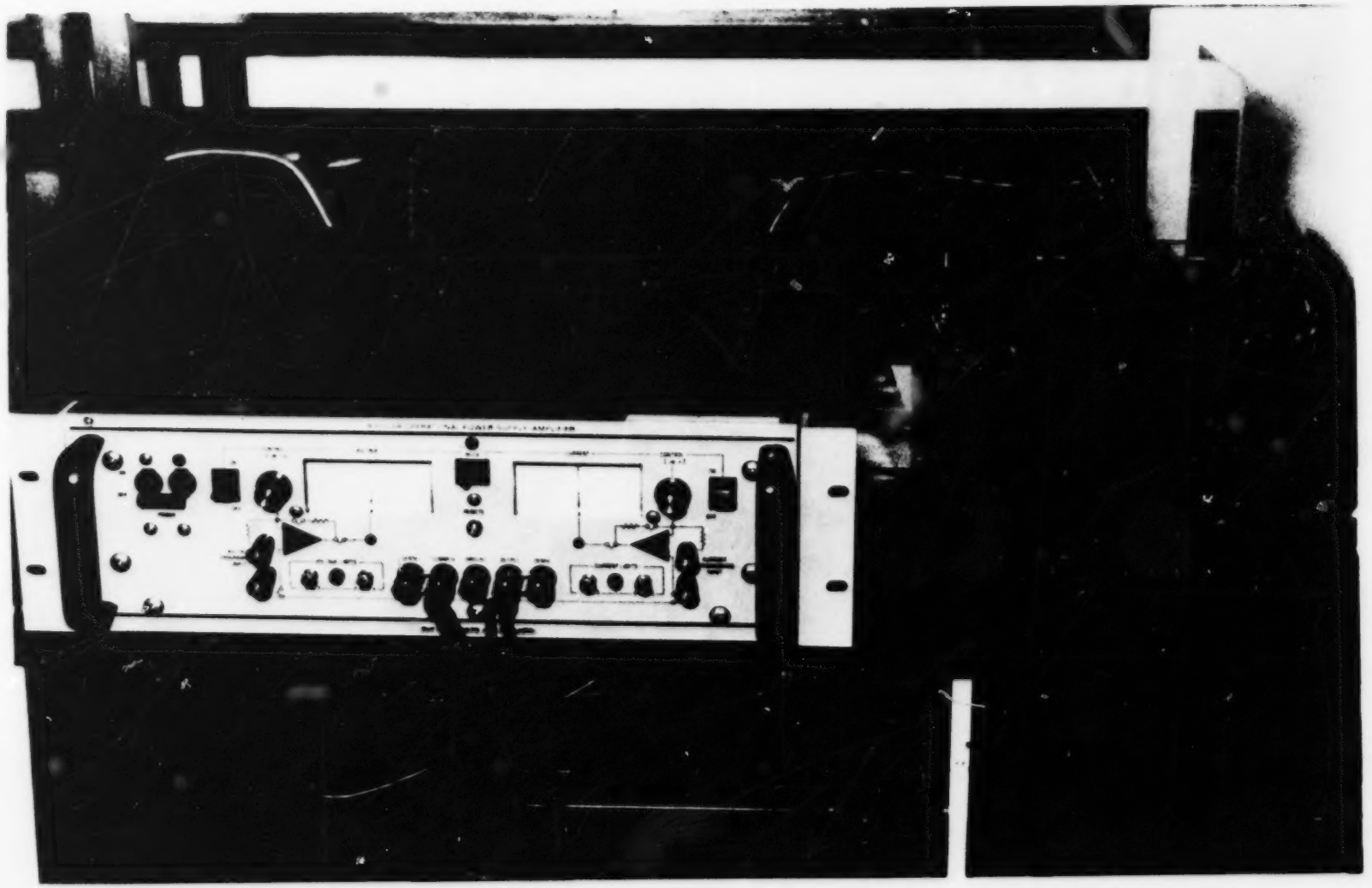

Figure 28 Shunt current test box

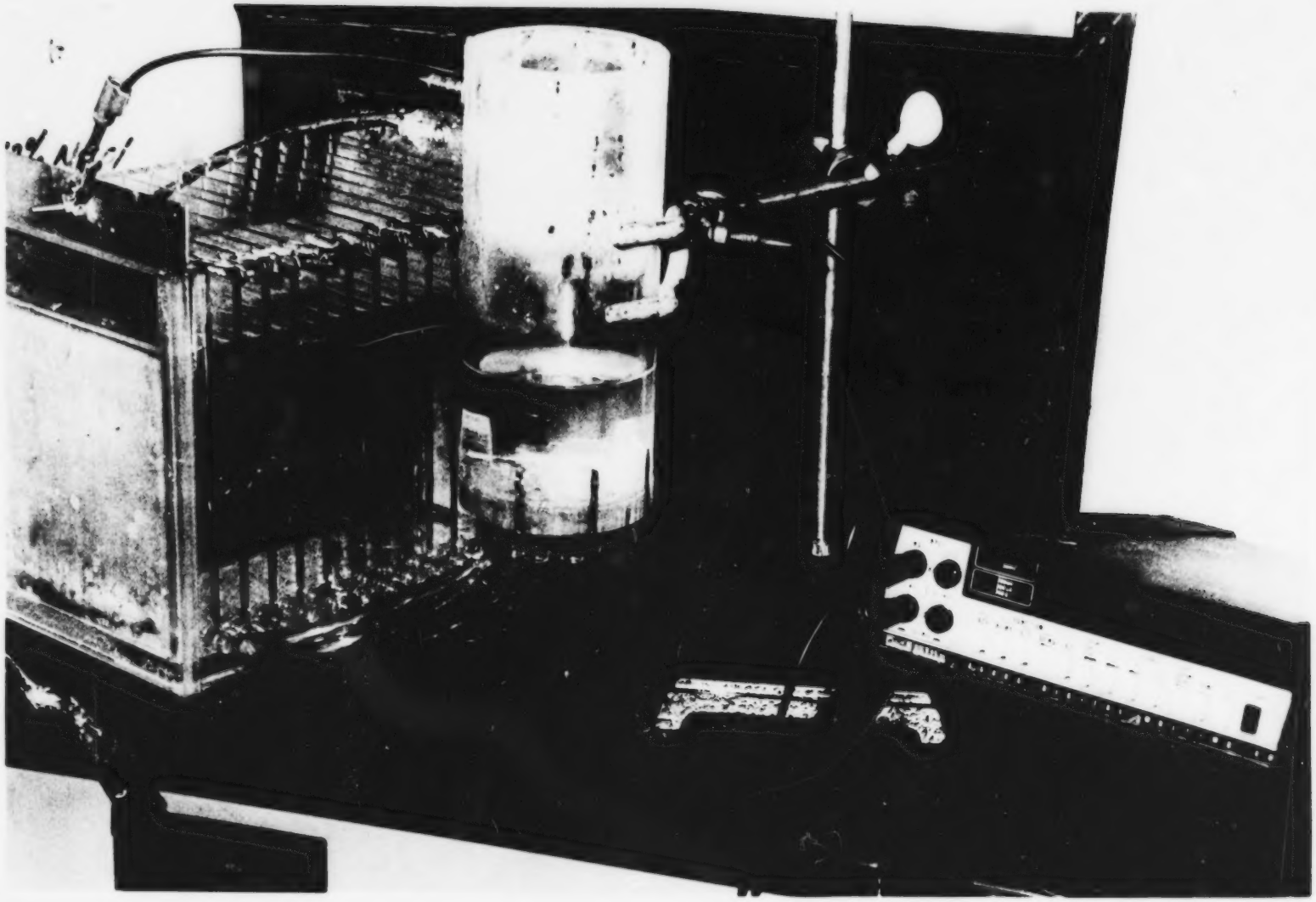

Figure 29 Shunt current test with common manifold

Figure 30 CADD design 3 (1)

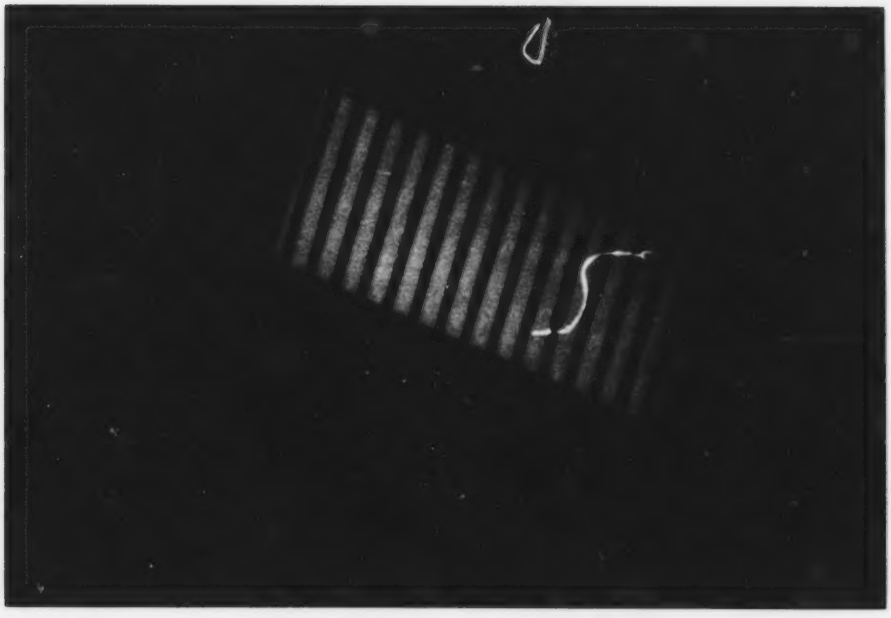

Figure 31 CADD design 3 (2)

Figure 32 CADD design 3 (3)

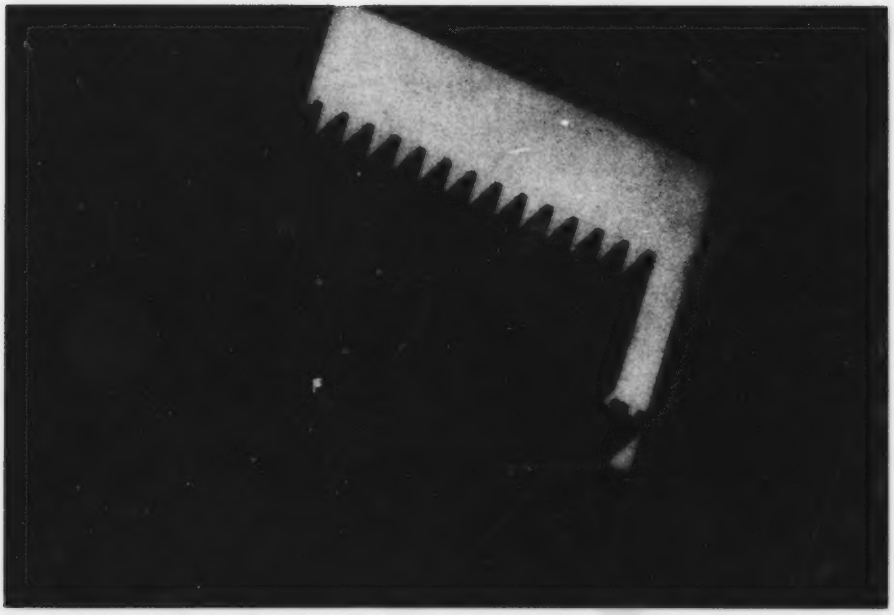

Figure 33 CADD design 3 (4)

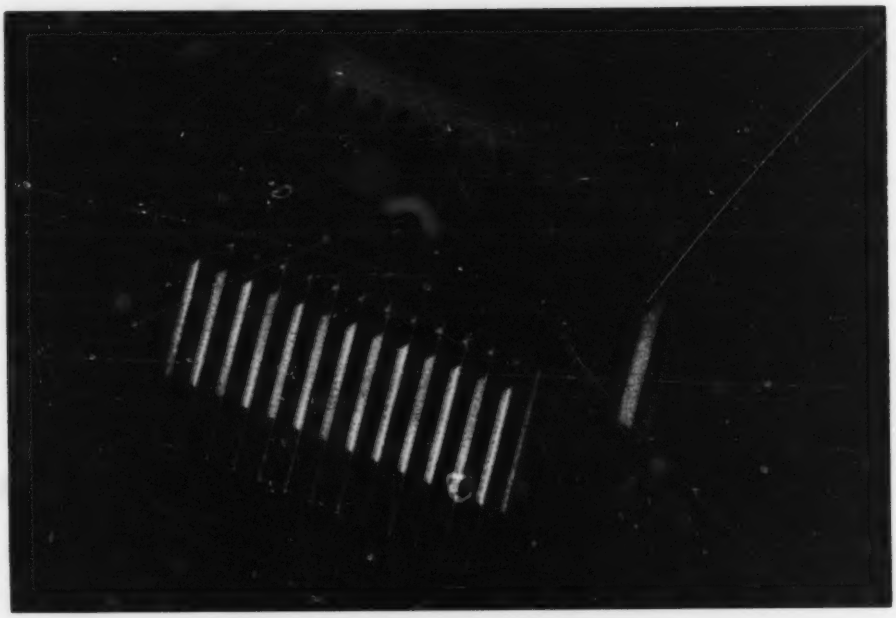

Figure 34 CADD design 3 (5)

Figure 35 CADD design 3 (6)

Figure 36 CADD design 3 (7)

Figure 37 CADD design 3 (8)

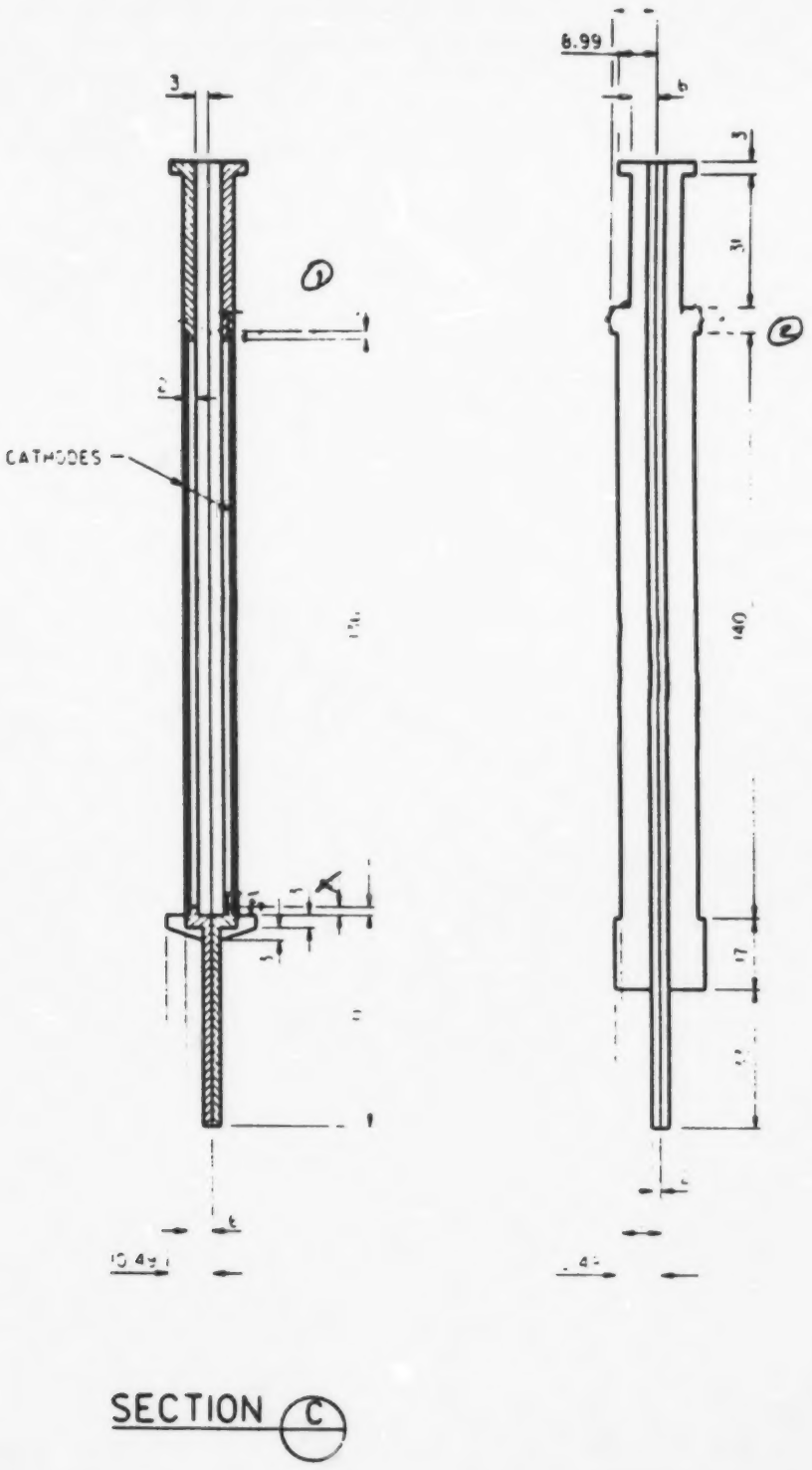

Figure 38 Three cell battery - air cathode cassette

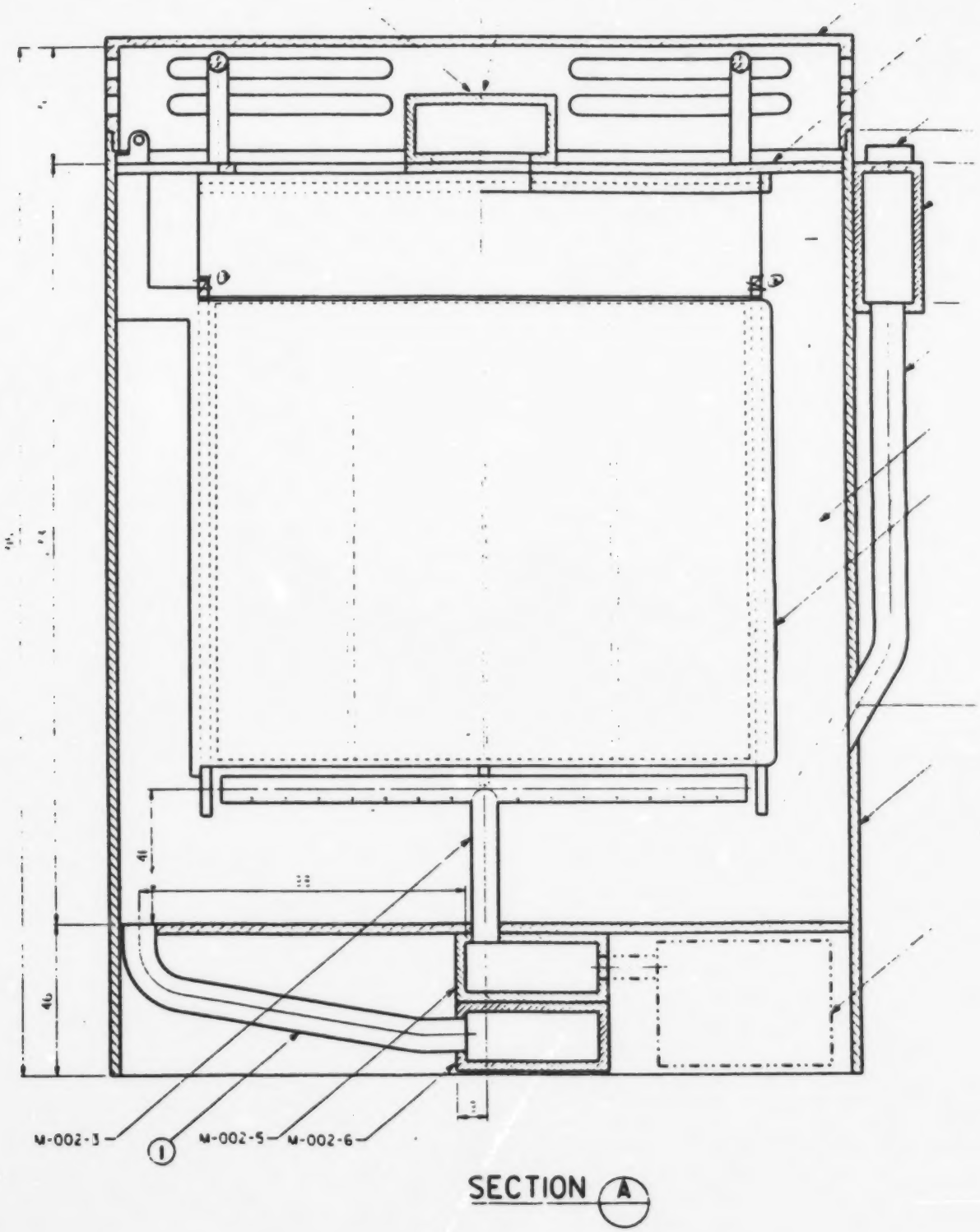

Figure 39 Three cell battery - front view

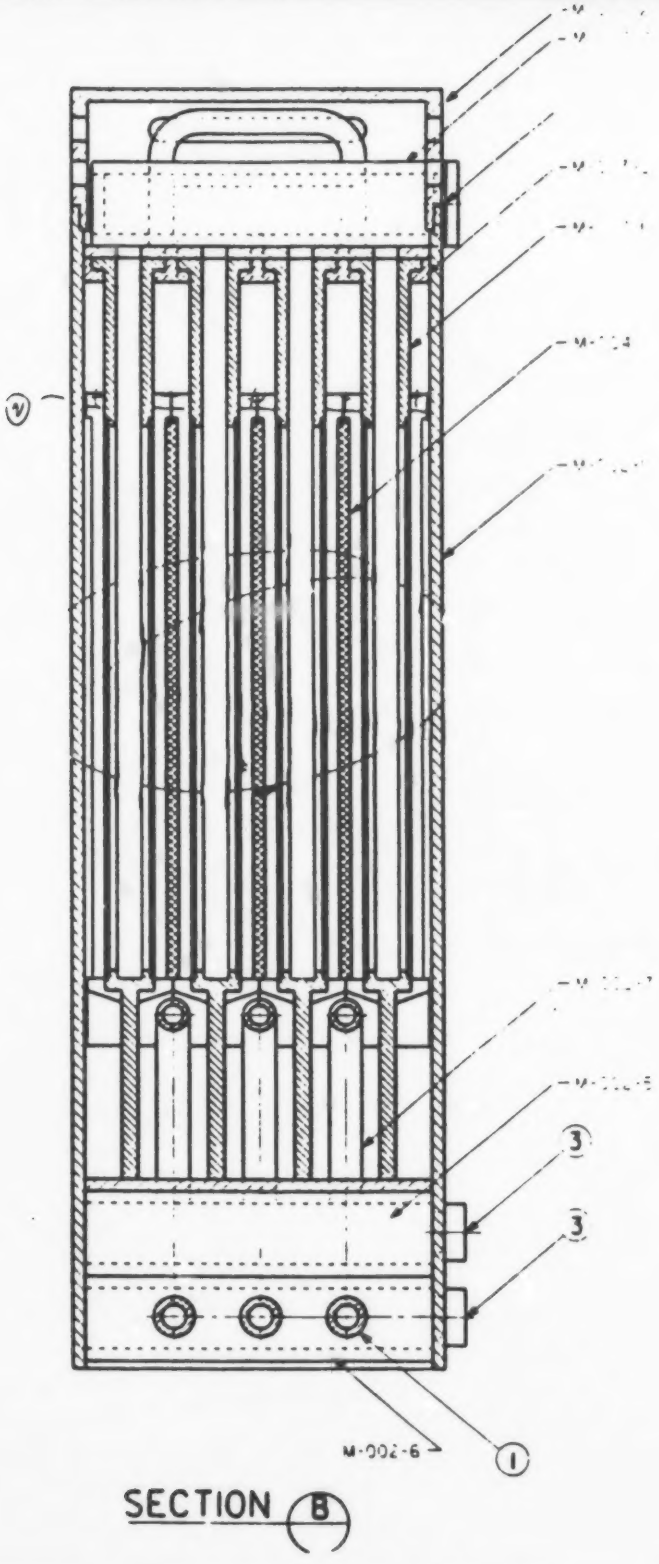

Figure 40 Three cell battery - side view

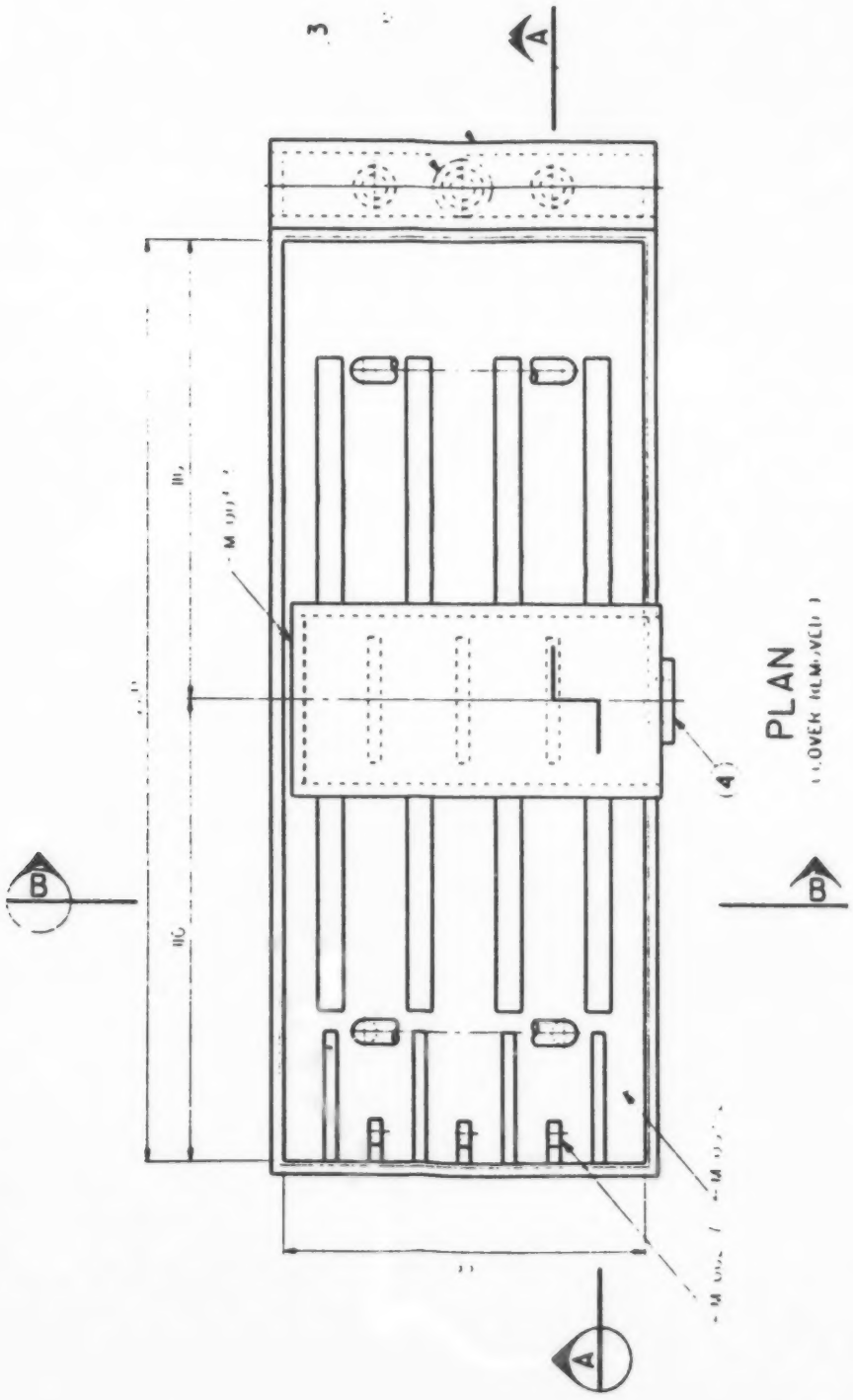

Figure 41 Three cell battery - top view

Figure 42 Three cell battery test apparatus

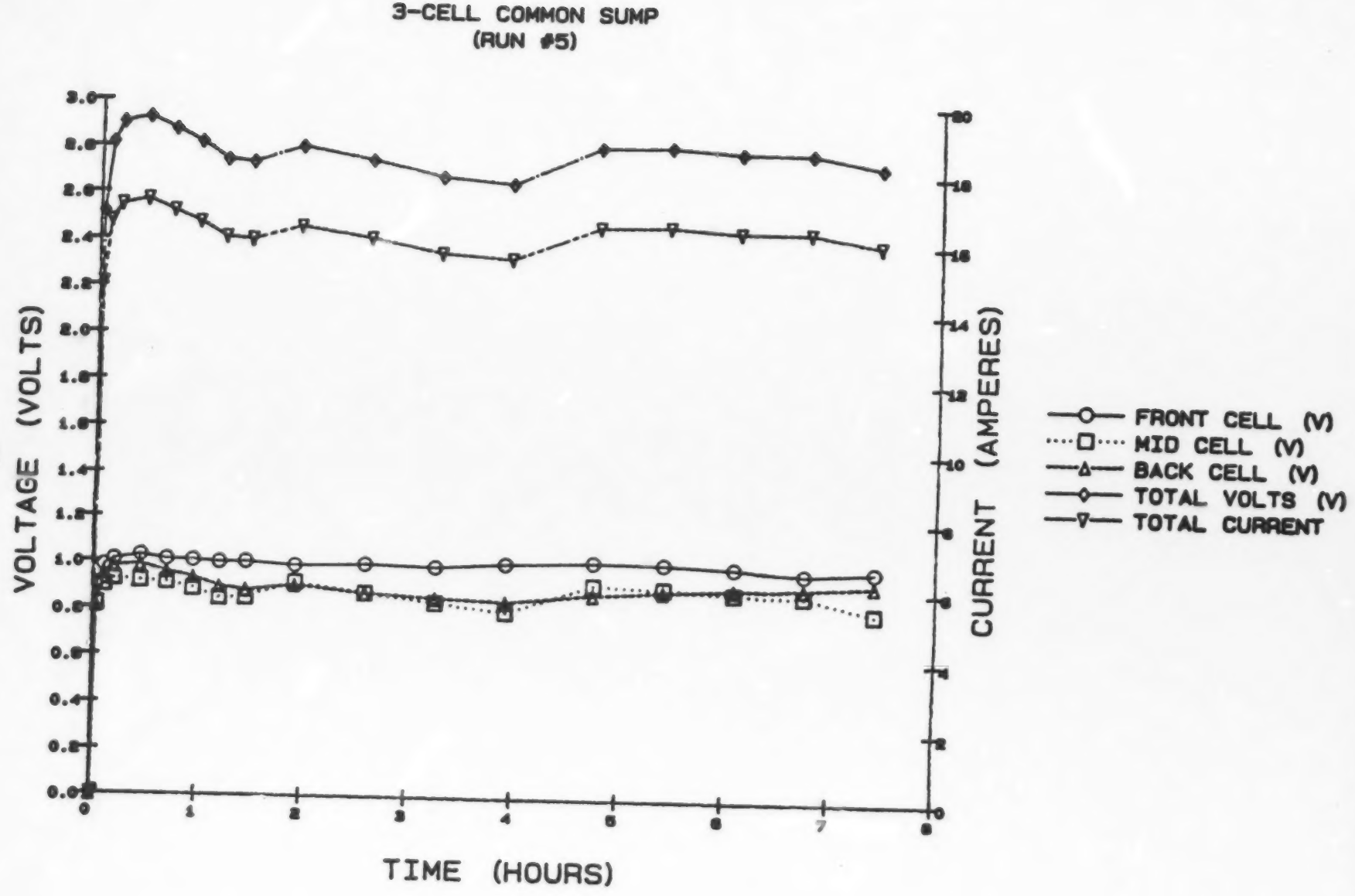

Figure 43 Three cell battery performance

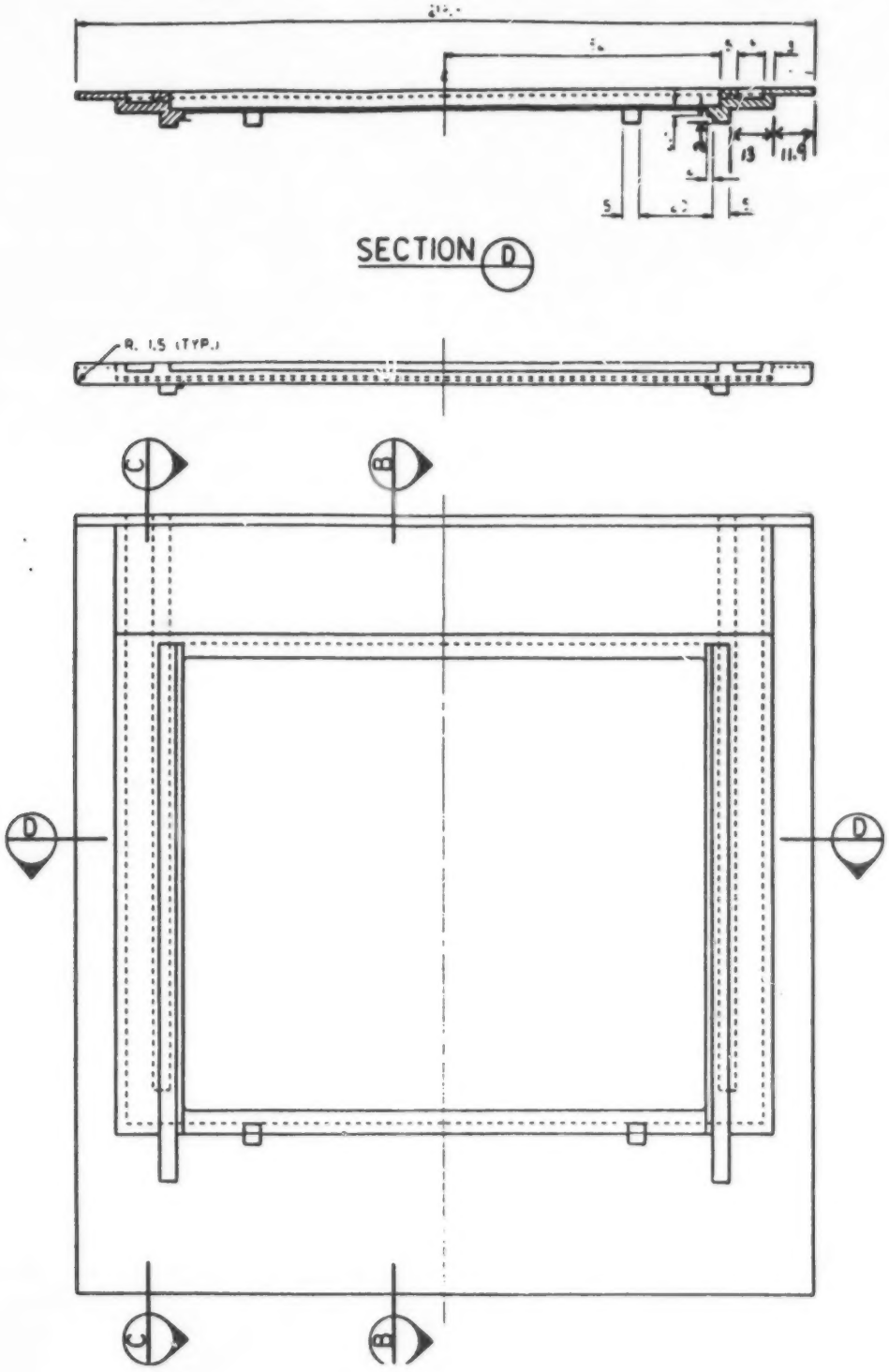

Figure 44 Final prototype design - air cathode cassette (front view)

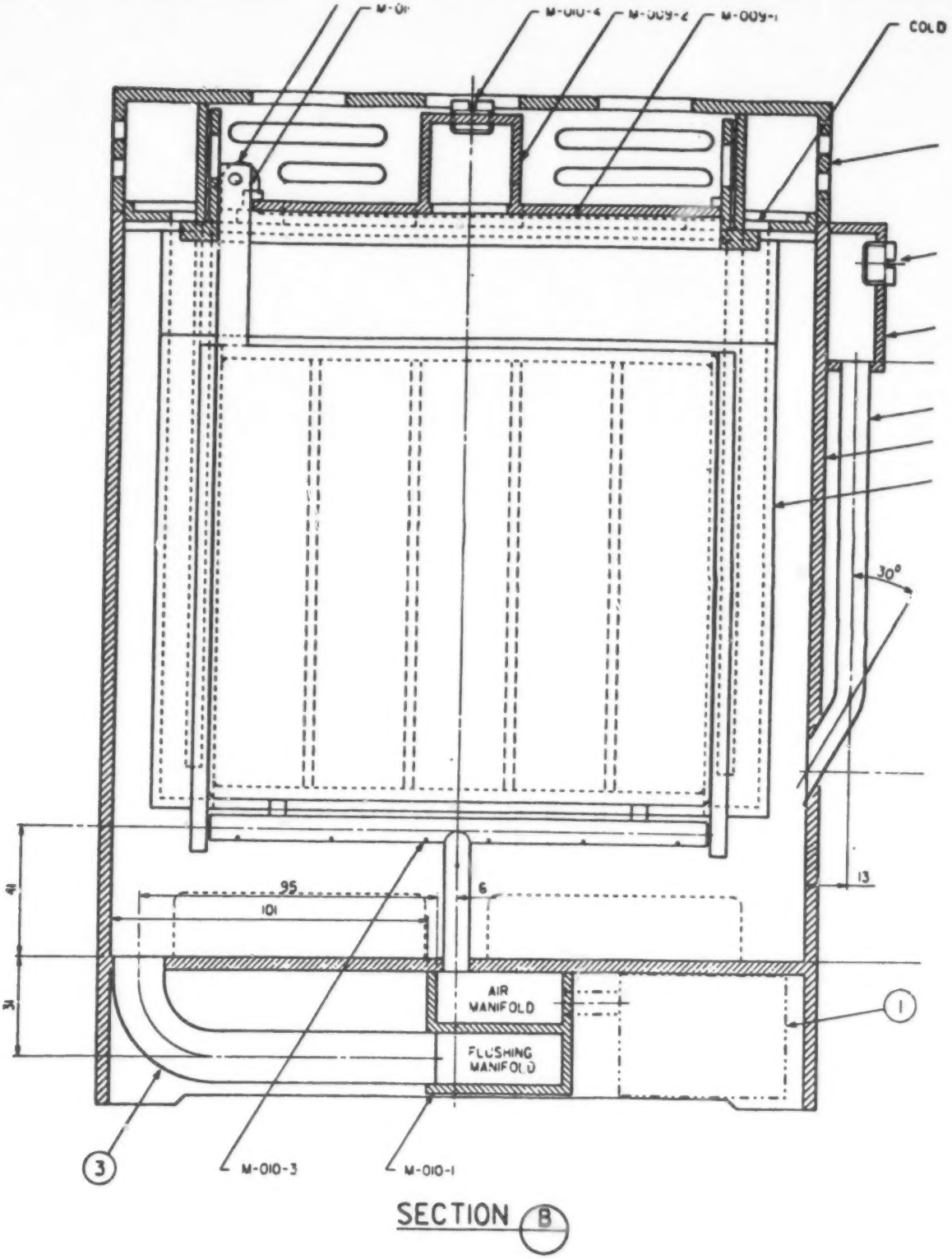

Figure 45 Final prototype design - battery end view

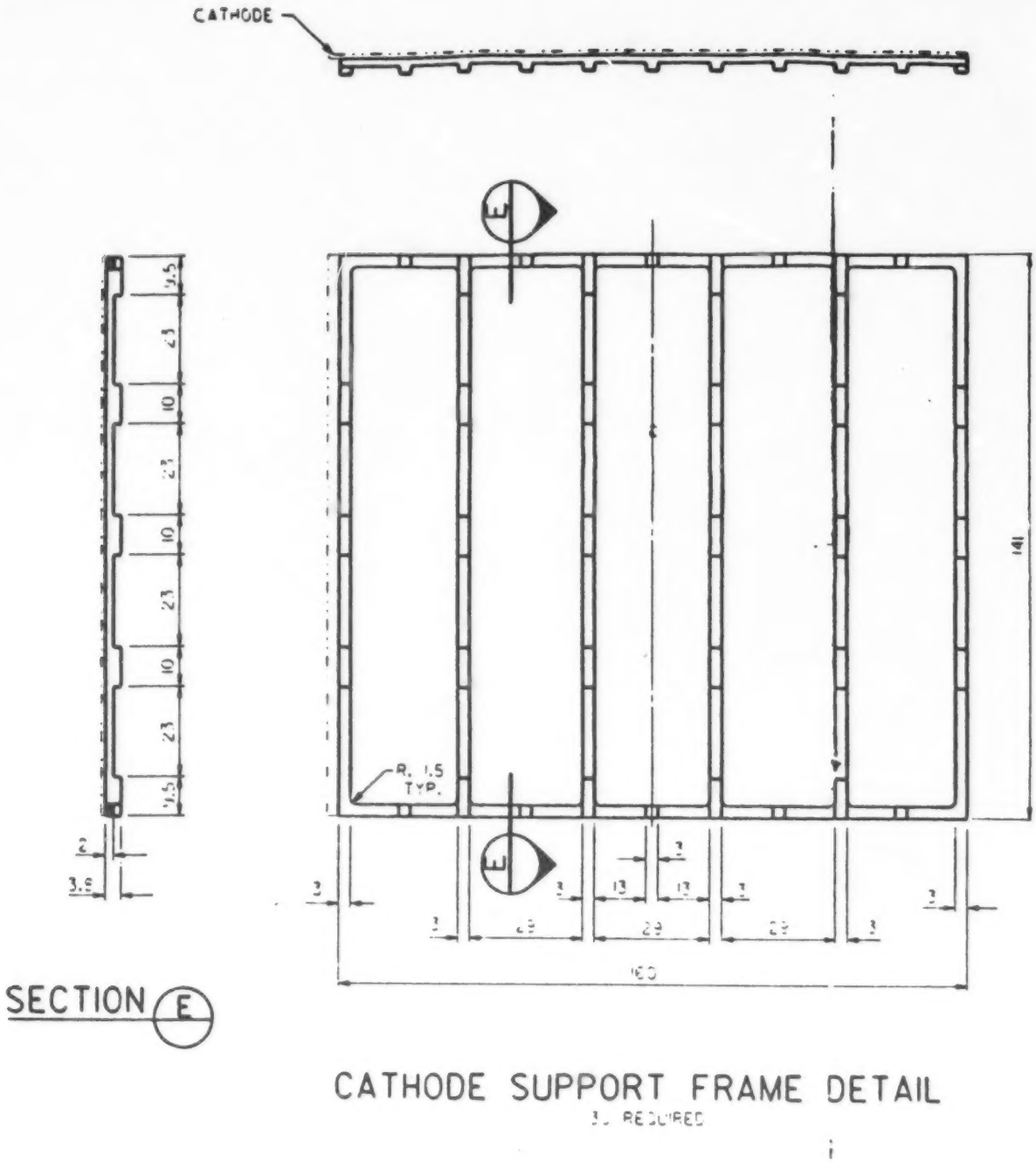

Figure 46 Final prototype design - cathode support frame

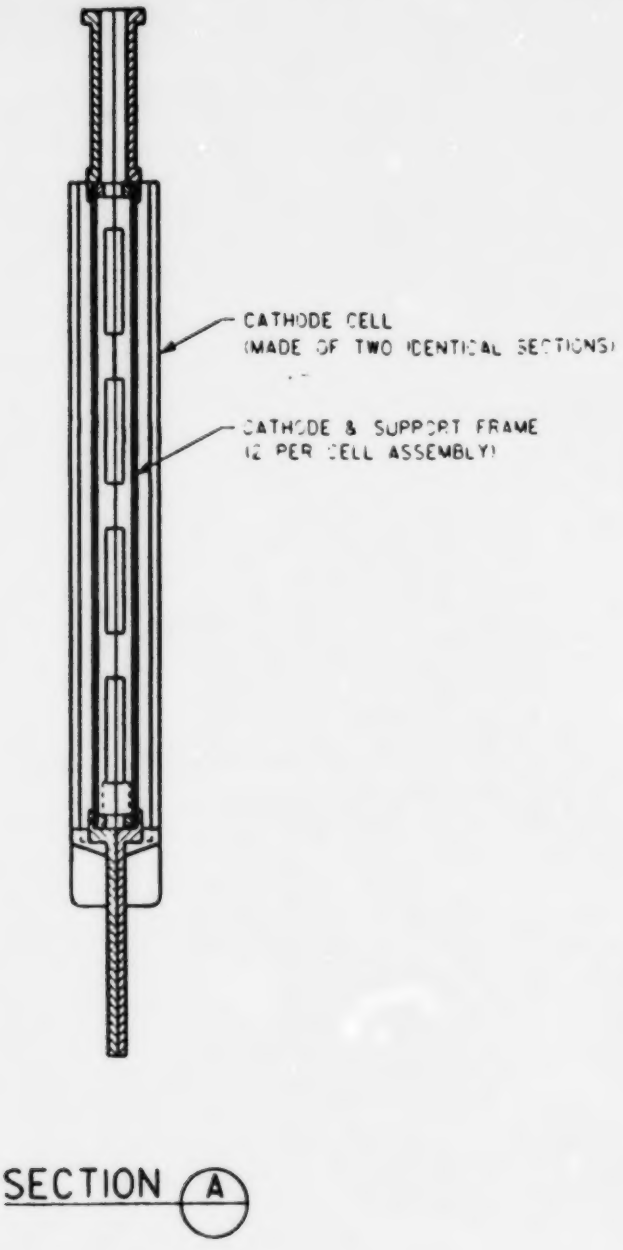

Figure 47 Final prototype design - cathode cassette assembly

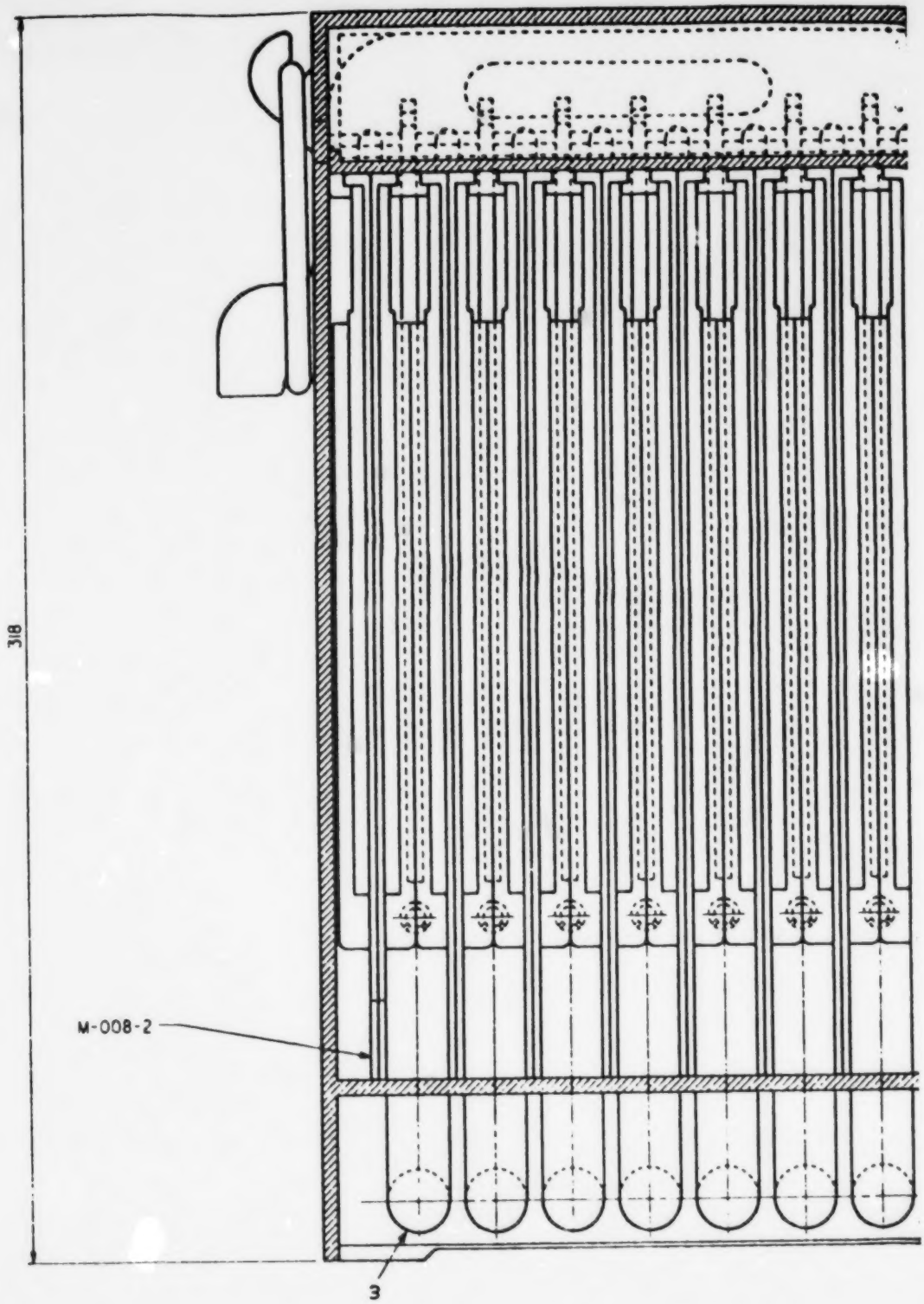

Figure 48 Final prototype design - partial side view

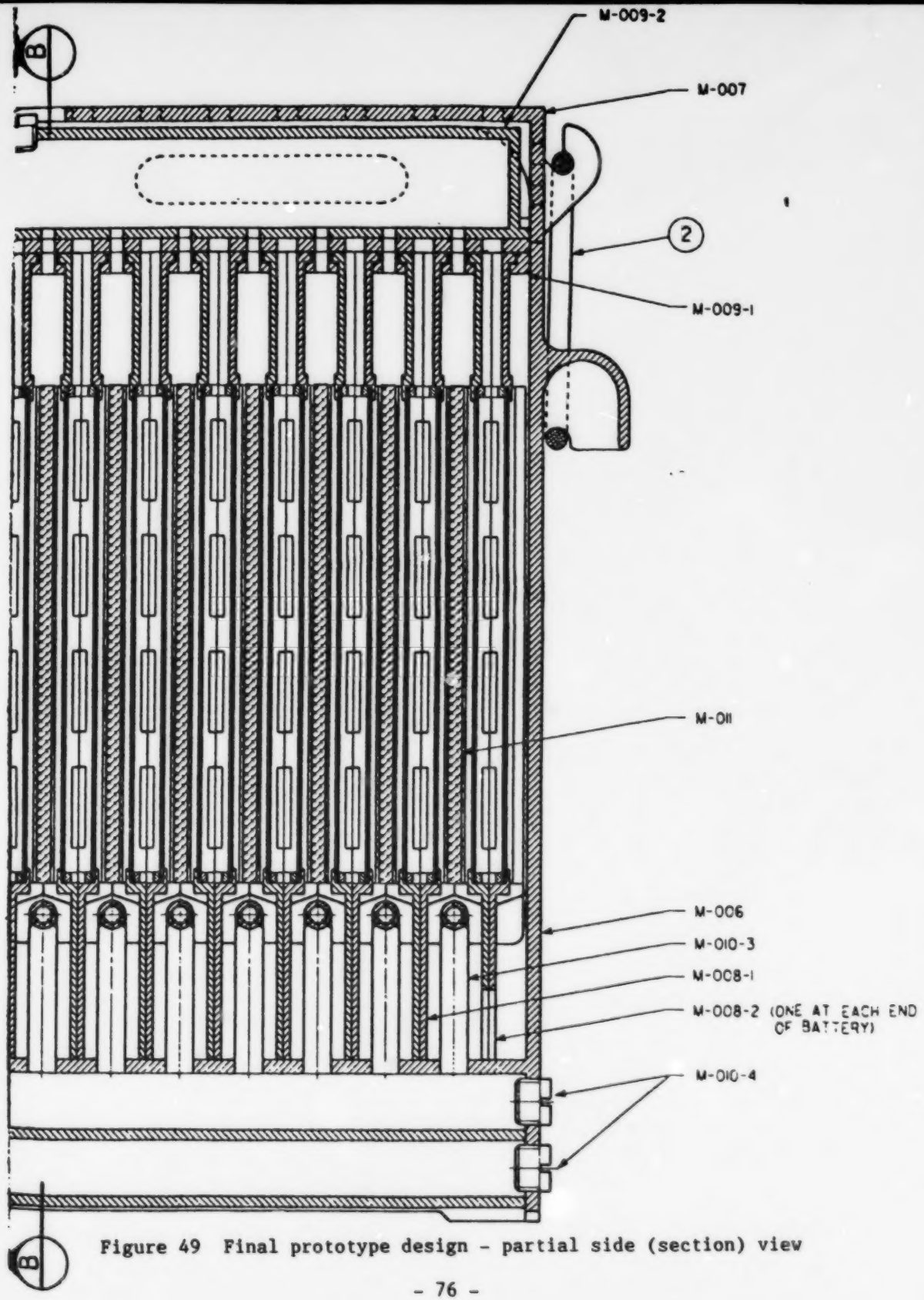

Figure 49 Final prototype design - partial side (section) view

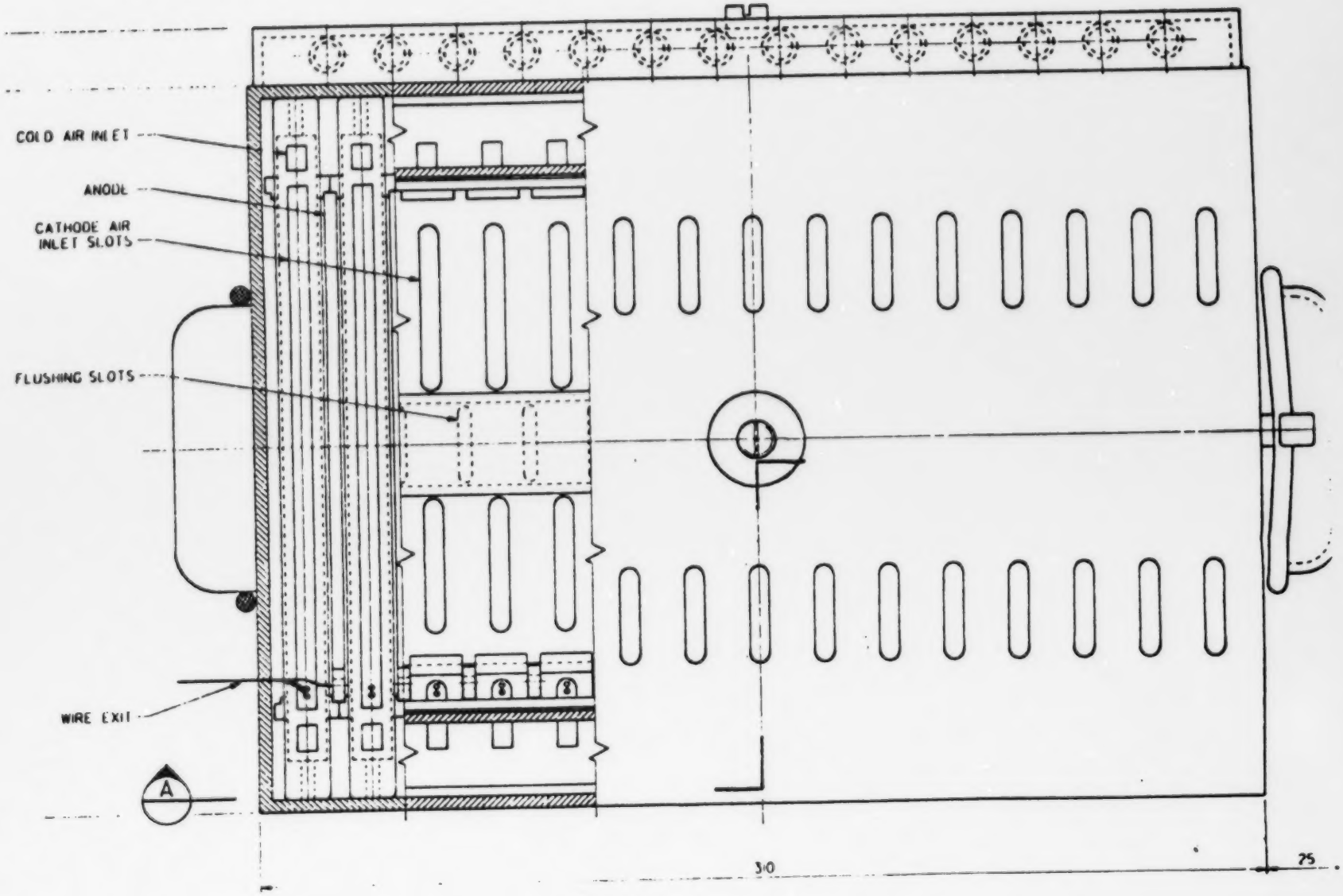

Figure 50 Final prototype design - top view

Figure 51 Final CADD design (1)

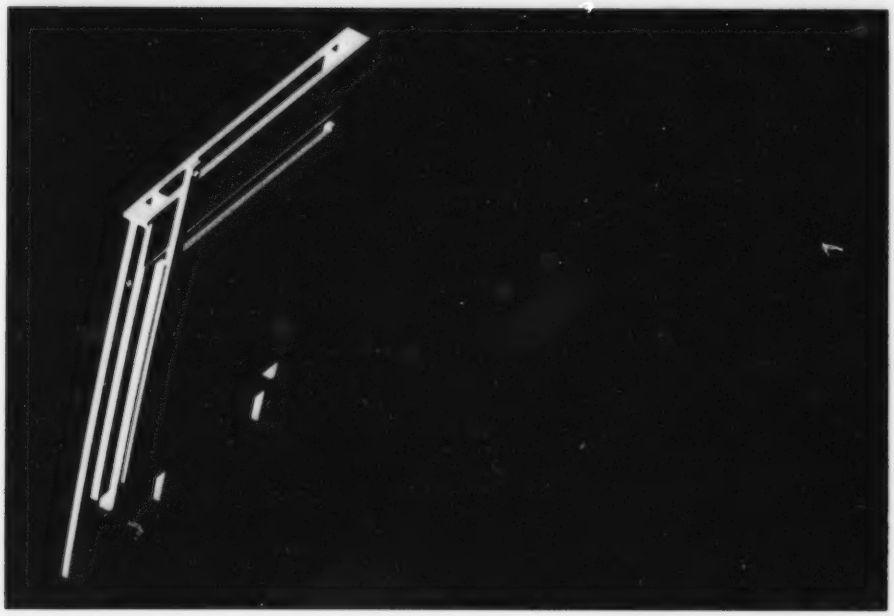

Figure 52 Final CADD design (2)

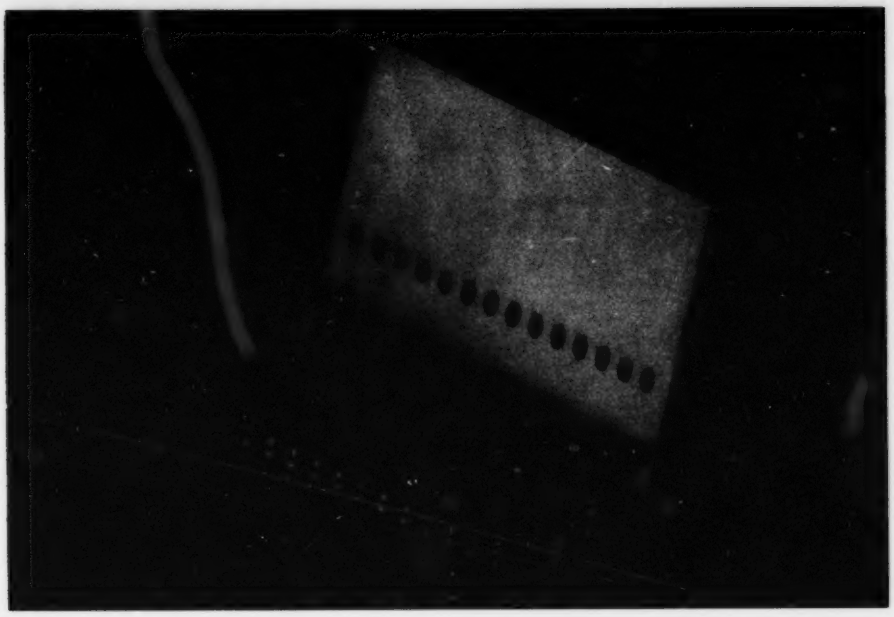

Figure 53 Final CADD design (3)

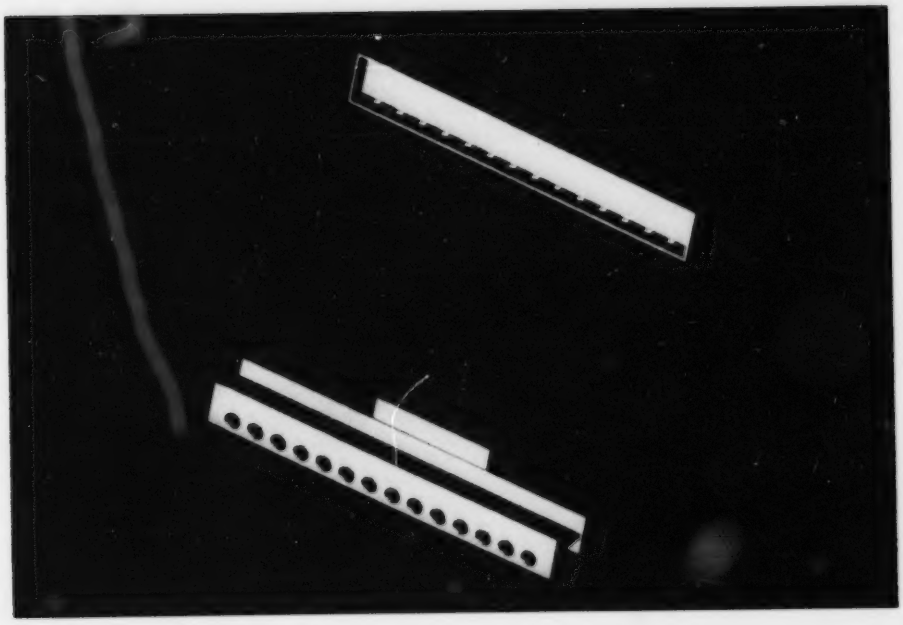

Figure 54 Final CADD design (4)

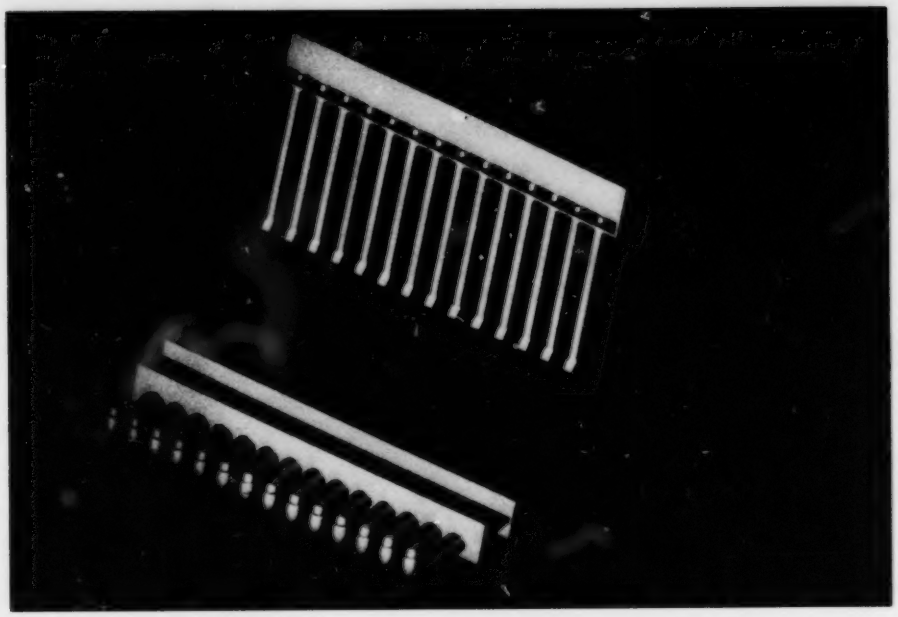

Figure 55 Final CADD design (5)

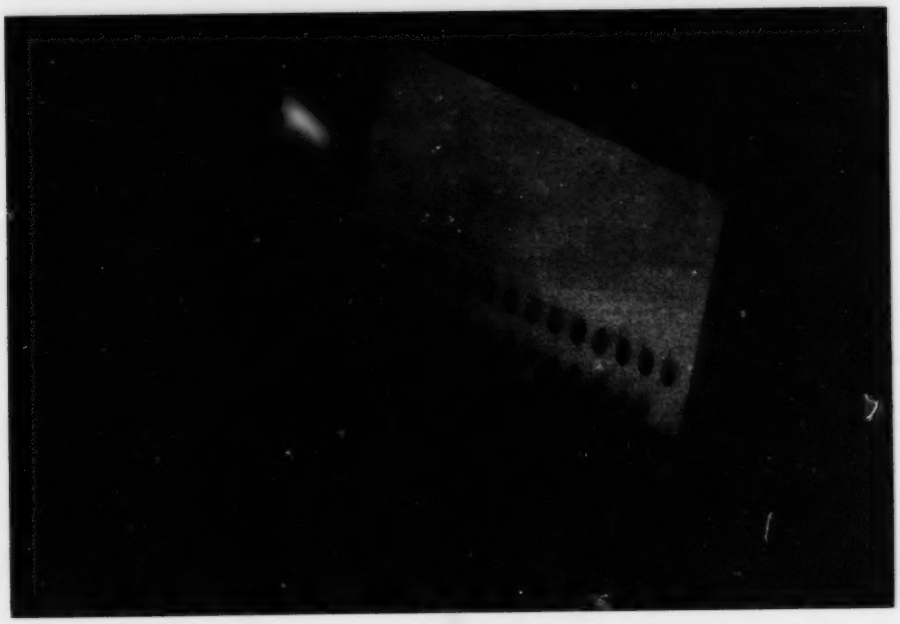

Figure 56 Final CADD design (6)

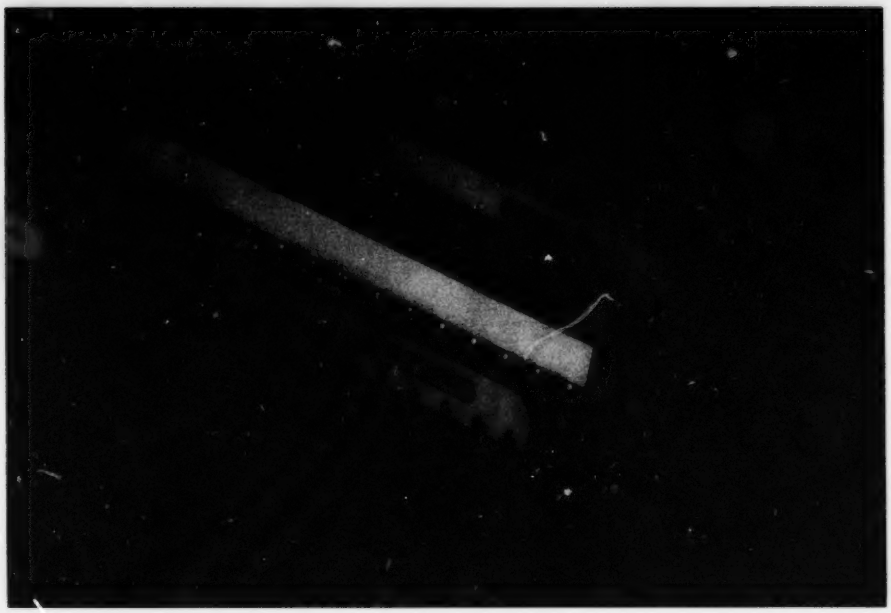

Figure 57 Final CADD design (7)

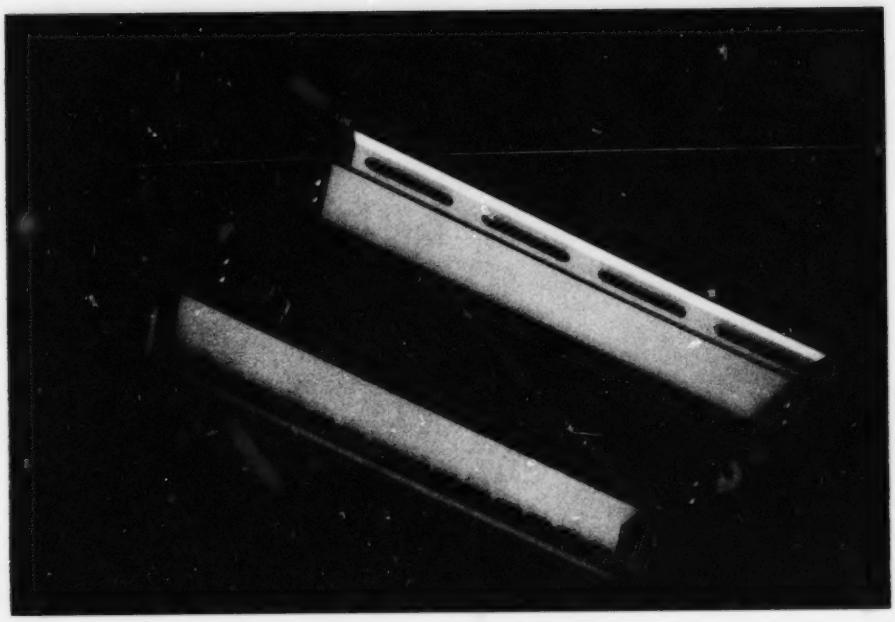

Figure 58 Final CADD design (8)

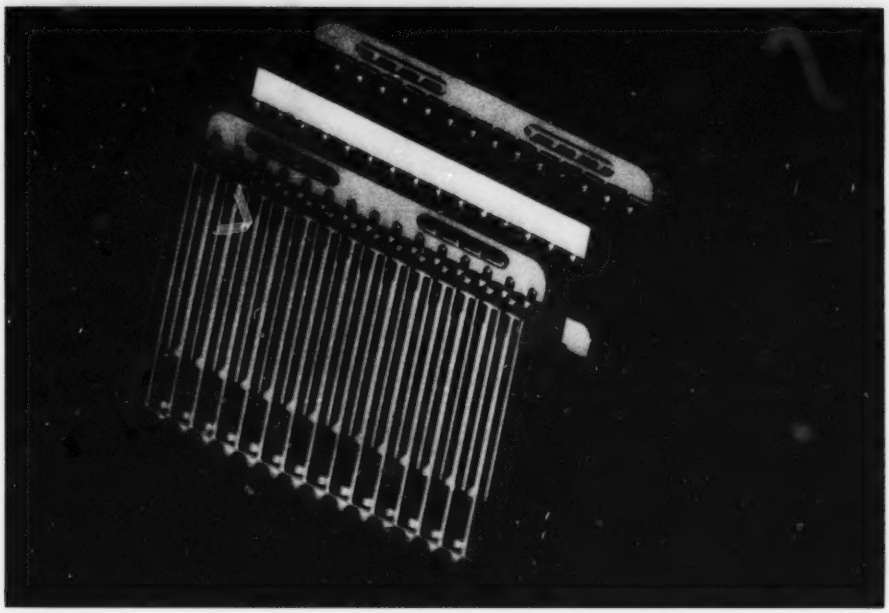

Figure 59 Final CADD design (9)

Figure 60 Final CADD design (10)

Figure 61 Final CADD design (11)

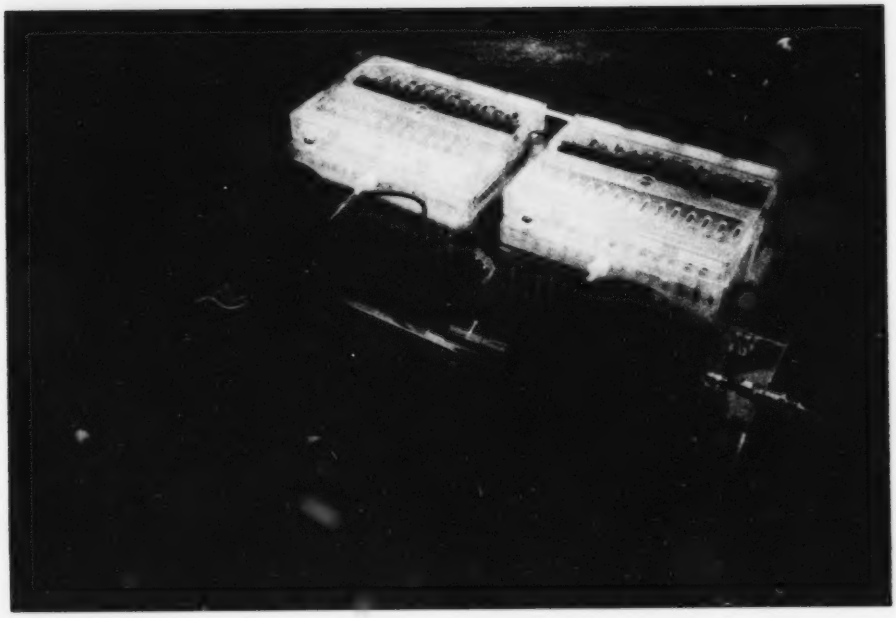

Figure 62 Constructed battery (1)

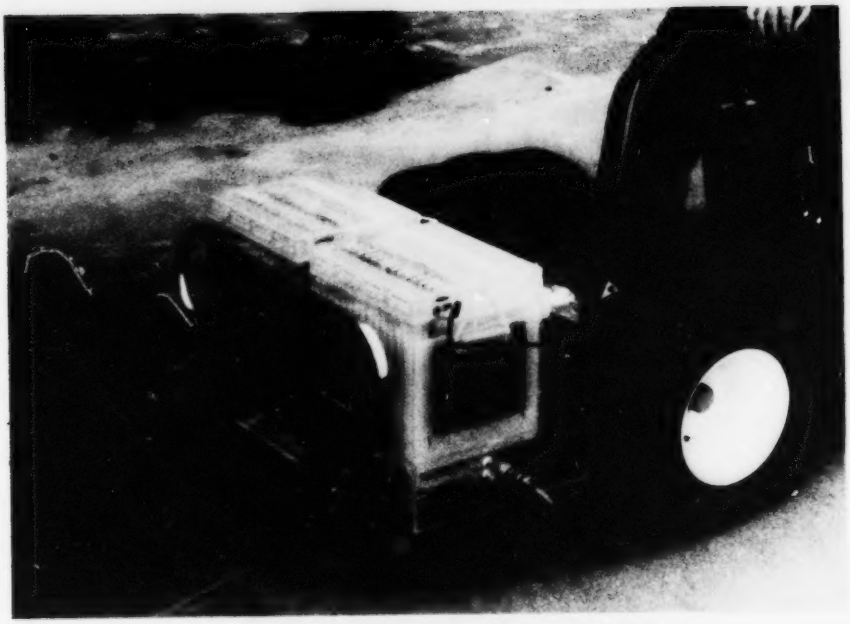

Figure 63 Constructed battery (2)

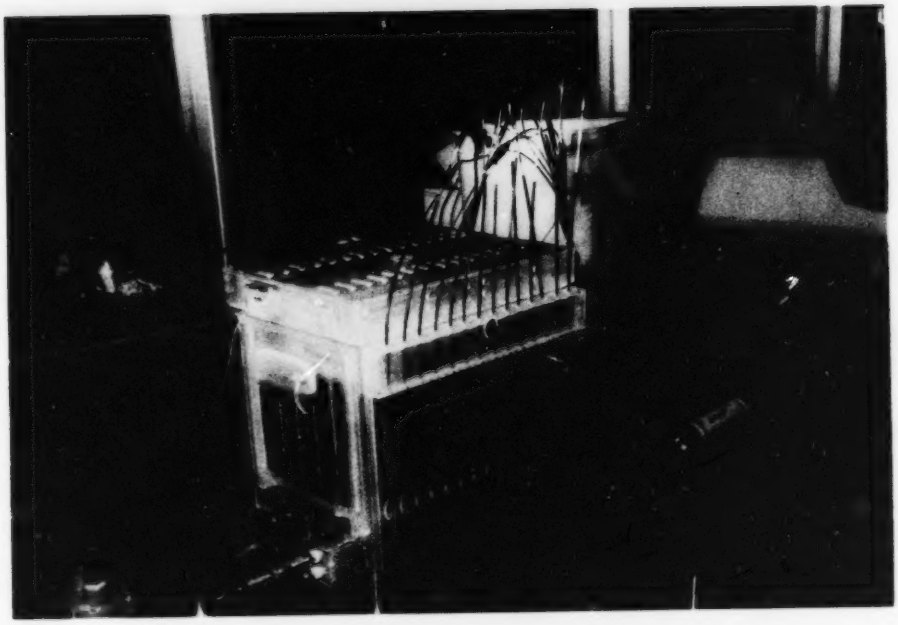

Figure 64 Final prototype battery bench test

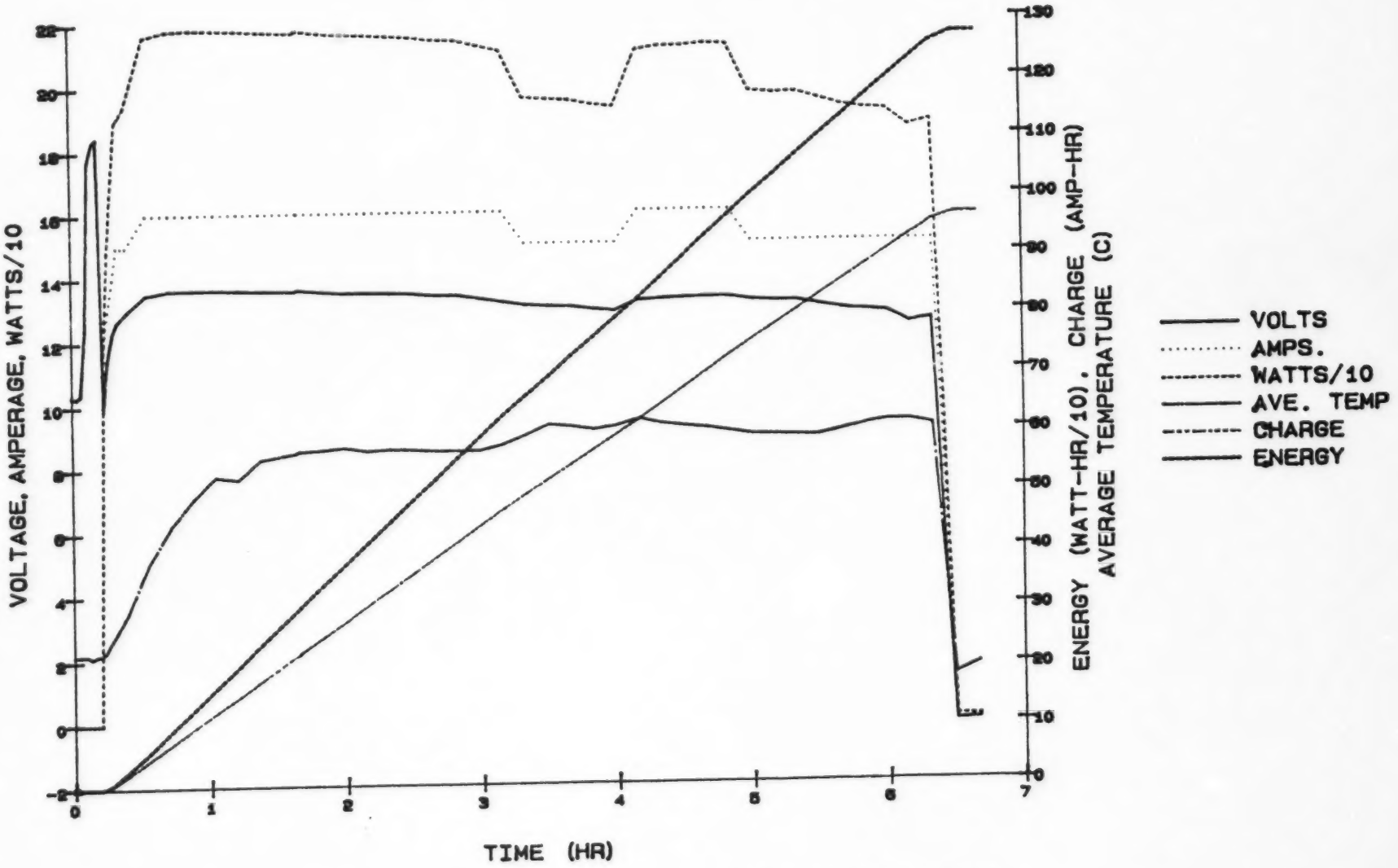

Figure 65 Final prototype battery performance test results

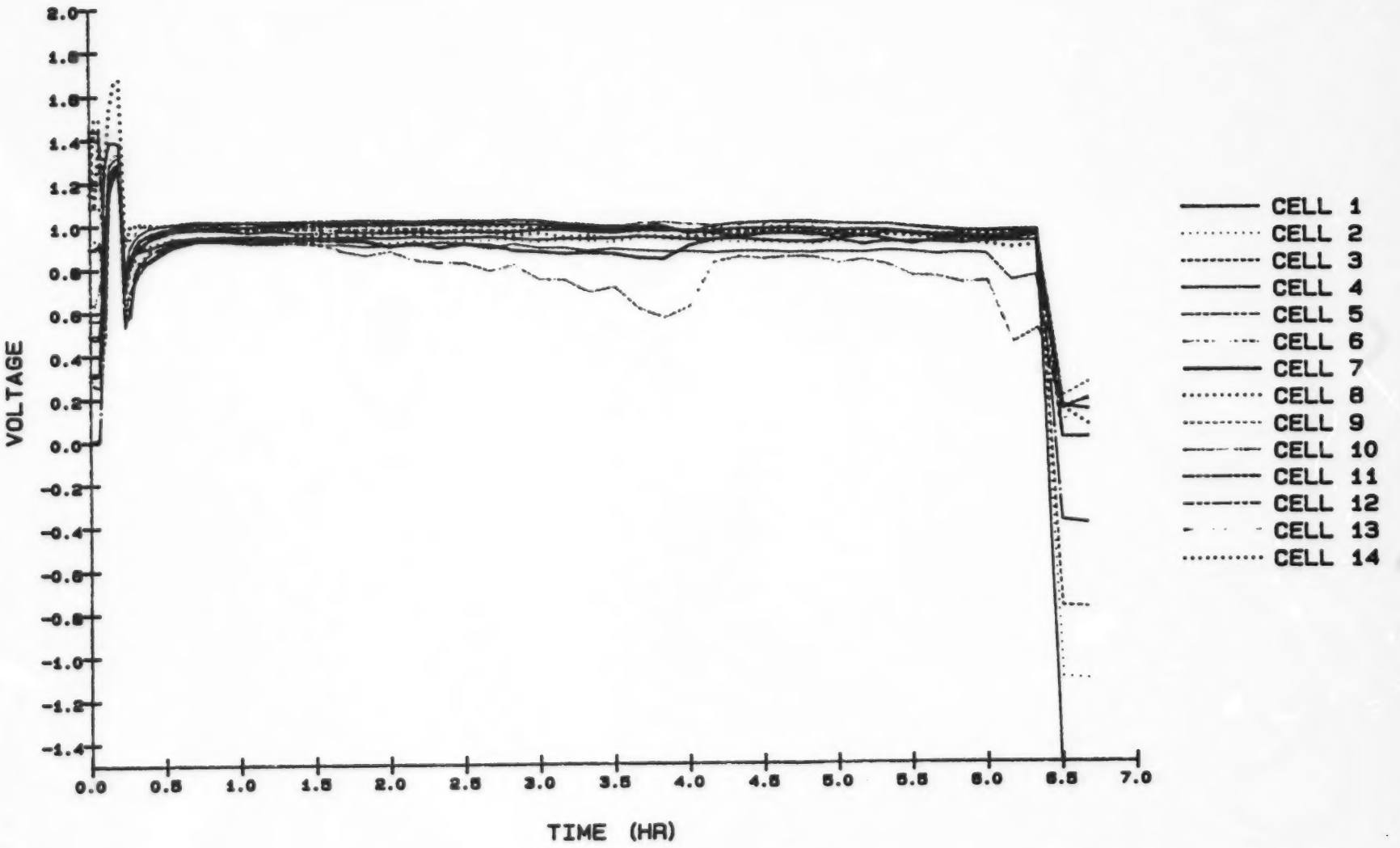

Figure 66 Final prototype battery cell voltages

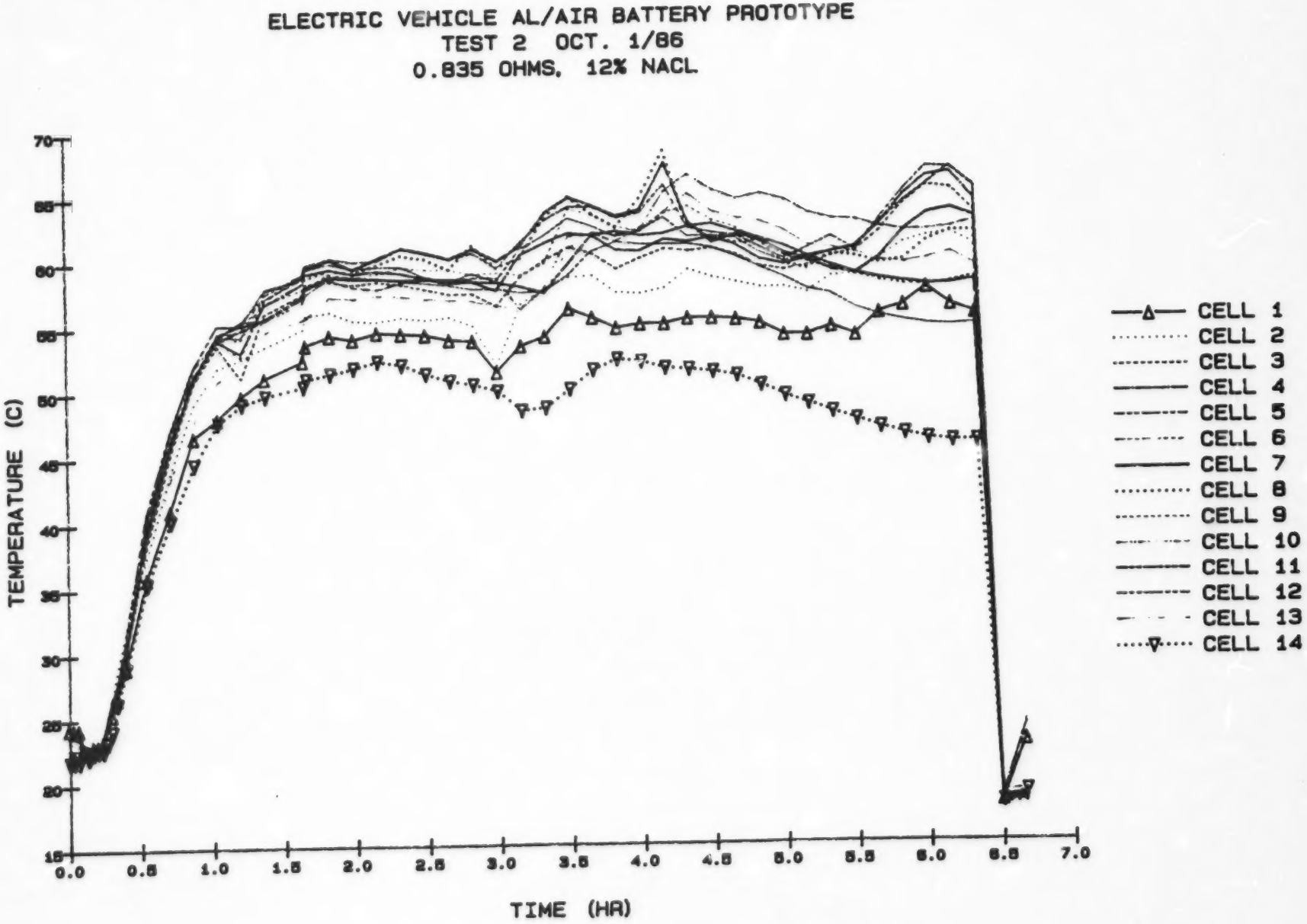

Figure 67 Final prototype battery temperatures

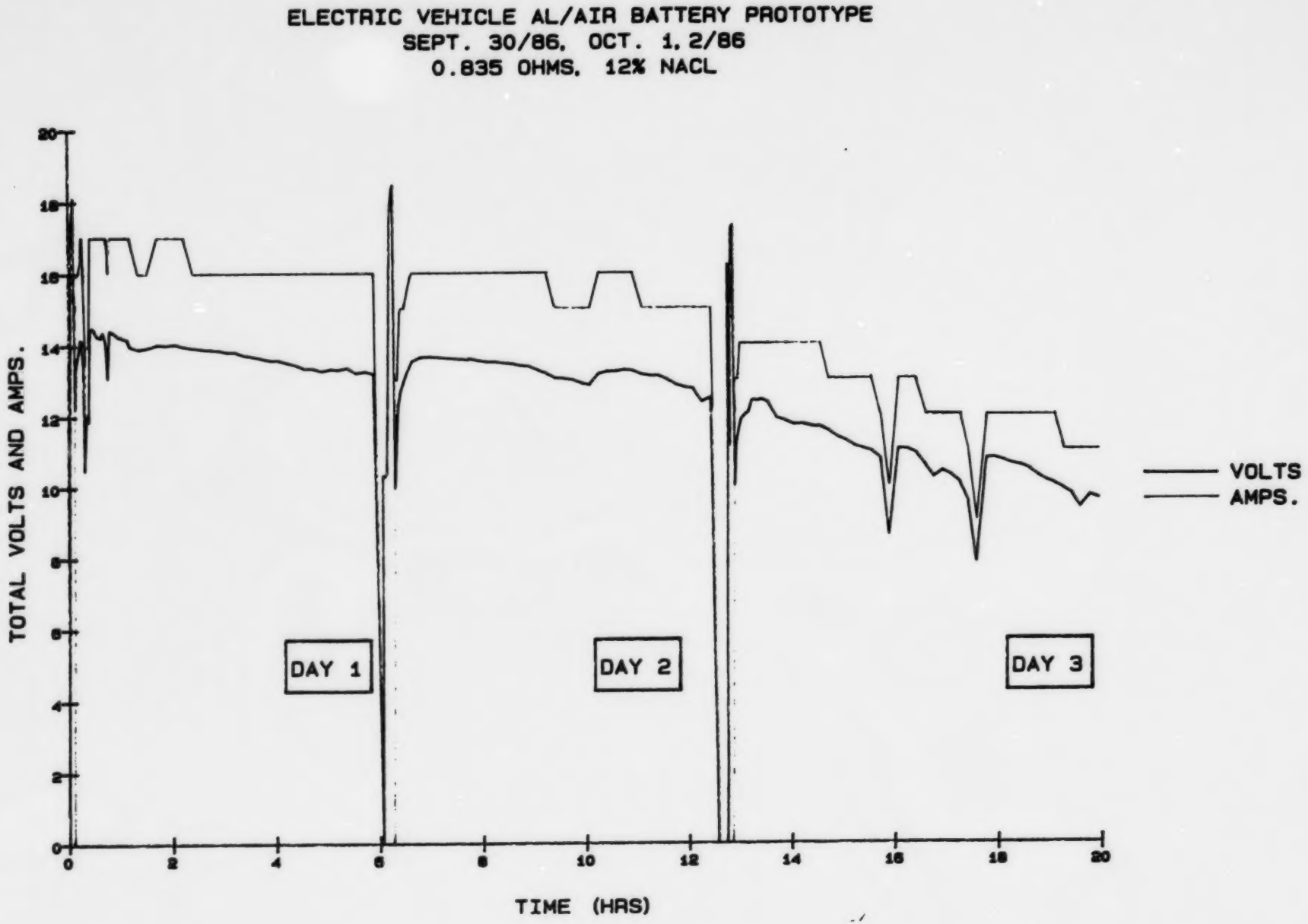

Figure 68 Final prototype battery - three day results

APPENDICES

APPENDIX A

Report on Work Done

Aluminium – Air
Lead – Acid
Interface

J.R van der Post

17th January 1987

INTRODUCTION

Alcan International Ltd has been engaged in a research contract with Transport Canada for the past two years. The objective of this research has been to run a small electric vehicle on a saline electrolyte Aluminium – Air battery: this objective has now been met. To do this it has been necessary firstly to develop the required energy capacity Aluminium – Air battery and secondly to interface this battery to the power demands of the electric vehicle. This interfacing work has been necessary because a saline electrolyte Aluminium – Air battery of sufficient energy capacity (100 – 300 A Hr at 24 V) has a maximum power output of approximately 500 W. A typical small electric vehicle, such as the Battricar Battricaddy used, has a peak power requirement on starting or while climbing of >2 kW; this power is only required for brief periods, and the total energies involved are in the region of 200 to 400 kJ.

This energy requirement can be met by a small 24 V Lead – Acid battery rated at 15 – 25 A Hr quite satisfactorily. As the average power requirement of the electric vehicle is only 500 – 600 W, the Aluminium – Air battery should be able to drive the vehicle quite satisfactorily on a light duty cycle nearly continuously, the principal halts being to refuel the Aluminium – Air battery.

The Lead – Acid battery should be continuously recharged by the Aluminium – Air battery, whilst the vehicle is running; at times of heavy power demand, the output required from the Aluminium – Air battery should be limited to the maximum of approximately 500 W, and the Lead – Acid battery should supply the remaining needs of the vehicle.

A Lead – Acid battery will gas if too high a voltage is applied to it during charging. The Lead – Acid battery will require frequent topping up of electrolyte if it is gassed, which makes the system more complex to operate; it is therefore desireable to be able to use a maintenance – free Lead – Acid battery if possible, which requires that the output voltage from the Aluminium – Air battery be limited to that which does not cause gassing (typically 27.6 V at 30 degrees Celsius for a 12 cell Lead – Acid battery).

The saline electrolyte Aluminium – Air battery has a low power density. In terms of the electrical characteristics of the battery, this low power density manifests itself as a high equivalent series resistance, so that output voltage falls off rapidly with increasing current. For this application of a Lead – Acid battery, it is desireable that the Lead – Acid battery be kept as close to fully charged as possible at all times and be charged as rapidly as possible. This requires a high charging current to be available when the Lead – Acid battery is close to fully charged.

A 19 cell Aluminium – Air battery could be constructed to suit the Lead – Acid battery's gassing requirements. This battery would have a typical open circuit voltage of 27.3 V, depending on the air cathode material and anode alloy used. This battery, however, would only typically deliver 7 A to a Lead – Acid battery discharged to 24 V, which would result in slow charging.

The solution to this problem is to use a higher voltage Aluminium – Air battery and some kind of charging controller. Hence the need for work on interfacing of the Aluminium – Air battery to the vehicle.

Work was done on this interfacing at the University of Southampton from October 1985 until April 1986, and a free running switch mode system tried on the bench for 12 V systems. A full report on this work was submitted in April 1986 (see Southampton University Electrical Engineering Department "Aluminium – Air Lead–Acid Interface", J.R. van der Post, April 1986).

From July 1986 until September, further work was done on this interface system, culminating in the construction of 3 prototype 24 V systems. Two of these prototypes were delivered to Alcan International, Kingston Laboratories, and fitted to the trial electric vehicle. The vehicle ran satisfactorily on Aluminium – Air batteries, using the controller. This report covers the design, function and assembly of the controller system.

FUNCTIONAL DESCRIPTION

A simplified block diagram of the system is shown in figure 3. The output from the Aluminium – Air battery (1) feeds via the switching device (2) to the large storage capacitor (3). The output from the capacitor flows through a current measurement resistor (4) and a reverse flow blocking diode (5) to the lead–acid battery (6). The output voltage is compared to two reference values (with hysteresis). The output current is similarly compared to a reference value.

If the output current is greater than the reference current, then the switching device will be turned off (comparator 7). If the output voltage is greater than the permitted maximum, then the switching device will be turned off (comparator 8). If the output voltage is less than the permitted minimum, then the switching device will be turned off. Only if all three conditions are satisfied will the switching device be turned on. If both the output current and the output voltage are below the allowed maximum values and if the output voltage is above the allowed minimum, then the switching device is turned on, allowing the capacitor to charge. If either output quantity is above the permitted maximums then the switching device is turned off, and the capacitor slowly discharges through the load until both quantities are below reference value, when the switch is again turned on.

If the output voltage is pulled below the allowed minimum, the output is shut off and will not turn on again until the unit is either turned off and on, or until the output voltage rises again to within allowed limits; this protects the controller from trying to charge a Lead – Acid battery that has been discharged excessively, beyond the point of possible damage to the Lead – Acid battery.

A detailed block diagram is shown in figure 4. The principal factor of note is the system required to provide the power supplies for the measurement circuitry. It is necessary to synthesise a positive supply to give symmetrical supplies for the comparators to minimise common mode pick – up. This synthesis is performed by an oscillator and a charge pump. The supply is initially regulated to provide a supply for the gate drive circuitry that does not exceed the allowable maximum V_{gs} of the FETs, and regulated to provide a negative supply that powers the oscillator, charge pump and measurement circuitry. The supply for the charge pump and the output from the charge pump are both then further regulated to eliminate the switching spikes from the power oscillator, giving a clean, symmetrical supply for the measurement circuitry.

The level shifting is performed by an opto – isolator. This requires a 5 V supply, which is provided by a 78L05 voltage regulator from the gate drive's supply. This 5 volt supply is split by a potential divider, and the result fed with the opto – isolator output to a comparator which then drives the gate drive transistors.

Detailed circuit diagrams are shown in figures 6, 7 and 8.

Power Supplies: in figure 6, the power board circuit diagram, the output of the Aluminium − Air battery is connected to terminals A and H. Terminal A (the positive terminal of the Aluminium − Air battery) is connected to the chassis tray and used as the 0 V reference point. The source terminals of the FETs are connected directly to terminal H − this point is nominally at −40 V. The gate circuit requires a fixed supply relative to this point. IC 2, D 13/14/15, C 5/6/11/12 and R 7/8 form a variable output voltage regulator, referred to the source terminals of the FETs; the output of this is set to approximately 12 V. D 13 limits the maximum input experienced by the IC to survivable levels, D 14 acts to allow C 6 to hold up the input to the IC when the supply falls momentarily during switching, and D 15 protects the regulator during turn − off. The output from this regulator is nominally −28 V, and is also used to power the receive half of the level shifter circuit in figure 7.

IC 1, D 11/12/16, C 3/4/9/10 and R 7/8 form a variable negative voltage regulator, referred to 0 V; the output from this regulator is set to −12 V and used indirectly to provide the power for all the measurement circuits in figure 7.

In figure 7, the −12 V supply is used to power an NE 555 oscillator, consisting IC 4, C 22/23/24 and R 34/35, and to power a −5 V regulator built from IC 2, C 12/13 and D 14. This regulator provides the negative supply for the measurement circuits. The output of this oscillator drives a charge pump built from C 14/18/19/20/21 and D 17/18. The output of the charge pump, which is positive with respect to the 0 V line, drives a +5 V regulator built from IC 1, C 10/11 and D 16. This regulator then provides the positive supply for the measurement circuitry. The output from the positive regulator is also used to power a simple voltage reference circuit consisting R 26, IC 5 and C 9.

Current Measurement Signal: the output current to the Lead − Acid battery is sensed by a resistor chain which is built in to the track pattern of the power PCB − see figure 6. Connections can be made to this resistor chain at one of 5 points: the lower the output current limit, the higher the resistance required. The voltage from the resistor chain, as a result of the current flowing through it, is fed to a buffer amplifier on the control board (see figure 7). This buffer is built around a CA 3140 operational amplifier, and consists of IC 6, R 1/2/3/4/5 and C 1/2. The output offset can be nulled by adjusting R 2 − this is done with no current signal (ground the input, line 8 in the ribbon cable). The gain of the amplifier is adjustable (R 4), and this is used to adjust the current sensitivity, by varying the signal fed to the comparator circuit.

Comparators: Figure 5 shows the basic comparator circuit used. R 1 and R 2 form a potential divider: the voltage at the inverting input (V 1) is given by:
$V\,1 = ((R\,1 \times V_{ref}) + (R\,2 \times V_{in}))/(R\,1 + R\,2)$

When the output is low, the non − inverting input (V 2) is at 0 V. When the output is high, the voltage at this input is given by:
$V\,2 = (R\,3 \times (V_{out} - \text{Diode forward drop}))/(R\,3 + R\,4)$

If the non − inverting input is at a greater voltage than the inverting input then the output will be low, and vica − versa. If a positive reference voltage is used, with a negative input, it can be seen that the system has hysteresis such that it will behave as follows: when the input is substantially more positive (i.e. less magnitude) than the value required for V 1 = 0 V, then the output will be negative. As the input reaches the value such that V 1 becomes greater than 0 V, then the output swings positive. The non − inverting input is then driven positive by the amount shown in the equation for V 2 above. Until the input swings to a magnitude such that V 1 is more positive than the voltage at the non − inverting input, the output will remain positive: when the crossover is reached, the output will swing negative again.

The amount of input overshoot that is required depends on the gain, the bandwidth and the slew rate of the operational amplifier or comparator used (the more the open loop gain, the less the input required to shift the output). The capacitor C 1 is a proven way of speeding up the switching of the circuit. It also prevents the circuit switching in the opposite direction until the capacitor has charged up to the difference between the output and 0 V via R 3.

The current buffer output drives a comparator of the type described above (see figure 7), which is built around IC 7a, R 6/7/8/9/10/14, C 4/5 and D 2. The input potential divider is built from R 6/7, which is fixed ratio − the trip level of the comparator is fixed, and the current level is adjusted by varying the gain of the buffer. R 14 adjusts the hysteresis of the comparator, and C 4 is used to provide latching out of any ground line signals resulting from the switching process.

The output voltage drives two comparators, one for output voltage regulation, and one for under voltage protection. The former is built from IC 8a, D 9/10/11/12/13, R 18/19/20/21/22/23/25 and C 8, the latter from IC 7b, D 3/4/5/7, R 11/12/13/15/17 and C 3/6. The voltage regulation comparator has a variable input potential divider which adjusts switching level and, hence, output regulation voltage; the maximum voltage swing of the IC's input is limited to safe areas by the voltage clamp formed by D 10/11/12/13 − these diodes have to be fast, low capacitance types. Hysteresis is adjusted by R 20. The under voltage protection comparator has a variable input comparator which adjusts the trip level; it is configured slightly differently to the simple comparator circuit in figure 5 − to operate for under voltage, instead of over voltage, the potential divider feeds the non − inverting input together with the feedback signal, and the resultant is compared to 0 V. This comparator is given substantial hysteresis, (see the output voltage characteristic − figure 17).

Combinational Logic: if the output of any comparator goes high, the FETs should be turned off. Hence, D 1/6/8 and R 24 (which form an "or" gate) are connected to the comparators' outputs. The signal from this "or" gate is buffered by IC 8b, R 24/28/29 and C 7. The output of this buffer drives the input side of the opto − isolator (IC 9), via a current limiting resistor R 27.

Level Shifter and Mosfet Gate Drive: the opto − isolator provides level shifting from the 0 V level to the −40 V level. IC 3, D 15 and C 15 provide a −35 V supply to drive the output side of the opto − isolator. R 31 is a pull − up resistor for the open − collector output of the opto − isolator. The output of the opto − isolator is compared to the output of a potential divider between the −35 V and −40 V rails (R 32/33 and C 16), by IC 10, R 30 and C 17 which buffer this signal and level shift it to a swing between the −28 V and −40 V rails. This signal is then carried by the ribbon cable from the control PCB to the power PCB, where it is used to drive the gate drive transistors (see figure 6). TR 3/4, R 3/4/9, C 7/8 and D 3/4/5/6/7/8/9/10 form the gate drive circuit. The transistors are power darlingtons, and they are driven by Baker clamp networks, zener shifters and speeded up current limiting resistors. R 1/2 limit the surge current into the gates of the FETs on switching to that which will produce switching at maximum rated speed, assuming a straight line, 3 time constant model.

To drive the FETs at maximum speed, the output current capacity of the driver stage should be as high as possible. If a single transistor (Class "A" style) output were used, the quiescent current of the stage would be high: for this reason, a push−pull drive is used: there are a range of possible circuits that could be used, some offering better quiescent current consumption than others. The circuit used is reasonably efficient, and has the advantage that its output swings to within 1 Vce sat of each supply rail, enabling the FETs to be turned hard off. With the base currents used, the transistors are capable of driving a current of up to 1 A (but not the presence of R 9 which limits this) in the gate lines.

Decoupling Capacitors: There is a large number of additional capacitors connected across the various low power supplies for smoothing and decoupling. Before any final production design is submitted, the number and position of these capacitors should be looked at − initially, an excess has been fitted to ensure adequate decoupling, and the number may be reducible, saving parts cost and assembly time.

RESULTS

The controller has been run satisfactorily on the test bench. No operating results have been received from Kingston. On the test bench, a peak efficiency of 94% was measured. Figures 17 and 18 show the operating curves. No − load voltage ripple was measured as $< 2\%$. Output current limit was initially set to 20 A. Output voltage regulation was set to 27.6 V. Under voltage protection was set to approximately 15 V. The overall weight of the sample assembly was approximately 1.7 kg.

PARTS LISTS

The parts lists follow on the next pages. The prices shown are approximate prices for sufficient parts for 100 units. The approximate price for the parts for a batch of 100 units is £85 per unit. The printed circuit boards are not included in the price or the parts lists. They should be produced to the drawings in figures 9 to 14. The control PCB should be made in 1 oz copper board with single thickness base, the power board in 2 oz copper with a double thickness base.

Parts List - Control Board, Sheet 1

Part	Value	Type and Source	Farnell Order Code		Price / 100
IC 1	LM 340T-5	National Semiconductor	STC/FARNELL	LM 340T-5	41.00
IC 2	LM 320T-5	National Semiconductor	STC/FARNELL	LM 320T-5	133.00
IC 3	78L05	National Semiconductor	STC/FARNELL	LM 78L05ACH	110.00
IC 4	NE 555	Signetics / National	STC/FARNELL	NE 555N	31.00
IC 5	ZN 458A	Ferranti	STC/FARNELL	ZN 458A	66.00
IC 6	CA 3140	R.C.A.	STC/FARNELL	CA 3140E	34.00
IC 7	LM 393	National Semiconductor	STC/FARNELL	LM 393N	39.00
IC 8	LM 393	National Semiconductor	STC/FARNELL	LM 393N	39.00
IC 9	6N 137	Hewlett Packard / G. Instrument	STC/FARNELL	6N 137	392.00
IC 10	LM 393	National Semiconductor	STC/FARNELL	LM 393N	39.00
IC 11	Socket Only -------	See page 3.			
D 1	OA 91	Mullard	FARNELL	OA 91-05	6.00
D 2	OA 91	Mullard	FARNELL	OA 91-05	6.00
D 3	OA 91	Mullard	FARNELL	OA 91-05	6.00
D 4	OA 91	Mullard	FARNELL	OA 91-05	6.00
D 5	OA 91	Mullard	FARNELL	OA 91-05	6.00
D 6	OA 91	Mullard	FARNELL	OA 91-05	6.00
D 7	OA 91	Mullard	FARNELL	OA 91-05	6.00
D 8	OA 91	Mullard	FARNELL	OA 91-05	6.00
D 9	OA 91	Mullard	FARNELL	OA 91-05	6.00
D 10	OA 91	Mullard	FARNELL	OA 91-05	6.00
D 11	OA 91	Mullard	FARNELL	OA 91-05	6.00
D 12	OA 91	Mullard	FARNELL	OA 91-05	6.00
D 13	OA 91	Mullard	FARNELL	OA 91-05	6.00
D 14	IN 4148	Fairchild / I.T.T.	STC/FARNELL	IN 4148	3.00
D 15	IN 4148	Fairchild / I.T.T.	STC/FARNELL	IN 4148	3.00
D 16	IN 4148	Fairchild / I.T.T.	STC/FARNELL	IN 4148	3.00
D 17	11 DQ 04	International Rectifier	STC/FARNELL	11 DQ 04	35.00
D 18	11 DQ 04	International Rectifier	STC/FARNELL	11 DQ 04	35.00

Parts List - Control Board, Sheet 2

Part	Value	Type and Source	Farnell Order Code	Price / 100
R 1	1.0 K 1% M.F.	Corning SMA0207 / Mullard MRS25	STC/FARNELL MRS25 + Value	1.18
R 2	10 K Multiturn	Dubilier D75-207 / Spectrol 64-W	STC/FARNELL 64-W + Value	93.00
R 3	1.0 K 1% M.F.	Corning SMA0207 / Mullard MRS25	STC/FARNELL MRS25 + Value	1.18
R 4	200 K Multiturn	Dubilier D75-207 / Spectrol 64-W	STC/FARNELL 64-W + Value	93.00
R 5	2.2 K 1% M.F.	Corning SMA0207 / Mullard MRS25	STC/FARNELL MRS25 + Value	1.18
R 6	10 K 1% M.F.	Corning SMA0207 / Mullard MRS25	STC/FARNELL MRS25 + Value	1.18
R 7	47 K 1% M.F.	Corning SMA0207 / Mullard MRS25	STC/FARNELL MRS25 + Value	1.18
R 8	3.3 K 1% M.F.	Corning SMA0207 / Mullard MRS25	STC/FARNELL MRS25 + Value	1.18
R 9	2.2 K 1% M.F.	Corning SMA0207 / Mullard MRS25	STC/FARNELL MRS25 + Value	1.18
R 10	1.0 K 1% M.F.	Corning SMA0207 / Mullard MRS25	STC/FARNELL MRS25 + Value	1.18
R 11	47 K 1% M.F.	Corning SMA0207 / Mullard MRS25	STC/FARNELL MRS25 + Value	1.18
R 12	22 K 1% M.F.	Corning SMA0207 / Mullard MRS25	STC/FARNELL MRS25 + Value	1.18
R 13	2.2 K 1% M.F.	Corning SMA0207 / Mullard MRS25	STC/FARNELL MRS25 + Value	1.18
R 14	1.0 M Multiturn	Dubilier D75-207 / Spectrol 64-W	STC/FARNELL 64-W + Value	93.00
R 15	1.0 K 1% M.F.	Corning SMA0207 / Mullard MRS25	STC/FARNELL MRS25 + Value	1.18
R 16	1.0 K 1% M.F.	Corning SMA0207 / Mullard MRS25	STC/FARNELL MRS25 + Value	1.18
R 17	100 K Multiturn	Dubilier D75-207 / Spectrol 64-W	STC/FARNELL 64-W + Value	93.00
R 18	1.0 K 1% M.F.	Corning SMA0207 / Mullard MRS25	STC/FARNELL MRS25 + Value	1.18
R 19	100 K Multiturn	Dubilier D75-207 / Spectrol 64-W	STC/FARNELL 64-W + Value	93.00
R 20	200 K Multiturn	Dubilier D75-207 / Spectrol 64-W	STC/FARNELL 64-W + Value	93.00
R 21	1.0 K 1% M.F.	Corning SMA0207 / Mullard MRS25	STC/FARNELL MRS25 + Value	1.18
R 22	1.0 K 1% M.F.	Corning SMA0207 / Mullard MRS25	STC/FARNELL MRS25 + Value	1.18
R 23	1.0 K 1% M.F.	Corning SMA0207 / Mullard MRS25	STC/FARNELL MRS25 + Value	1.18
R 24	6.8 K 1% M.F.	Corning SMA0207 / Mullard MRS25	STC/FARNELL MRS25 + Value	1.18
R 25	2.2 K 1% M.F.	Corning SMA0207 / Mullard MRS25	STC/FARNELL MRS25 + Value	1.18
R 26	1.5 K 1% M.F.	Corning SMA0207 / Mullard MRS25	STC/FARNELL MRS25 + Value	1.18
R 27	1.5 K 1% M.F.	Corning SMA0207 / Mullard MRS25	STC/FARNELL MRS25 + Value	1.18
R 28	47 K 1% M.F.	Corning SMA0207 / Mullard MRS25	STC/FARNELL MRS25 + Value	1.18
R 29	4.7 K 1% M.F.	Corning SMA0207 / Mullard MRS25	STC/FARNELL MRS25 + Value	1.18
R 30	1.5 K 1% M.F.	Corning SMA0207 / Mullard MRS25	STC/FARNELL MRS25 + Value	1.18
R 31	1.2 K 1% M.F.	Corning SMA0207 / Mullard MRS25	STC/FARNELL MRS25 + Value	1.18
R 32	4.7 K 1% M.F.	Corning SMA0207 / Mullard MRS25	STC/FARNELL MRS25 + Value	1.18
R 33	4.7 K 1% M.F.	Corning SMA0207 / Mullard MRS25	STC/FARNELL MRS25 + Value	1.18
R 34	3.3 K 1% M.F.	Corning SMA0207 / Mullard MRS25	STC/FARNELL MRS25 + Value	1.18
R 35	10 K 1% M.F.	Corning SMA0207 / Mullard MRS25	STC/FARNELL MRS25 + Value	1.18

Parts List - Control Board, Sheet 3

Part	Value	Type and Source		Farnell Order Code	Price / 100
C 1	0.1 uF, 100 V, PETP	Mullard 368 series, 10%,	STC/FARNELL	368 25104	4.80
C 2	0.1 uF, 100 V, PETP	Mullard 368 series, 10%,	STC/FARNELL	368 25104	4.80
C 3	0.1 uF, 100 V, PETP	Mullard 368 series, 10%,	STC/FARNELL	368 25104	4.80
C 4	33 uF, 250 V, PETP	Mullard 368 series, 10%,	STC/FARNELL	368 45333	4.90
C 5	0.1 uF, 100 V, PETP	Mullard 368 series, 10%,	STC/FARNELL	368 25104	4.80
C 6	0.1 uF, 100 V, PETP	Mullard 368 series, 10%,	STC/FARNELL	368 25104	4.80
C 7	0.1 uF, 100 V, PETP	Mullard 368 series, 10%,	STC/FARNELL	368 25104	4.80
C 8	0.1 uF, 100 V, PETP	Mullard 368 series, 10%,	STC/FARNELL	368 25104	4.80
C 9	0.1 uF, 100 V, PETP	Mullard 368 series, 10%,	STC/FARNELL	368 25104	4.80
C 10	0.1 uF, 100 V, PETP	Mullard 368 series, 10%,	STC/FARNELL	368 25104	4.80
C 11	0.1 uF, 100 V, PETP	Mullard 368 series, 10%,	STC/FARNELL	368 25104	4.80
C 12	0.1 uF, 100 V, PETP	Mullard 368 series, 10%,	STC/FARNELL	368 25104	4.80
C 13	0.1 uF, 100 V, PETP	Mullard 368 series, 10%,	STC/FARNELL	368 25104	4.80
C 14	1,000 uF, 35 V, EL.	Dubilier CEB / Nippon C.C.SMVB	STC/FARNELL	STC - 23787F	32.00
C 15	0.1 uF, 100 V, PETP	Mullard 368 series, 10%,	STC/FARNELL	368 25104	4.80
C 16	0.1 uF, 100 V, PETP	Mullard 368 series, 10%,	STC/FARNELL	368 25104	4.80
C 17	0.1 uF, 100 V, PETP	Mullard 368 series, 10%,	STC/FARNELL	368 25104	4.80
C 18	0.1 uF, 100 V, PETP	Mullard 368 series, 10%,	STC/FARNELL	368 25104	4.80
C 19	100 uF, 35V, ELECT.	Dubilier CEB / Nippon C.C.SMVB	STC/FARNELL	STC - 23783C	8.20
C 20	0.1 uF, 100 V, PETP	Mullard 368 series, 10%,	STC/FARNELL	368 25104	4.80
C 21	1.0 uF, 100 V, PETP	Mullard 368 series, 10%,	STC/FARNELL	368 25105	4.80
C 22	330 pF, 63 V, Cer.	Dubilier low K Ceramic Disc	STC/FARNELL	146 490	5.00
C 23	0.1 uF, 100 V, PETP	Mullard 368 series, 10%,	STC/FARNELL	368 25104	4.80
C 24	0.1 uF, 100 V, PETP	Mullard 368 series, 10%,	STC/FARNELL	368 25104	4.80
TP 1-8	1.0 mm diameter pin	Lektrokit pins / BICC Vero pin C	STC/FARNELL	LK3011 (8 off)	17.60
Misc.	8 pin DIL socket	Low Prof. Harwin IC 4/6/7/8/9/10	STC/FARNELL	170 798 (6 off)	36.00
	16 pin DIL socket	Midland Ross wire wrap IC11	STC/FARNELL	175 330	51.00
	22 SWG TCW	For links, STC / FARNELL	STC/FARNELL	TCW22	3.56
	M3 x 6 mm PH screw	2 required per pcb	FARNELL	104 421 (2 off)	2.04
	M3 nut	2 required per pcb	FARNELL	101 449 (2 off)	1.34
	M3 star washer	2 required per pcb	FARNELL	101 473 (2 off)	0.68
	8 pin DIL Heatsink	Aavid slide-on type, for IC4	VEROSPEED	Verospeed order for pack of 5 253-39693D	30.00

Parts List - Power Board, Sheet 1

Part	Value	Type and Source		Farnell Order Code	Price / 100
IC 1	LM 337	National Semiconductor	STC/FARNELL	LM 337T	98.00
IC 2	LM 317	National Semiconductor	STC/FARNELL	LM 317T	76.00
IC 3	Socket Only -------	See page 2			
D 1	42 V Zener	Thomson CSF DTZ56A Transworld Scientific		Transworld Scientific DTZ56A	97.90
D 2	42 V Zener	Thomson CSF DTZ56A Transworld Scientific		Transworld Scientific DTZ56A	97.90
D 3	IN 4148	Fairchild / I.T.T.	STC/FARNELL	IN 4148	3.00
D 4	IN 4148	Fairchild / I.T.T.	STC/FARNELL	IN 4148	3.00
D 5	IN 4148	Fairchild / I.T.T.	STC/FARNELL	IN 4148	3.00
D 6	IN 4148	Fairchild / I.T.T.	STC/FARNELL	IN 4148	3.00
D 7	IN 4148	Fairchild / I.T.T.	STC/FARNELL	IN 4148	3.00
D 8	IN 4148	Fairchild / I.T.T.	STC/FARNELL	IN 4148	3.00
D 9	3.3 V Zener	400mw BZX79/61 BZY88	STC/FARNELL	BZY88C3V3 DO35	6.00
D 10	3.3 V Zener	400mw BZX79/61 BZY88	STC/FARNELL	BZY88C3V3 DO35	6.00
D 11	4.7 V Zener	5.0 W IN5337B	STC/FARNELL	IN5337B	37.00
D 12	11 DQ 06	International Rectifier	STC/FARNELL	11 DQ 06	54.00
D 13	4.7 V Zener	5.0 W IN5337B	STC/FARNELL	IN5337B	37.00
D 14	11 DQ 06	International Rectifier	STC/FARNELL	11 DQ 06	54.00
D 15	IN 4148	Fairchild / I.T.T.	STC/FARNELL	IN 4148	3.00
D 16	IN 4148	Fairchild / I.T.T.	STC/FARNELL	IN 4148	3.00
D 17	11 DQ 06	International Rectifier	STC/FARNELL	11 DQ 06	54.00
R 1	47 Ohm 1% M.F.	Corning SMA0207 / Mullard MRS25	STC/FARNELL	MRS25 + Value	1.18
R 2	47 Ohm 1% M.F.	Corning SMA0207 / Mullard MRS25	STC/FARNELL	MRS25 + Value	1.18
R 3	10 K 1% M.F.	Corning SMA0207 / Mullard MRS25	STC/FARNELL	MRS25 + Value	1.18
R 4	10 K 1% M.F.	Corning SMA0207 / Mullard MRS25	STC/FARNELL	MRS25 + Value	1.18
R 5	4.7 K Trimmer	Egen 2322-482-3 + Value/or equiv	STC/FARNELL	146 748	28.00
R 6	220 Ohm 1% M.F.	Corning SMA0207 / Mullard MRS25	STC/FARNELL	MRS25 + Value	1.18
R 7	4.7 K Trimmer	Egen 2322-482-3 + Value/or equiv	STC/FARNELL	146 748	28.00
R 8	220 Ohm 1% M.F.	Corning SMA0207 / Mullard MRS25	STC/FARNELL	MRS25 + Value	1.18
R 9	22 Ohm 5% MF 1W+	Corning FP1-1W / FP2-2W SERIES	STC/FARNELL	STC - 42468XM OR 16222RM	31.20 40.90

Parts List - Power Board, Sheet 2

Part	Value	Type and Source		Farnell Order Code	Price / 100
TR 1	IRFP 150 Mosfet	International Rectifier	STC/FARNELL	IRFP 150	983.00
TR 2	IRFP 150 Mosfet	International Rectifier	STC/FARNELL	IRFP 150	983.00
TR 3	TIP 110 Darlington	S.G.S. or equivalent	STC/FARNELL	TIP 110	41.00
TR 4	TIP 115 Darlington	S.G.S. or equivalent	STC/FARNELL	TIP 115	42.00
C 1	NOT FITTED				
C 2	15,000 uF	Filmcap Prosec 85C 15,000/40V	FARNELL	EP560	597.00
C 3	1,000 uF 63 V	Dubilier CEA / Nippon C.C. SMT	STC/FARNELL	143 672	51.30
C 4	1,000 uF 63 V	Dubilier CEA / Nippon C.C. SMT	STC/FARNELL	143 672	51.30
C 5	1,000 uF 63 V	Dubilier CEA / Nippon C.C. SMT	STC/FARNELL	143 672	51.30
C 6	1,000 uF 63 V	Dubilier CEA / Nippon C.C. SMT	STC/FARNELL	143 672	51.30
C 7	100 pF polystyrene	Mullard 425/6/7 series 160/630 V	STC/FARNELL	427 41001	12.40
C 8	100 pF polystyrene	Mullard 425/6/7 series 160/630 V	STC/FARNELL	427 41001	12.40
C 9	0.1 uF, 100 V, PETP	Mullard 368 series, 10%,	STC/FARNELL	368 25104	4.80
C 10	0.1 uF, 100 V, PETP	Mullard 368 series, 10%,	STC/FARNELL	368 25104	4.80
C 11	0.1 uF, 100 V, PETP	Mullard 368 series, 10%,	STC/FARNELL	368 25104	4.80
C 12	0.1 uF, 100 V, PETP	Mullard 368 series, 10%,	STC/FARNELL	368 25104	4.80
TP 1-5	1.0 mm diameter pin	Lektrokit pins / BICC Vero pin C	STC/FARNELL	LK3011 (pack of 100)(5 packs reqd)	11.00
Misc.	16 pin DIL socket	Midland Ross wire wrap IC3	STC/FARNELL	175 330	51.00
	22 SWG TCW	For Links, sufficient in Control Board list.	STC/FARNELL	TCW22	N.A.
	M3 x 6 mm PH screw	6 required per pcb	FARNELL	101 421 (6 off)	6.12
	M3 x 12 mm PH scr.	2 required per pcb	FARNELL	101 425 (2 off)	1.78
	M3 flat washer	2 required per pcb	FARNELL	101 465 (2 off)	0.42
	M3 x 8 mm spacers	2 required per pcb, M 3 tap.	VEROSPEED	Verospeed order code (pack of 50) 87 25977] (4 packs reqd.)	14.84
	Heatsink	see separate drawing and assembly parts list			
	TO 220 Insulator	Greaseless, Warth International	FARNELL	170 649 (pack of 10) 4 reqd.	79.60
	TO 3P Insulator	Greaseless, Warth International	FARNELL	170 651 (pack of 10) 2 reqd.	31.20

Parts List - Assembly, Sheet 1

Part	Value	Type and Source		Farnell Order Code	Price / 100
Misc.	Heatsink	Machined from Pinfin, blank from	PANTECHNIC	N.A.	840.00 (appr)
	Chassis Pan	Made from 16 Ga. mild steel, see separate drawing		N.A.	270.00 (appr)
	Ribbon Cable	7.5", 16 way, DIL to DIL, see separate drawing		N.A. (complete assembly can be obtained from Farnell or STC)	370.00
	M3 x 6 mm PH screw	5 required per assembly	FARNELL	101 421 (5 off)	5.10
	M3 nut	8 required per assembly	FARNELL	101 449 (8 off)	5.36
	M3 star washer	6 required per assembly	FARNELL	101 473 (6 off)	2.04
	M3 x 8 mm spacers	3 required per assmbly	VEROSPEED	Verospeed order code (pack of 50) 87 25977J (6 packs reqd.)	22.26
	M3 x 20mm PH screw	3 required per assembly	FARNELL	101 427 (3 off)	3.24
	Capacitor Mtg.	1 required per assembly	FARNELL/FILMCAP	DT2254	27.00
	M6 x 20mm PH screw	6 required per assembly	FARNELL	101 639 (6 off)	31.62
	M6 nut	6 required per assembly	FARNELL	101 451 (6 off)	3.48
	M6 flat washer	6 required per assembly	FARNELL	101 467 (6 off)	1.26
	Crimp eyes	12 required per assembly	T&B/FARNELL	DRC6Y (12 off per assembly)	81.60
	Input diode	75HQ045 International Rect.	IR/FARNELL	75HQ045	486.00
	Output diode	50HQ045 International Rect.	IR/FARNELL	50HQ045	437.00
	Diode insulators	SIL PAD D05 Large	WARTH INT.	Warth Int. order code SILPAD D05 LARGE (2 per assembly) WITH BUSHING.	25.00 (appr.)
	Cable (6 mm^2)	1.5 m required per unit, appr.	FARNELL	147 276 (6 reels required)	60.24
	Connectors	Input and output connectors to suit			
	M3 flat washer	4 required per assembly	FARNELL	101 465 (2 off)	0.42
	M3 x 12mm PH screw	2 required per assembly	FARNELL	101 425 (2 off)	1.78

CONCLUSION

The system has two principal advantages over commercially available switch mode voltage regulators, its low weight and its high efficiency. It has not been possible to follow through on the design work as insufficient information is available from Kingston on the results of trying the regulator in the target system. A specification for the Aluminium – Air battery has still not been received.

Figure 1 -- The Complete Interface

Figure 2 -- The Complete Interface

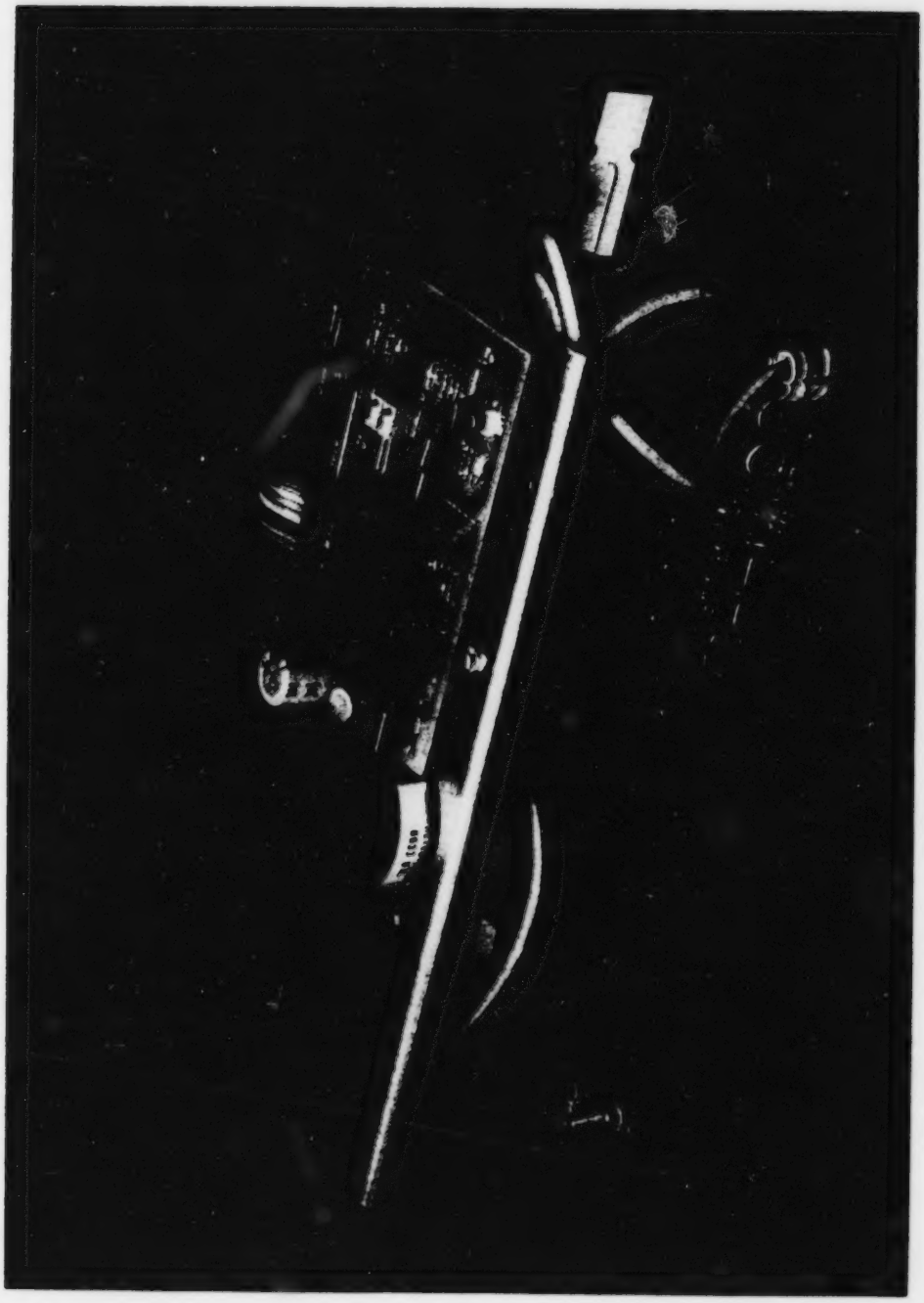

Figure 3 - Simplified Block Diagra

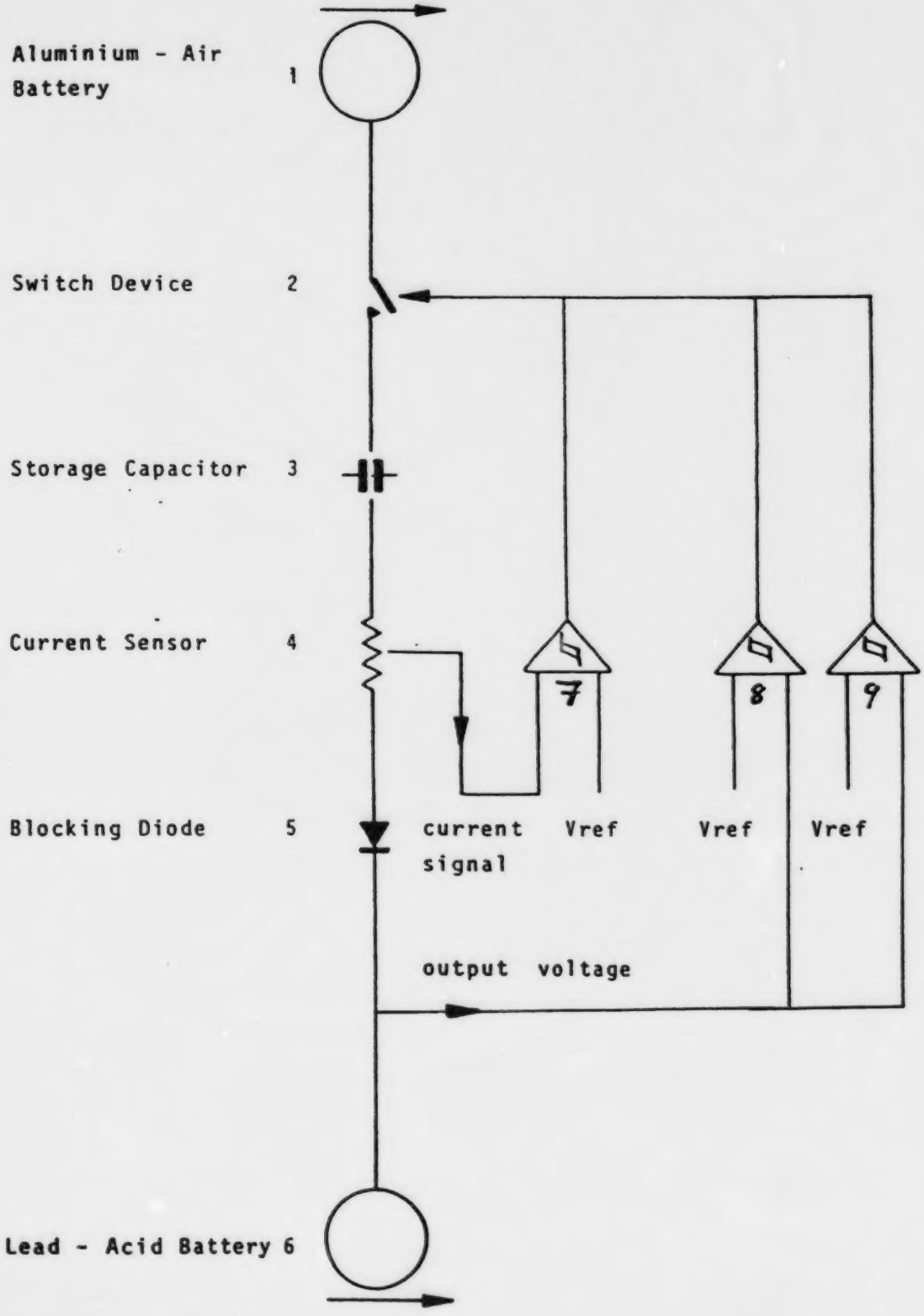

Figure 4 – Full Block Diagram

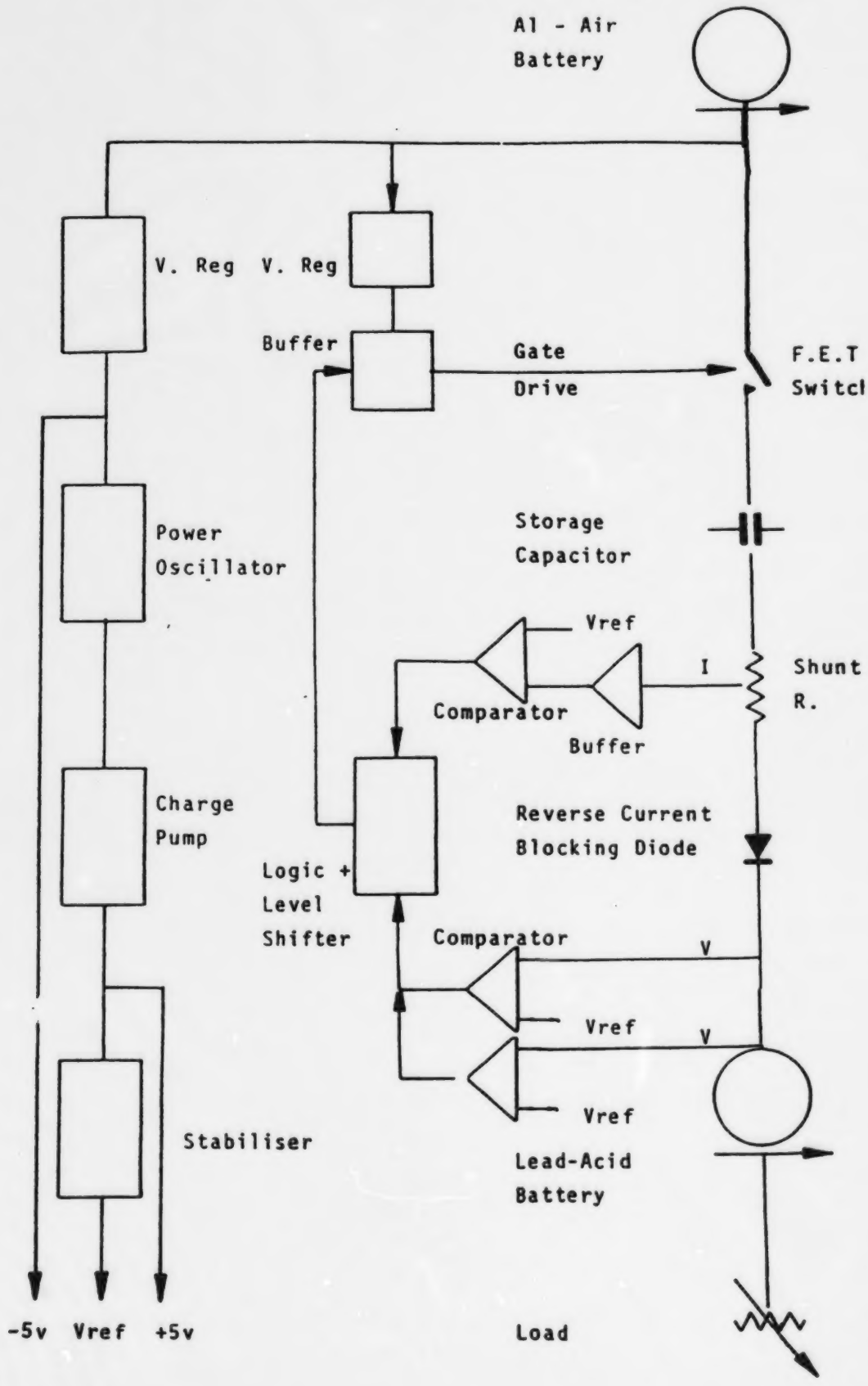

Figure 5 - Comparator Circuit

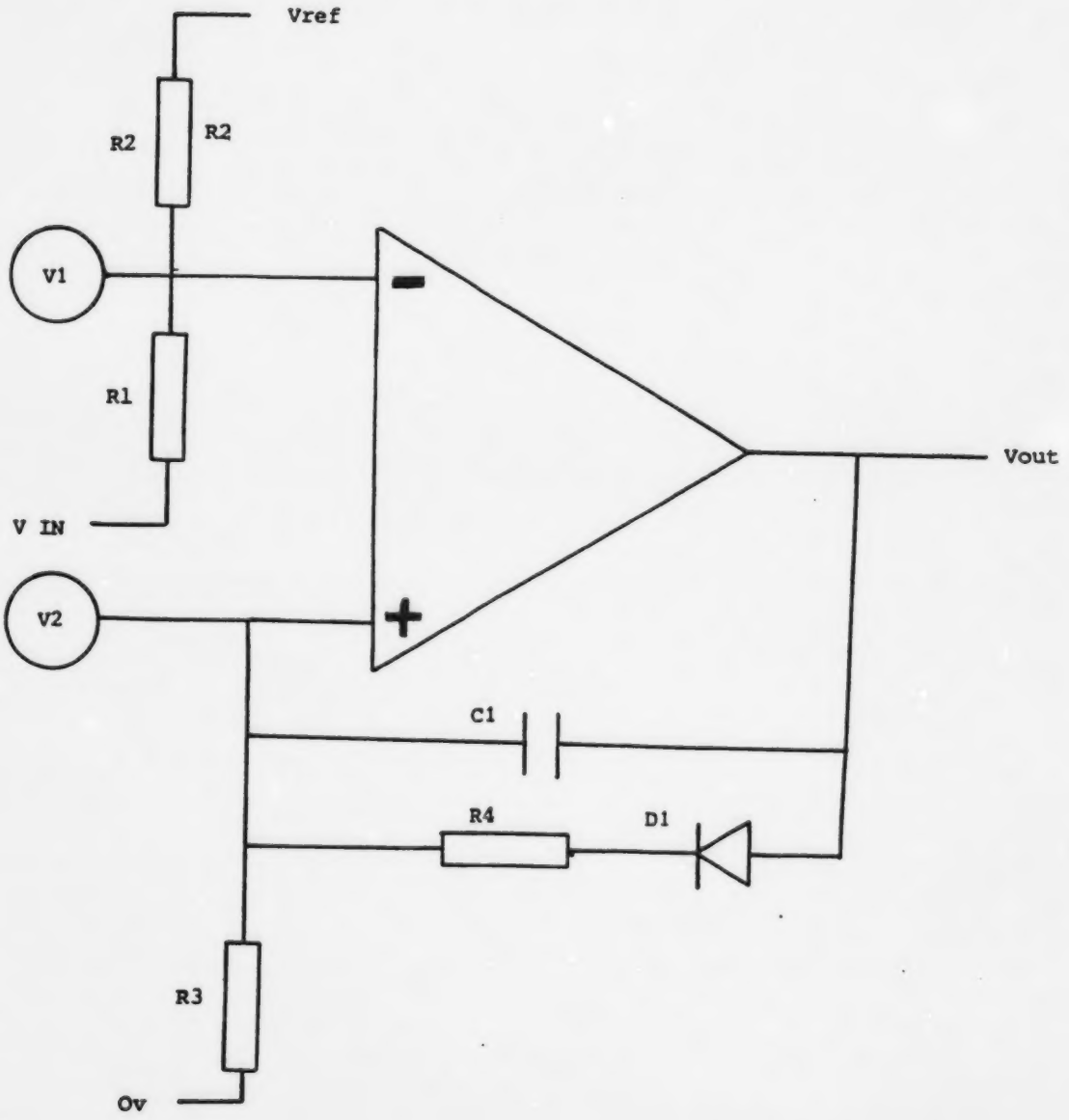

Figure 6 - Power Board Circuit

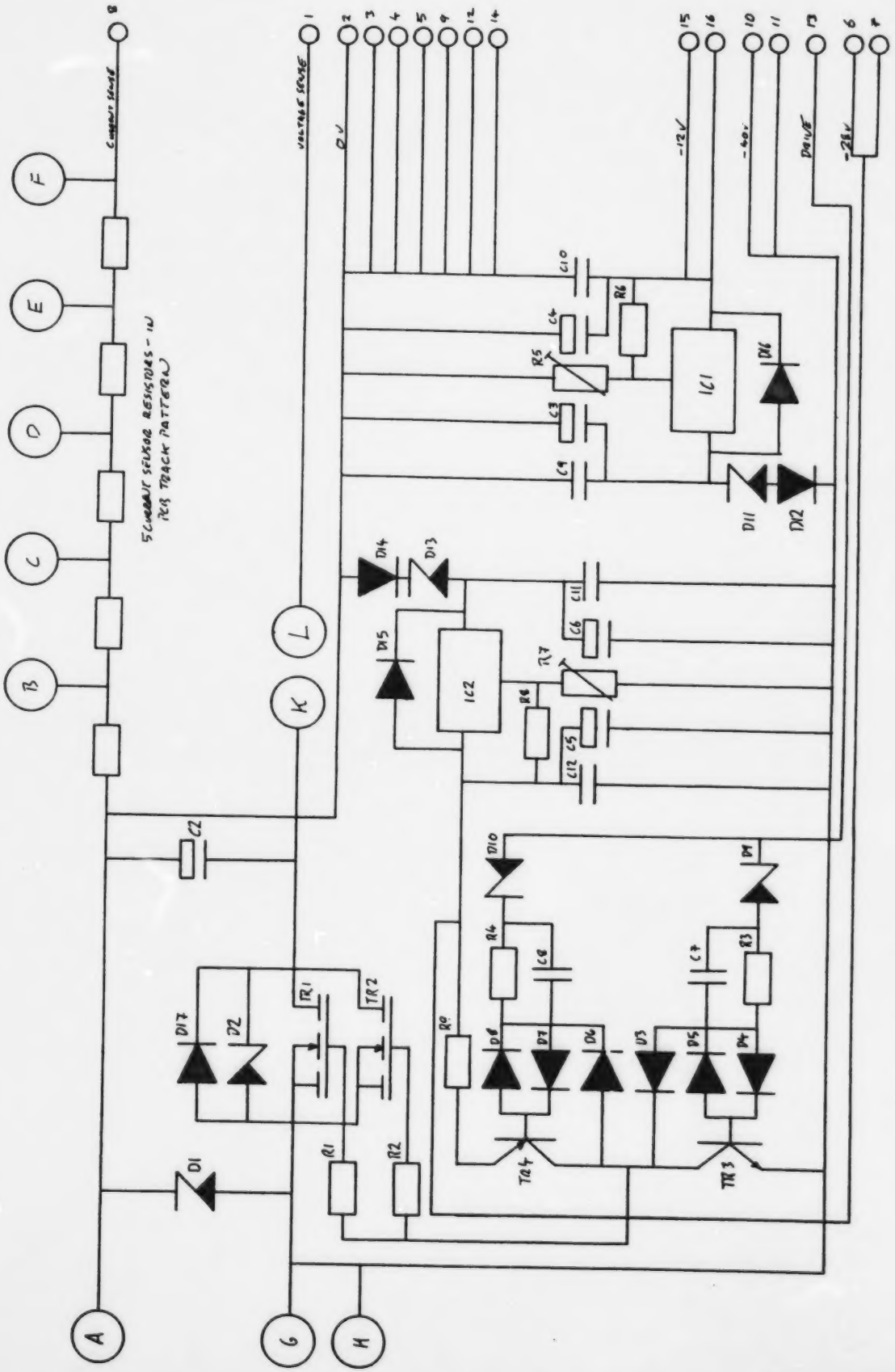

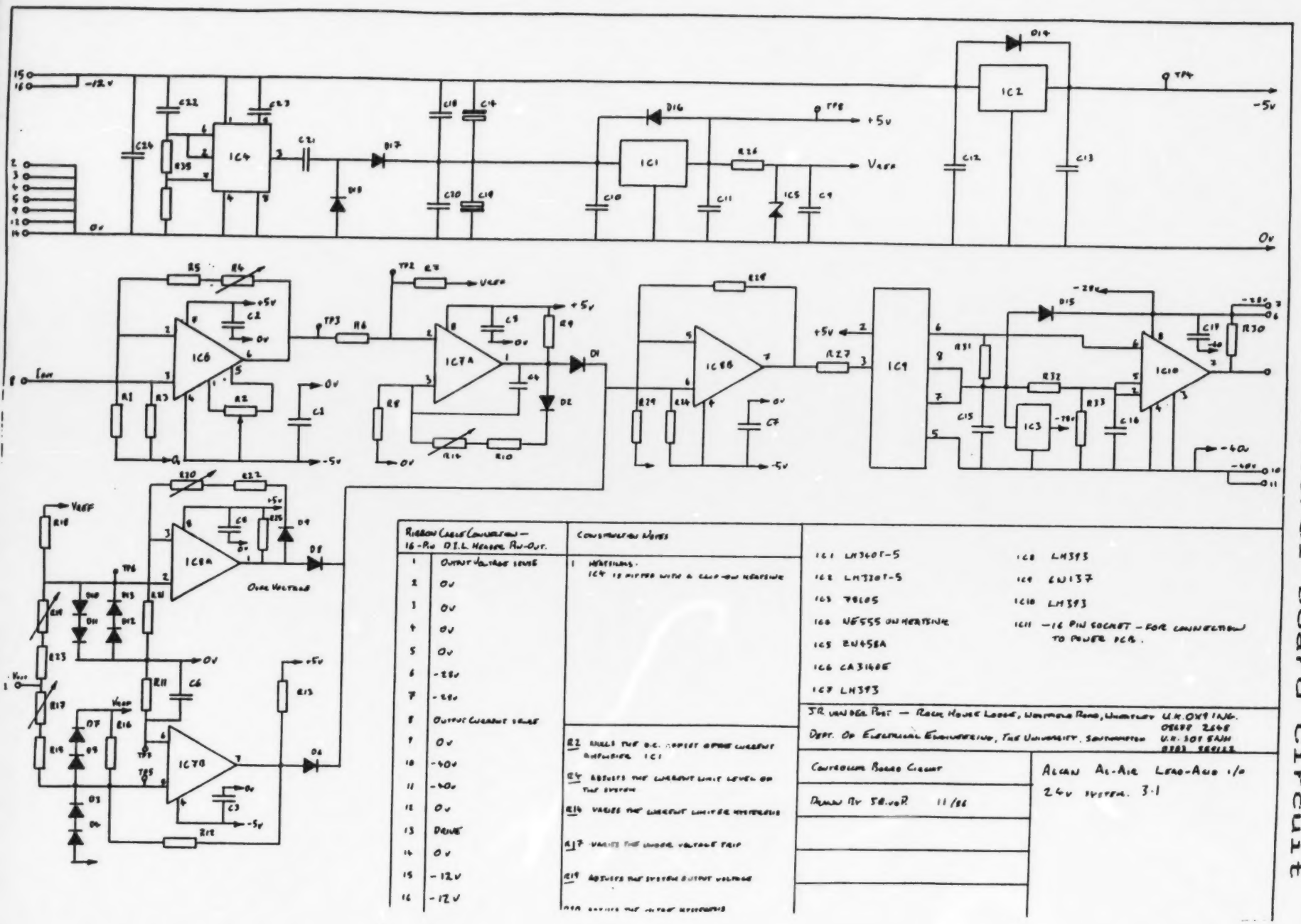

Ribbon Cable Connections — 16-Pin D.I.L. Header Plug-Out.	
1	Output Voltage Sense
2	0v
3	0v
4	0v
5	0v
6	-28v
7	-28v
8	Output Current Sense
9	0v
10	-40v
11	-40v
12	0v
13	Drive
14	0v
15	-12v
16	-12v

Construction Notes

1. Heatsinks.
   IC4 is fitted with a clip-on heatsink

R2 Sets the D.C. output current limiting IC1

R4 Adjusts the current limit level of the system

R14 Varies the current limiter hysteresis

R17 Varies the under voltage trip

R19 Adjusts the system output voltage

R20 Varies the voltage hysteresis

IC1	LM360T-5
IC2	LM320T-5
IC3	7905
IC4	NE555 on heatsink
IC5	ZN458A
IC6	CA3140E
IC7	LM393
IC8	LM393
IC9	LM137
IC10	LM393
IC11	-16 Pin socket - for connection to power PCB.

J.R. van der Post — Rock House Lodge, Westmead Road, Wimbledon U.K. SW19 1NG. 01-879 2648

Dept. of Electrical Engineering, The University, Southampton U.K. SO1 5NH 0703 559122

Controller Board Circuit

Drawn by J.R.v.d.P. 11/86

Alcan Al-Air Lead-Acid 1/o 24v system. 3-1

Figure 7 - Control Board Circuit

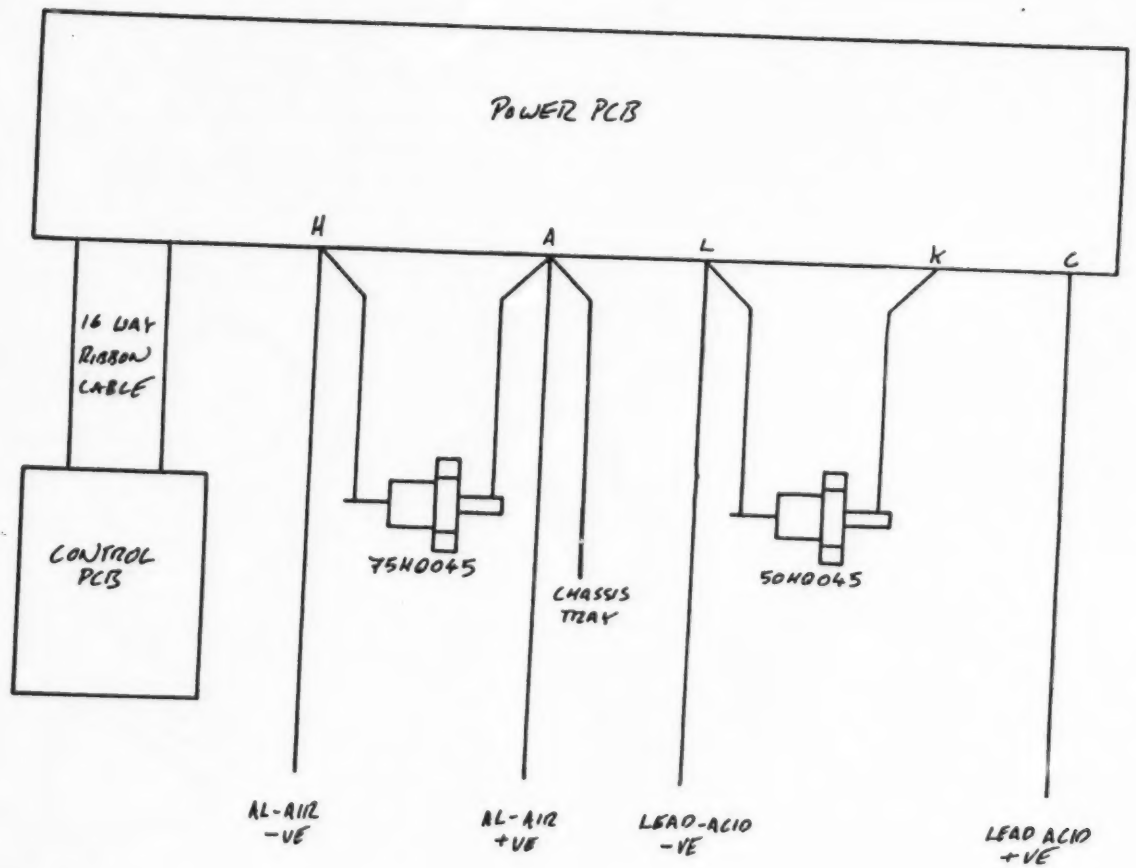

Figure 8 - System Wiring Diagram

Figure 9 - Control Board Artwork

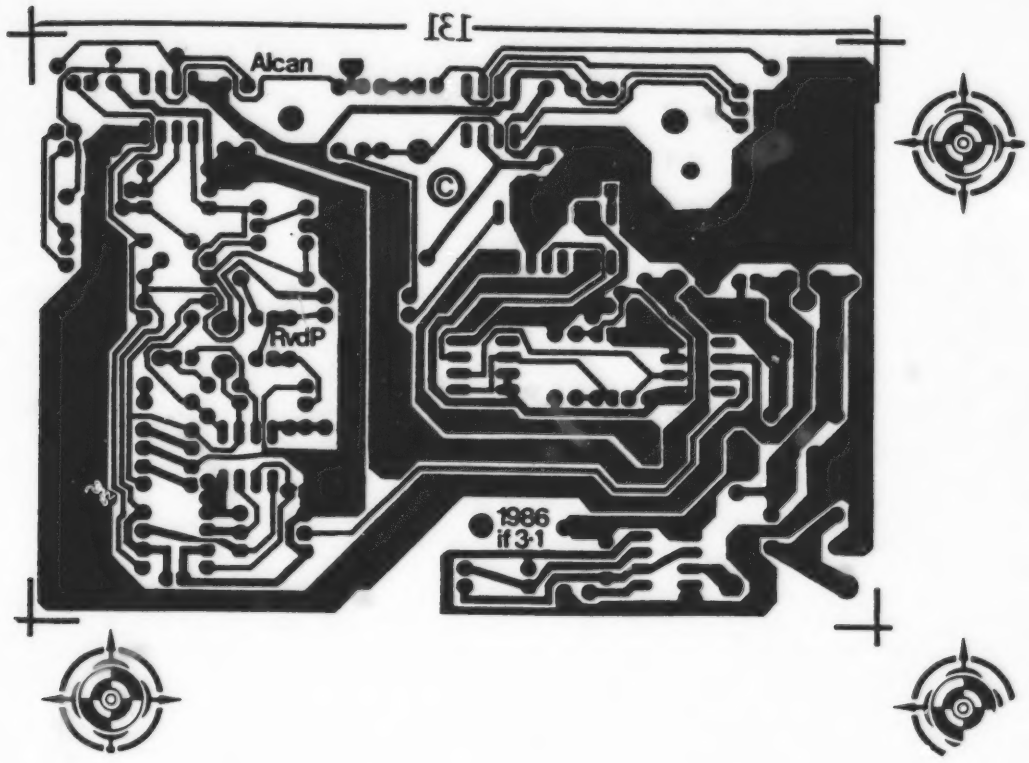

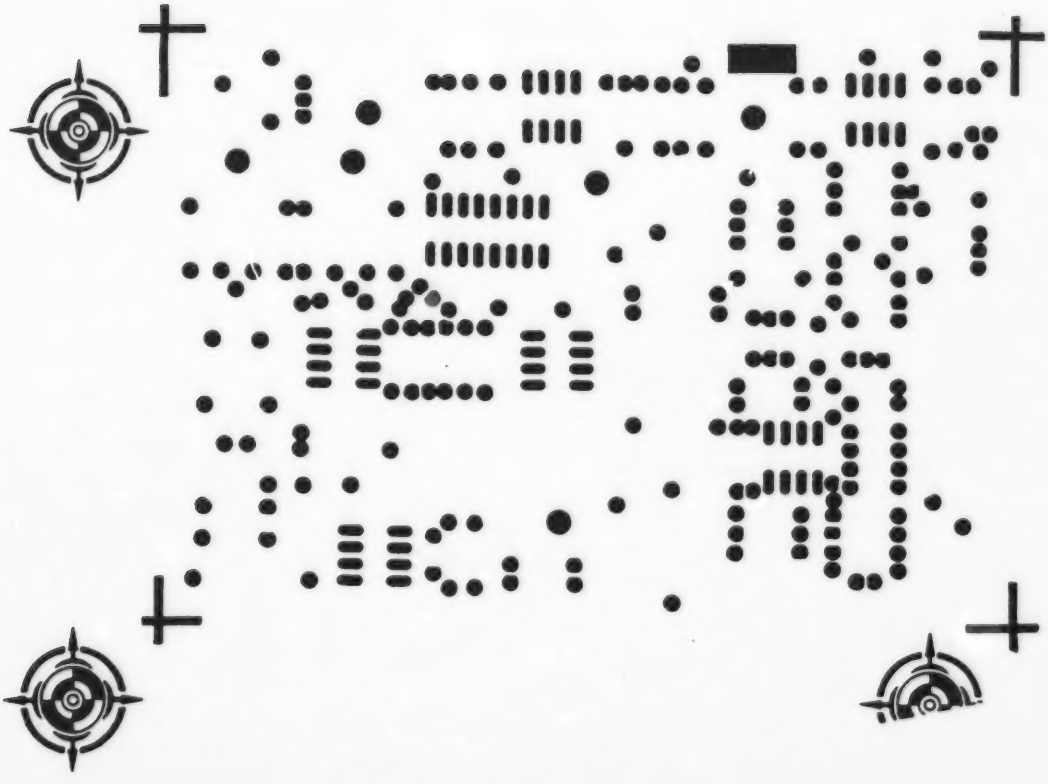

Figure 10 - Control Board Artwork

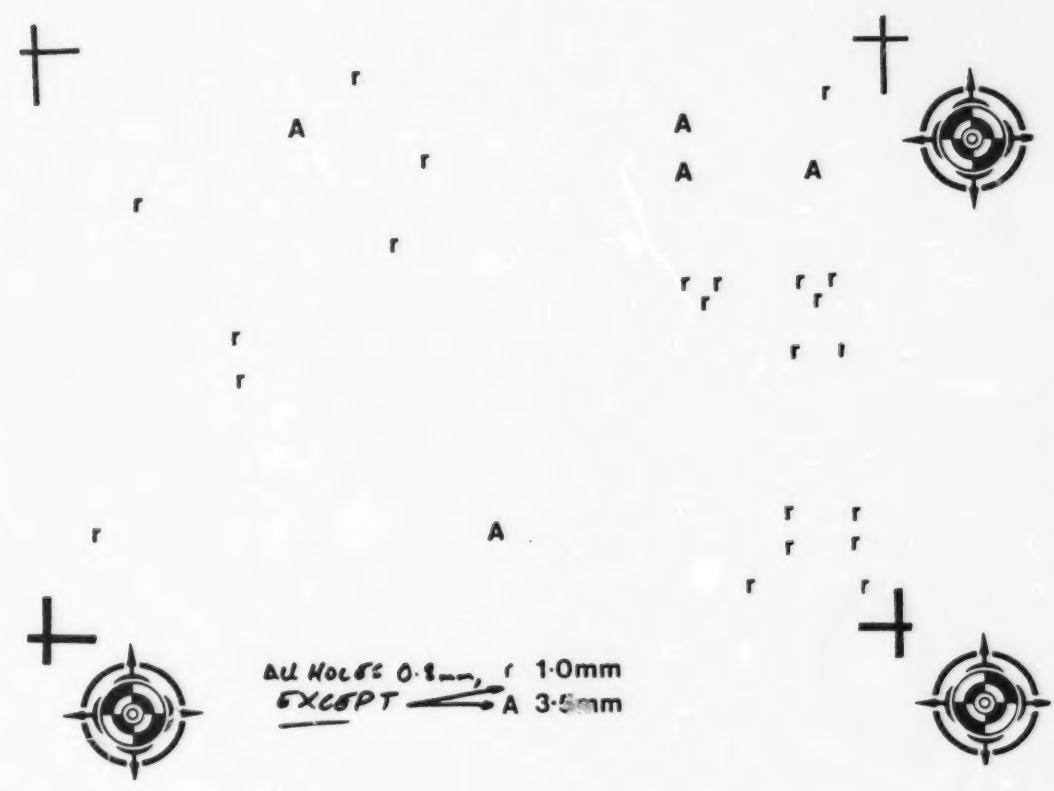

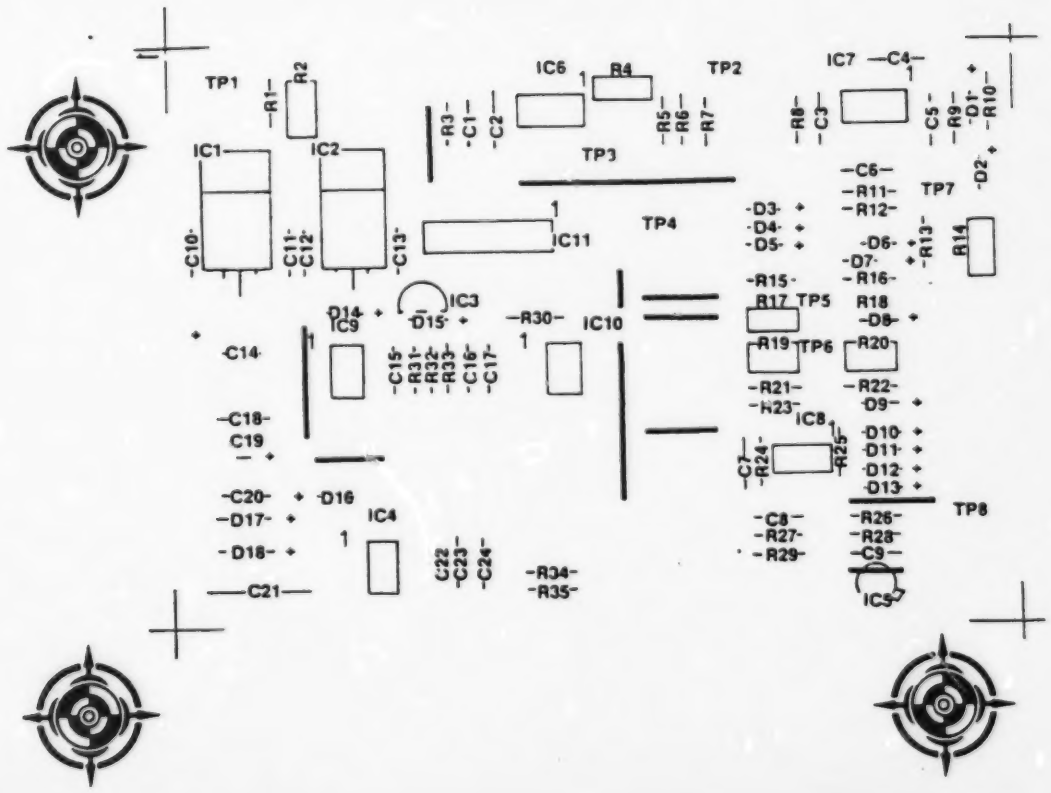

Figure 11 – Power Board Artwork

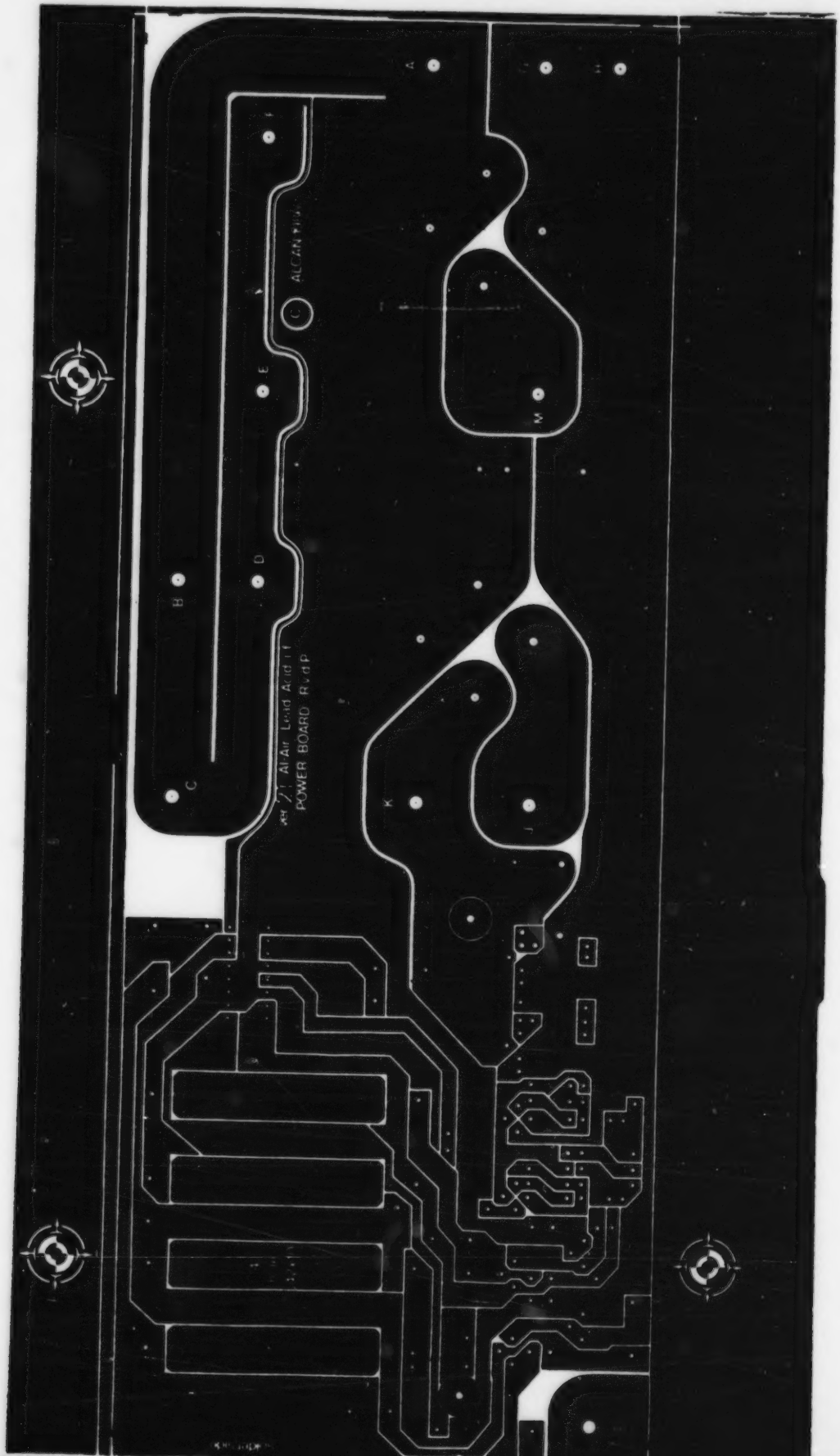

Power Board Artwork

Figure 13 – Power Board Artwork

Figure 14 – Power Board Artwork

Figure 15 – Chassis Tray

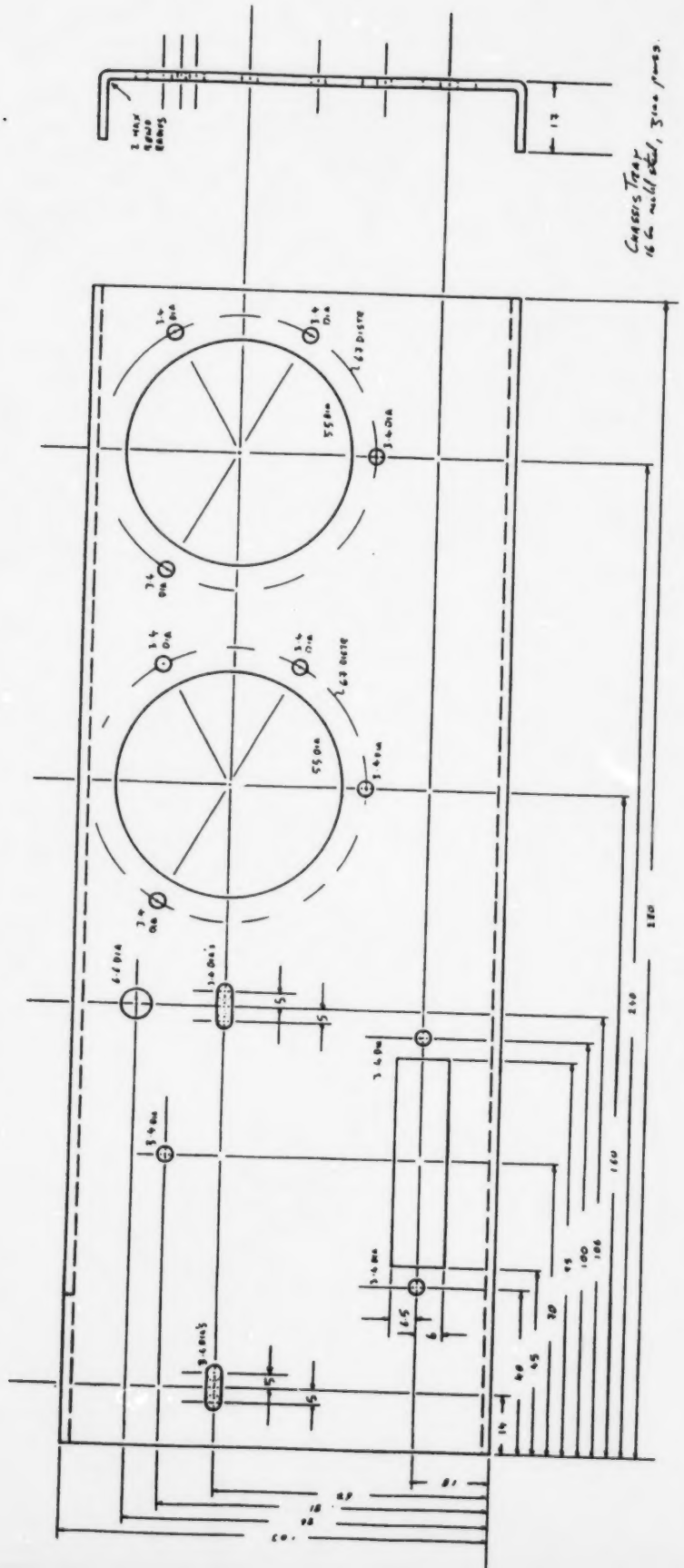

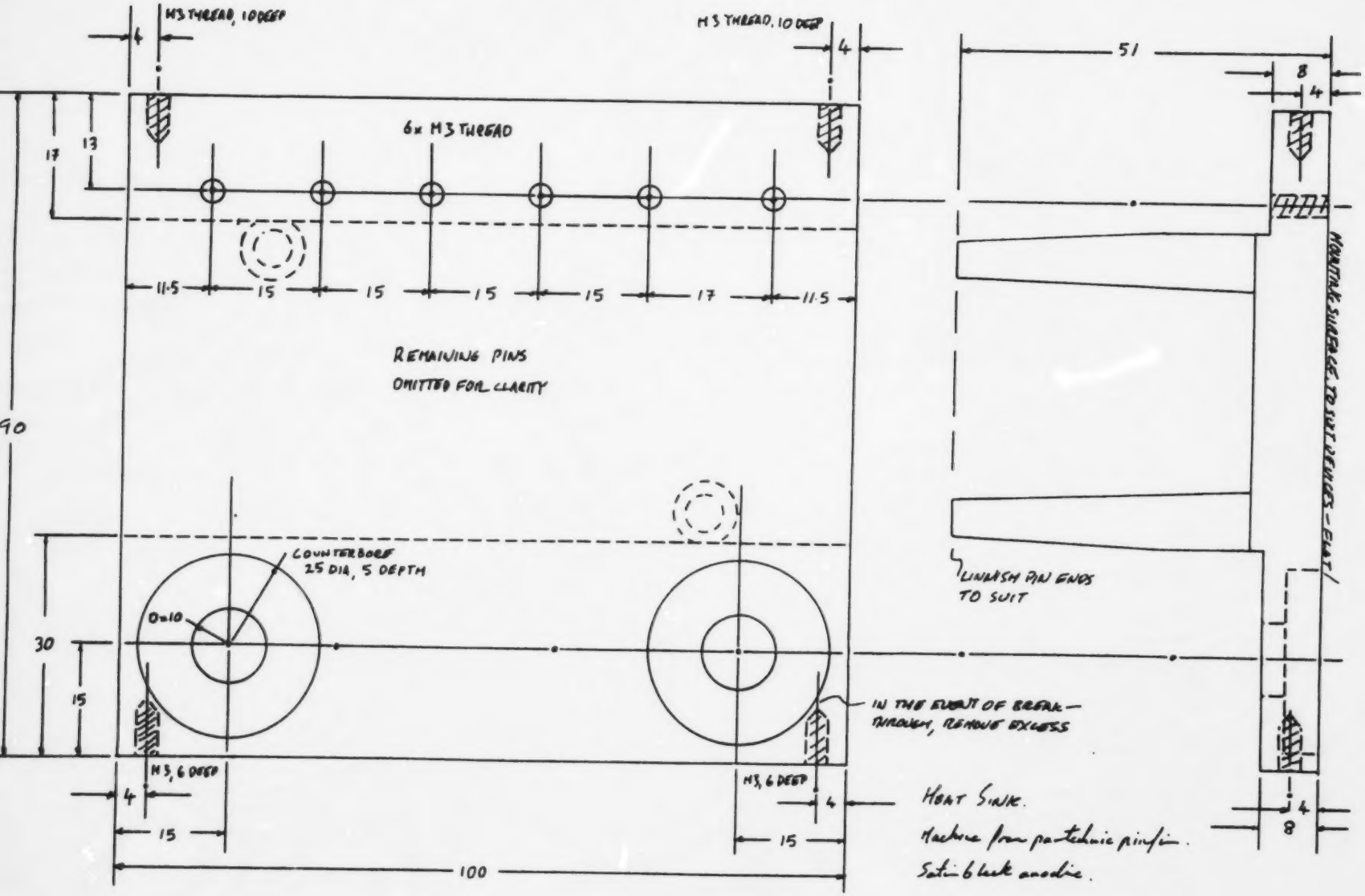

Figure 16 - Heatsink

Figure 17 - Voltage Characteristic

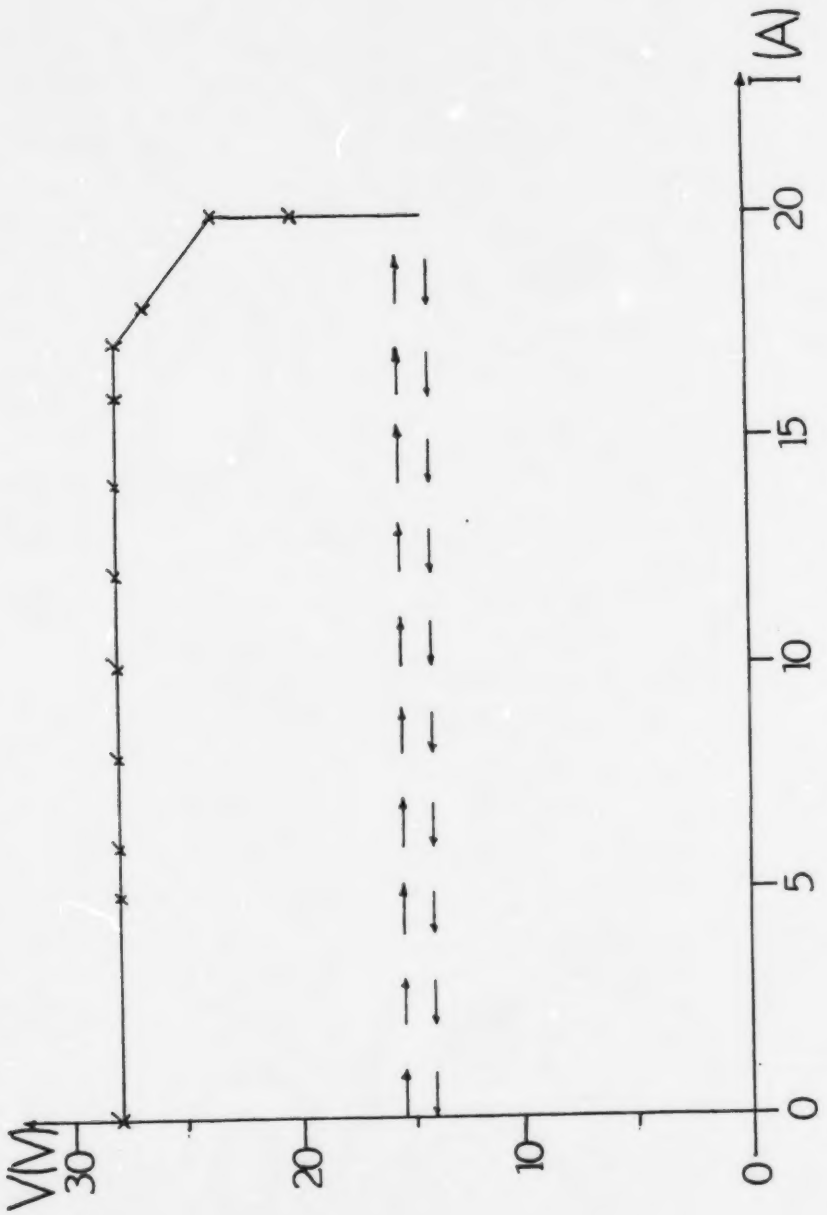

Figure 18 - Efficiency Curve

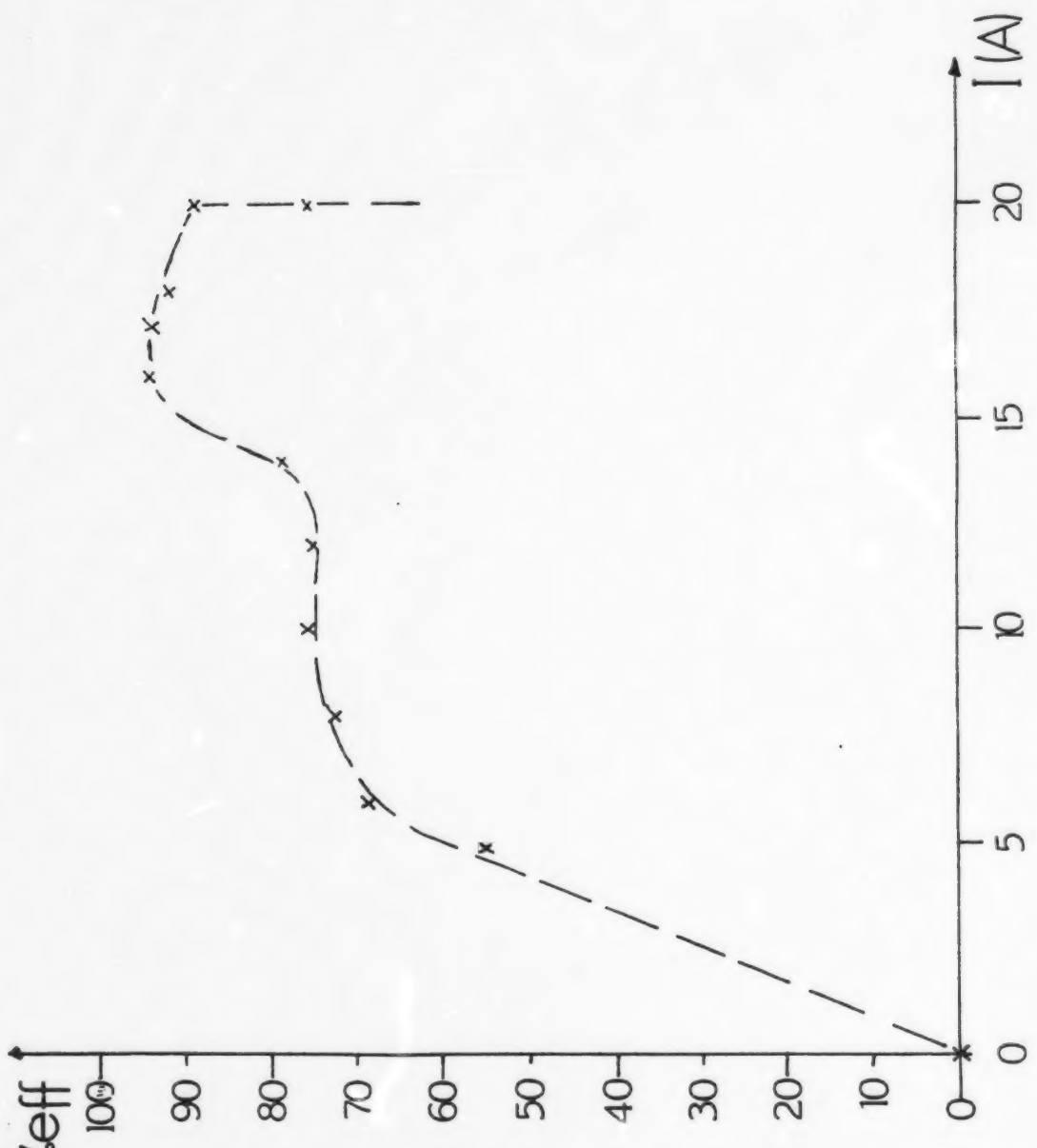

APPENDIX B

Alcan International Limited
Kingston, Ontario

Mail Address: Box 8400, Kingston, Ontario, Canada K7L 4Z4
Telephone: 613/549-4500 • Telex—05-25236 • Cable: Alcanint

13 December 1985

To: Mr. D.S. Strong, CONFIDENTIAL

From: N.P. Fitzpatrick

Subject: E.V. Analysis (corrected November 1987)

I thought a letter describing the analysis that I presented 27 November, with symbols defined, might be helpful for the next quarterly report.

The three batteries discussed were Pb-acid, saline Al-air and alkaline Al-air. The properties ascribed to them were:

Battery	Wh/kg	W/kg	Mass
Pb-acid	30	150	M_p
Saline Al-air	100	20	M_s
Alkaline Al-air	300	150	M_a

The figures for the latter battery are hypothetical, the former are realistic.

The maximum power that could be delivered by a hybrid combination of Pb acid and saline Al-air is

$$P_{max} = 150\ M_p + 20\ M_s \quad \text{kW}$$

and the maximum energy contained would be

$$E_{max} = 30\ M_p + 100\ M_s \quad \text{kWh}$$

The power for cruising would be

$$P_{cruise} = 20\ M_s$$

which could be maintained on the salt water battery alone.

The time the maximum power could be maintained would be $T_{pmax} - 30\ M_p/150\ M_p$. As an example we considered a 30 kWh capacity vehicle with a 20 kW power output,

If 3kWh of the energy was in the Pb/acid battery

P_{max} = 20 kW
M_p = 100 kg, i.e. 3 kWh capacity
M_s = 270 kg, i.e. 27 kWh capacity

and the total weight would be 370 kg.

P_{cruise} would be 5.4 kW and the maximum time the maximum acceleration could be maintained would be <12 minutes. (Mr. J. Morgan pointed out that this would reduce the energy capacity of the Pb-acid battery.) An intermediate power level of 10 kW could be sustained for 30 minutes. Similarly we analysed a Pb-acid/alkaline Al-air hybrid and found for 30 kWh capacity

M_p = 100 kg for 3 kWh
M_a = 90 kg for 27 kWh

Total weight = 190 kg 30 kWh

30 kWh of pure alkaline Al-air would have a weight of 100 kg and of Pb-acid 1000 kg. If all the vehicles had a base weight of 500 kg and used 0.15 Wh/kg.km we obtain

System	Vehicle Weight kg	Wh/km	Range km (30 kWh)
Al-air (alkaline)	590	89	337
Pb-acid	1500	300	100
Alkaline Al-air/Pb-acid	700	105	285
Saline Al-air/Pb-acid	870	130	230

Costs

Commercial purity alloys may perform quite well in saline electrolytes and yield 3 kWh/kg at 1.50/kg. In alkaline electrolytes the most optimistic results at present suggest 4 kWh/kg at 3.00/kg. Thus a kWh cost could be

Saline	$0.50/kWh	
Alkaline	$0.75/kWh	
Electrical energy	$0.07/kWh	(75% efficient charger)

The saline hybrid has enough capacity in its rechargeable battery such that 22 km could be managed on wall electricity. The alkaline hybrid vehicle has enough energy for 32 km.

With a hybrid a mixture of short and long trips could result in low average costs.

System		Average Cost cents/km	Al cost Assumed
Al-air alkaline	any combination	6.7	$3/kg
Pb-acid	any combination	2.1	
Hybrid:			
Alkaline Al-air/Pb-acid	90% < 32 km	1.4	$3/kg
(7.8 cents/km aluminum)	70% < 32 km	2.9	
(0.73 cents/km Pb-acid)	50% < 32 km	4.3	
Hybrid:			
Saline Al-air/Pb-acid	90% < 22 km	1.4	$1.50/kg
(6.5 cents/km aluminum)	70% < 22 km	2.6	
(0.91 cents/km Pb-acid)	50% < 22 km	3.7	

Discussion

We can see from the above analysis that because of the weight reduction energy consumption/km can be reduced by a factor of 3X with a hybrid battery. This increase compensates to some extent for the increased fuel costs of aluminum.

If the mission is not full range at full speed and some recharging is possible, then for some users the cost of energy used by a hybrid can be cut below that of wall electricity.

Conclusions

- o A practical saline Al-air system (100 Wh/kg 20 W/kg) not only has dramatic input upon the range of a hybrid electric vehicle but can reduce running costs below those of a pure electric vehicle for short missions. Obviously the costs are dramatically less than those of a pure Al-air vehicle.

- For a wide range of missions, doubling of aluminum cost with an alkaline system does not dramatically affect the cost per average kilometre, provided the gains in energy density and energy efficiency in a hybrid materialize.

- A hybrid system (Al-air saline or Al-air alkaline plus Pb-acid) would dramatically increase available vehicle range while producing a fuel cost structure acceptable to the average consumer.

- Since hybrid Al-air/secondary systems have such dramatic impacts upon both range and running cost, it is possible that the electric vehicle market (presently $200 million for batteries alone) can be expanded.

- Aluminum cost per se is not the key factor in bringing the technology to market performance: practicality at this time has greater influence.

NPF:VM:10.80

Copies to:

Mr. J.A. Hirschfield
Dr. H.R. Wynne-Edwards: Montreal
Dr. R.P. Hamlen: Alupower

Mr. D. Schwartz, Deta Inc.